

Mechanisms of vascular morphogenesis and stabilization by VEGF dose

Inauguraldissertation

zur

Erlangung der Würde eines Doktors der Philosophie

vorgelegt der

Philosophisch-Naturwissenschaftlichen Fakultät

der Universität Basel

von

Elena Groppa

von Italien

Basel, 2014

Genehmigt von der Philosophisch- Naturwissenschaftlichen Fakultät auf Antrag
von

Prof Markus Affolter

Dr Andrea Banfi

Prof Michael Heberer

Prof Mauro Giacca

Basel, den 18. Juni 2013

Prof Dr Jörg Schimbler
Dekan

Table of contents

1. ANGIOGENESIS	1
1.1 Vascular activation	3
1.1.1 Endothelium activation	3
1.1.1.1 VEGF ligands and receptors	4
1.1.1.2 VEGF-A isoforms	5
1.1.1.3 VEGF-A regulation	6
1.1.1.4 VEGF-A receptors	7
1.1.1.5 VEGFs and NPs co-receptors	8
1.1.1.6 NPs and Sema3 ligands	10
1.2 Modes of vascular growth	11
1.2.1 Sprouting angiogenesis	11
1.2.2 Intussusception angiogenesis	14
 2. MECHANISMS OF VASCULAR MATURATION AND STABILIZATION	 17
2.1 Vascular maturation	17
2.2 Vascular stabilization	17
2.3 Pericytes: heterogeneous but unique cells	18
2.3.1 PDGF ligands and receptors	20
2.3.1.1 PDGF-BB/PDGFR β signaling in embryonic vascular development	21

2.4 Pericyte-endothelium paracrine signals	23
2.4.1 TGF- β family and its receptors	23
2.4.1.1 TGF- β activation	25
2.4.1.2 TGF- β /TGF β R signaling in endothelial cells	25
2.4.1.3 TGF- β /TGF β R signalling in mural cells	27
2.4.2 Tie receptors and their Ang-1 and Ang-2 ligands	28
2.4.2.1 Angs/Tie signaling in embryonic vascular development	29
2.4.2.2 Angs/Tie signaling activation	30
2.4.3 Eph receptors and their Ephrin ligands	31
2.4.3.1 Vascular distribution of EphB4 receptor and EphrinB2 ligand	32
2.4.3.2 EphrinB2/EphB4 signaling in embryonic vascular development	33
2.4.3.3 EphrinB2/EphB4 signaling in physiological and pathological angiogenesis	34
2.5 Accessory cells in angiogenesis	34
3. THERAPEUTIC ANGIOGENESIS	36
3.1 Peripheral arterial disease	36
3.2 Angiogenic therapy	37
3.2.1 The issues with VEGF for therapeutic angiogenesis	39
3.3 Myoblast-based gene transfer system	42
AIMS OF THE THESIS	51

References:	i
-------------	---

EPHRINB₂/EPHB₄ SIGNALING CONTROLS THE SWITCH BETWEEN NORMAL AND

ABERRANT ANGIOGENESIS BY INCREASING VEGF DOSES 54

Introduction 54

Materials and Methods 57

Results 63

Discussion 79

Supplementary Informations 83

References i

INCREASING VEGF DOSES IMPAIR VASCULAR STABILIZATION BY DIRECTLY

INHIBITING THE SEMA₃A/CD11b⁺ NP-1⁺ MONOCYTE/TGF- β ₁ AXIS 85

Introduction 85

Materials and Methods 87

Results 94

Discussion 107

Supplementary Informations 112

References: i

SUMMARY AND FUTURE PROSPECTIVE 114

References i

Introduction

1. Angiogenesis

Angiogenesis is the formation of new capillary branches from preexisting blood vessels and occurs in development following vasculogenesis, which is the de novo formation of the initial vascular plexus in the embryo (Fig. 1) (1). In adult life, with the exception of the ovary, the endometrium, and the placenta, vessels are quiescent, although endothelial cells retain high plasticity to recognize and respond to angiogenic signals (2). The maintenance of endothelial quiescence is controlled by co-existence of endogenous negative regulators and pro-angiogenic factors in different tissues (2, 3). However, in certain conditions, such as wound healing, inflammation, or pathological situations, positive angiogenic factors prevail and the endothelium is induced to form new vessels. Angiogenesis comprises two phases, i.e. an activation phase that is the initiation and progression of the angiogenic process, and a resolution phase during which vessels newly formed become mature and stable (2).

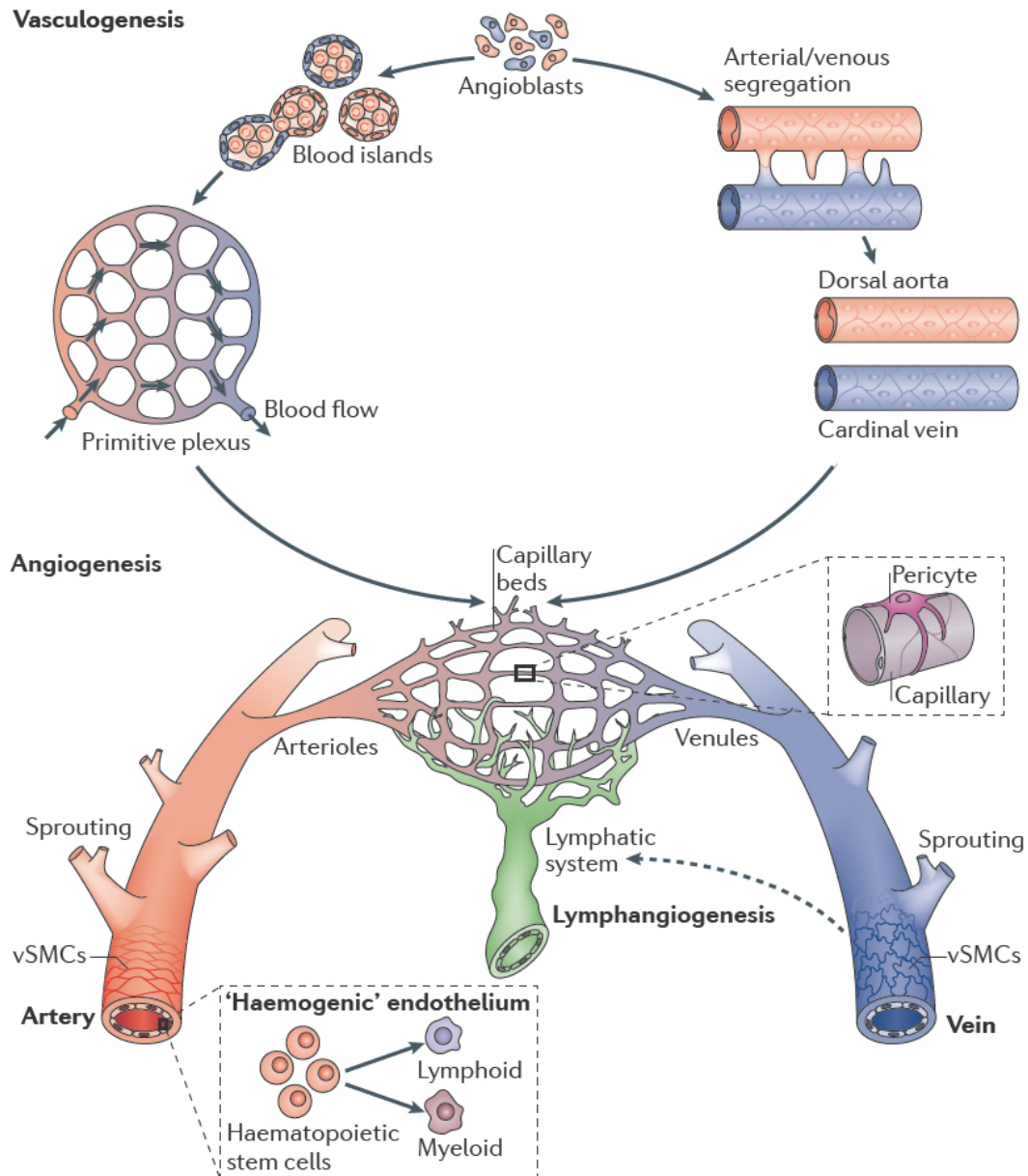


Figure 1 Development of a functional vasculature from endothelial progenitor cells. Endothelial progenitors (angioblasts) differentiate from mesodermal cells during early vertebrate development. Once formed, angioblasts may undergo arterial (red) or venous (blue) specification and coalesce to generate the first embryonic blood vessels, i.e. the dorsal aorta and cardinal vein. Angioblasts also aggregate to form blood islands, which fuse and remodel in response to haemodynamic stimuli or inherent genetic factors to create a primitive network of arterial and venous plexi. Following their vasculogenic assembly, angiogenic remodelling of the dorsal aorta, cardinal vein and vascular plexi generates a complex hierarchical network of arteries, arterioles, capillary beds, venules, and veins. Besides, the sprouting of lymphatic endothelial cells from venous vessels (lymphangiogenesis) seeds the lymphatic system (indicated by a dotted arrow) (adapted from Herbert et al, 2011).

1.1 Vascular activation

In a healthy adult, quiescent endothelial cells form a monolayer of cells sealed by junctional molecules. Here, endothelial cells have long half-life because they are protected against insults by the action of maintenance signals, such as Angiopoietin-1 (Ang-1) and low doses of Vascular Endothelial Growth Factor (VEGF), secreted by pericytes that are tightly associated with the endothelium into the basement membrane (BM) (3). However, metabolic and hemodynamic changes may disturb quiescent vessels and activate endothelial cells, which start a cascade of events that give rise to new capillaries (3, 4). In general, angiogenic factors released by the tissue in response to hypoxia induce sprouting angiogenesis, whereas high levels of shear stress lead to intussusception angiogenesis (4).

1.1.1 Endothelium activation

Signaling involved in angiogenic activation of endothelium occurs via extracellular signals, which are mainly secreted paracrine factors, frequently ligands of surface transmembrane receptors, and extracellular matrix components that usually bind to integrins and to specialized receptors. The main transmembrane receptors that transduce angiogenic signals are tyrosine kinase receptors (RTK) and tyrosine-kinase-associated receptors (5). Most RTKs are single subunit receptors, and each of them is constituted by a single hydrophobic transmembrane-spanning domain, an extracellular N-terminal region, and an intracellular C-terminal region. The extracellular N-terminal region exhibits a variety of conserved elements including

immunoglobulin (Ig)-like or epidermal growth factor (EGF)-like domains, fibronectin type III repeats, or cysteine-rich regions that are characteristic for each subfamily of RTKs. These domains contain primarily a ligand-binding site, which binds extracellular ligands, for example a particular growth factor. The intracellular C-terminal region comprises catalytic domains responsible for the kinase activity of these receptors, which catalyses receptor autophosphorylation and tyrosine phosphorylation of RTK substrates. Ligand binding to the extracellular domain induces formation of receptor dimers (Wikipedia).

VEGF ligands and their cognate RTK receptors, VEGFRs, play major roles in the endothelium activation in physiological as well as pathological angiogenesis (6).

1.1.1.1 VEGF ligands and receptors

Mammalian VEGF family consists of five members, VEGF-A, VEGF-B, VEGF-C, VEGF-D, and placenta growth factor (PlGF). VEGF-A was initially identified as an inducer of tumor vascular permeability factor (VPF) (7). Over the past decades, the idea that VEGF-A is one of the master players of vessel formation has taken root, and much work of vascular biology research has been focused on it (8).

Secreted VEGF in dimeric form binds to VEGF receptor and activate its downstream signaling. Three structurally-related receptors, VEGFR1 (Flt1), VEGFR2 (Flk1), and VEGFR3 (Flt4) are the RTKs of VEGF ligand family. VEGFR1 binds to VEGFA, VEGFB, and PlGF, whereas VEGFR2 binds exclusively to VEGFA. VEGFR3 bind specifically to VEGFC and VEGFD. Proteolytic processed VEGFC and VEGFD are able to bind also to VEGFR2 (9).

1.1.1.2 VEGF-A isoforms

The human VEGF-A (hereafter VEGF) is organized in eight exons, interrupted by seven introns and is localized in chromosome 6p21.3. Exon splicing generates four isoforms, having 121, 165, 189, and 206 amino acids (Fig. 2). VEGF₁₆₅ does not have the exon 6, whereas VEGF₁₂₁ lacks the regions encoded by exon 6 and 7. VEGF₁₆₅ is a heparin-binding homodimeric glycoprotein and is the major VEGF isoform (10). VEGF₁₂₁ is an acidic polypeptide that does not bind heparin, thus is freely diffusible protein. VEGF₁₈₉ and 206 are highly basic and bind to heparin with high affinity such that they are almost completely sequestered in the extracellular matrix (ECM) (11). VEGF₁₆₅ resembles intermediate properties with respect to the other isoforms, because it is secreted, but a significant fraction bound to the cell surface and ECM. The plasmin cleavage of heparin-bound VEGF-isoforms at the COOH terminus produces bioactive VEGFA fragments (10). The corresponding mouse isoforms, VEGF₁₂₀, VEGF₁₆₄, and VEGF₁₈₈, are all one amino acid shorter than their human counterparts, but they possess similar functional characteristics (12). The different heparin binding properties of the VEGF isoforms determine the formation and the shape of extracellular VEGF gradient, which is a fundamental factor to decide between directional sprouting through tip cell migration, and circumferential enlargement through non-directional endothelial proliferation (refer to section 1.2) (13). Genetic manipulation of each of these isoforms in mouse tumor model of VEGF driven angiogenesis, hindbrain, and retina, showed that VEGF₁₂₀ induces fewer and less branched vessels that grow by diameter enlargement rather than by sprouting due to the lack of VEGF gradient. In contrast, VEGF₁₈₈ causes hypervascularisation, but is unable to promote vessel

growth, because most vessels are of small caliber and they fail to connect the vessels to the systemic vasculature due to the steep VEGF gradient. Differently from these isoforms, VEGF₁₆₄ is able to support normal angiogenic growth forming properly branched and pervasive vessel network (14, 15).

The deletion of one VEGF allele (VEGF^{+/-}) resulted in embryonic lethality with developmental anomalies such as defective vascularization in several organs (16). Interestingly, two- to threefold overexpression of VEGF from its endogenous locus also resulted in severe abnormalities in vascular development, for example the formation of oversized epicardial vessels, and embryonic lethality between d 12.5 and d 14 (17). These results highlighted that the VEGF activity during vascular development is tightly controlled by its gene-dosage (10).

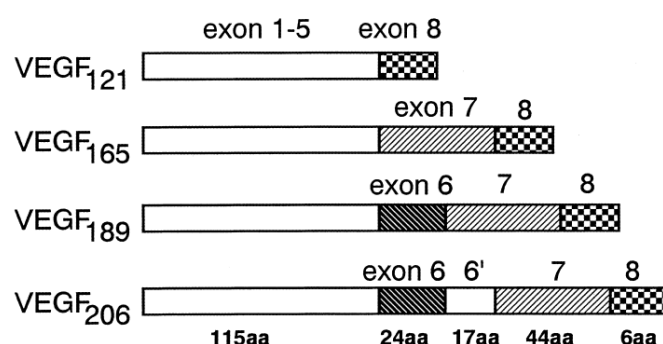


Figure 2 Comparison of structures of VEGF-A isoforms derived from alternative splicing (adapted from Shibuya et al, 2001).

1.1.1.3 VEGF-A regulation

VEGF gene is regulated by a variety of stimuli, such as hypoxia, nitric oxide, growth factors, p53-mutation, hormones, and tumor promoters. However, hypoxia represents the most relevant condition that triggers VEGF up-regulation. Under insufficient oxygen availability, transcriptional factors HIF1 α and HIF2 α are translocated to the nucleus and cooperate with other factors, such as HIF β , to

activate VEGF gene expression via a specific motif hypoxia response element (HRE). Contrary, under normoxic conditions, von Hippel Lindau (VHL) protein is involved in the degradation of VEGF protein (6).

1.1.1.4 VEGF-A receptors

VEGF-A can bind two RTKs, VEGFR1 (Flt1), and VEGFR2 (KDR, human; Flk1, mouse) (Fig. 3). Both receptors are expressed in endothelial cells, but VEGFR1 is also expressed in monocyte/macrophages, hematopoietic stem cells, and even some tumor cells (18). VEGFR1 has high affinity for VEGF, while weak tyrosine autophosphorylation in response to it (6). VEGFR1 exists also as soluble form and has a decoy receptor function to regulate in a negative manner the activity of VEGF on the vascular endothelium by sequestering it to VEGFR2 (19). Flt1^{-/-} null mice presented excessive and disorganized vasculature and died in utero between day 8.5 and day 9.5. This indicated that, at least during development, VEGFR1 is a negative regulator of VEGF action (10). Other studies, instead, revealed VEGFR1 to lead chemotaxis of endothelial progenitors or monocytes that directly or indirectly contribute to vessel formation (20). These conflicting results suggest that VEGFR1 has a dual function in angiogenesis, acting either in a positive or negative manner in different circumstances (10).

VEGFR2 binds VEGF with lower affinity compared to VEGFR1, but stronger tyrosine activity. The key role of this receptor was observed in Flk1^{-/-} null mice that lacked of vasculogenesis and organized blood vessels and died in utero between day 8.5 and day 9.5 (6). Based on this and further investigations, nowadays it is believed that VEGFR2 is the major mediator of mitogenic, angiogenic, and permeability-

enhancing effects of VEGF, by acting through mitogen-activated protein kinase (MAPKs) and phosphoinositide 3-kinases (PI3Ks), AKT, phospholipase Cy, and small GTPase (10, 19).

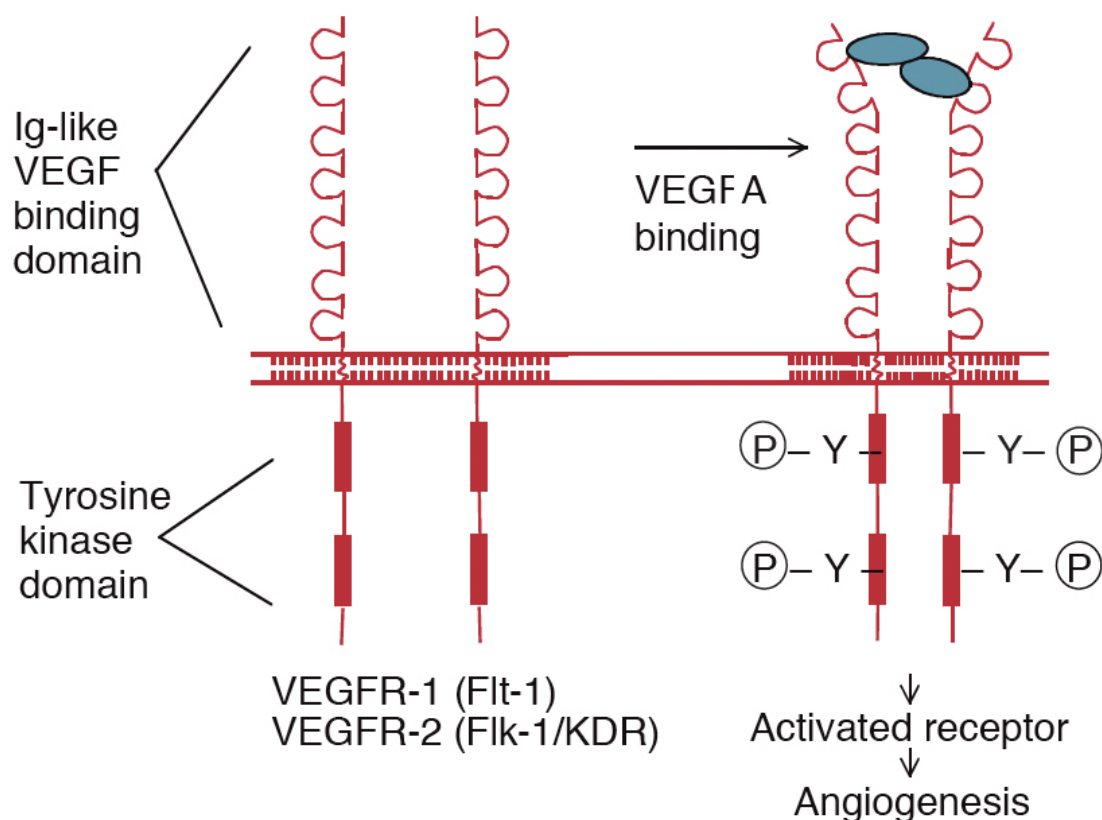


Figure 3 Representative structure of VEGF tyrosine kinase receptors. The VEGF binding domain is represented by seven immunoglobulin-like loops in the extracellular domain. Two VEGF receptors form a dimer to lead autophosphorylation of tyrosine residues on the cytoplasmic domain. Ig=immunoglobulin; VEGF=vascular endothelial growth factor; Y-Ⓟ=phosphorylated tyrosine residues (adapted from McMahon et al, 2000).

1.1.1.5 VEGFs and NPs co-receptors

In addition to RTKs, VEGF isoforms interact with a family of co-receptors, the neuropilins (NP-1 and -2) (10). NPs are single-pass transmembrane receptors with a large extracellular region comprising five modular domain named a1, a2, b1, b2, and c, joined to a transmembrane helical region and short cytoplasmic domain (21); NPs lack intrinsic enzymatic activity (22). NP-1 and NP-2 were first studied in nervous system and then identified in artery and vein endothelial cells,

respectively. They exhibit 44% sequence identity, and differ in the subset of ligands that they bind, such that NP-1 binds the heparin binding isoforms of VEGF-A, -B, and PlGF, while NP-2 interacts with VEGF-A, -C, and -D (21). The role of NPs in the development of the vascular system was addressed by gene-targeting studies that revealed a spectrum of vascular abnormalities leading to embryonic lethality in NP-1 null mice; conversely, embryonic vasculature was only partially affected by NP-2 deletion and mice were viable (21, 23). Further studies in development and adult angiogenesis showed that NP-1 improves VEGF-dependent angiogenesis by presenting VEGF₁₆₅ to VEGFR2 (Fig. 4) (23, 24). Binding of VEGF₁₆₅ to NP-1 occurs at the sites of the VEGF heparin binding domain (sequence derived from exon 7), whereas VEGF₁₆₅ binds VEGFR2 in correspondence of the region encoded by exons 3 and 4 (21).

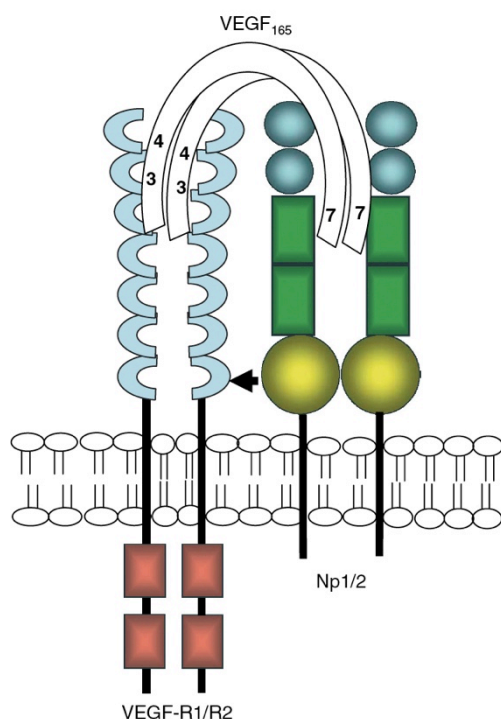


Figure 4 The interaction between VEGF₁₆₅, NP-1, and VEGFR2. VEGF₁₆₅ creates homodimers that bind to VEGFR1/R2 via the regions encoded by exons 3 and 4, causing receptor dimerization, and therefore signal transduction through the intracellular kinase domains. Simultaneously, VEGF₁₆₅ can bind to the b1/b2 domain of NP-1 via the region encoded by exon 7, thereby causing dimerization of NP-1, and enhancing signal transduction through VEGFR2 (adapted from Staton et al, 2007).

1.1.1.6 NPs and Sema3 ligands

NPs can also bind class 3 semaphorins, a family of secreted polypeptides that were initially described to have key roles in axonal guidance. Class 3 semaphorin has a single immunoglobulin domain and a basic C-terminus tail. NP-1 is a co-receptor for semaphorin-3A, -3C, and -3F, while NP-2 for semaphorin-3B, -3C, and -3F (24). The major semaphorin ligand for NP-1 is Sema3A (also called collapsin-1) that is expressed by endothelial cells in development and experimental angiogenesis (24, 25). The binding of Sema3A to NP-1 is enhanced by the Sema3A co-receptor Plexin-A1, and the Sema3A/NP-1/Plexin-A1 signaling is believed to act through Plexin-A1 cytoplasmatic region, which contains GTPase-activating proteins (GAP) homology domains (24). Sema3A binds both a and b domains of NP-1, while VEGF165 recognizes b1/b2 sites, therefore, Sema3A and VEGF165 compete for NP-1 binding (26). This competition leads to Sema3A to negatively regulate the activity of VEGF165/NP-1/VEGFR2 complex, by inhibiting endothelial proliferation, tubule formation, migration, and integrin expression (Fig. 5) (24, 25). Loss of Sema3A activity in favor of VEGF165 regulates the switch from monoclonal gammopathy of undetermined significance to multiple myeloma, whereas, overexpression of Sema3A reduces tumor growth (27-30). Narazaki and Tosato investigated how NP-1 receptor achieves opposite signaling via Sema3A or VEGF165, and demonstrated a mechanism for ligand prioritization, by which the ligand with higher affinity for NP-1 causes NP-1 internalization reducing surface NP-1 available for binding to the competitor ligand. In this work, they showed that VEGF165 preferentially binds and internalizes NP-1 compared to Sema3A, but requires VEGF receptors (31).

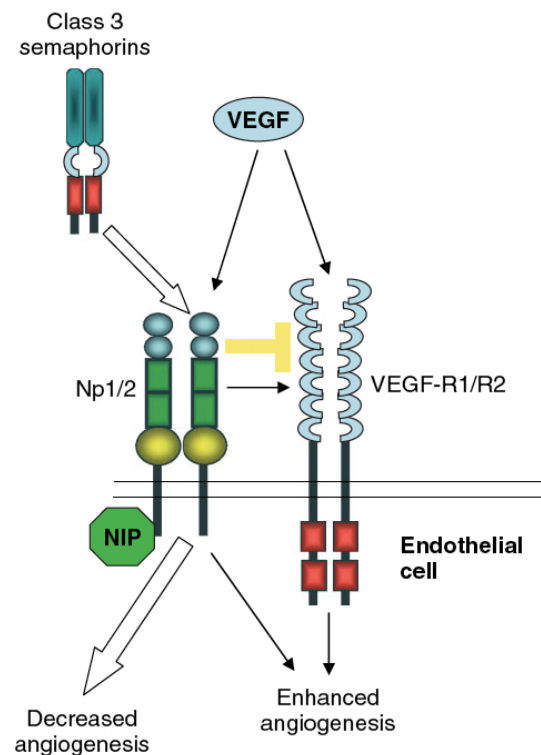


Figure 5 VEGF and class 3 semaphorins compete for binding to neuropilins. In endothelial cells, VEGF can bind to both NP-1 and VEGFR1/R2, causing enhanced signaling through VEGFR1/R2 as well as potential signaling through the NP-1 cytoplasmic domain. Class 3 semaphorins compete with VEGF for binding to NP-1, therefore preventing NP-1 from associating with VEGFR1/R2 and leading to inhibitory signals in the cell through neuropilin interacting protein (NIP), thus decreasing the angiogenic signal in two ways (adapted from Staton et al, 2007).

1.2 Modes of vascular growth

1.2.1 Sprouting angiogenesis

VEGF is the master regulator of new blood vessel sprouting during development, growth, and disease (1, 32, 33). In this mechanism of angiogenesis, VEGF precisely coordinates endothelial cells, selecting tip cells that migrate to lead the sprout, and stalk cells that proliferate to support the vessel growth. This vessel patterning depends on two features of the extracellular VEGF distribution by which VEGF regulates different cellular response by endothelial cells. The first is the VEGF gradient that induces migration of tip cells, and the second is the VEGF

concentration that regulates the proliferation of stalk cells (34). Moreover, VEGF cooperates with Notch family to determine the branching pattern of sprouting (35). The mammalian Notch signaling pathway is composed of four Notch receptor (Notch 1-4), and five ligands (Jagged 1 and 2, and Delta-like (Dll) 1,3, and 4) (36). The ligands are transmembrane-type protein and, therefore, Notch signaling is often mediated by cell-cell interaction (36). After ligand binding, Notch receptors undergo two proteolytic cleavages, upon which the intracellular domain is released and translocates to the nucleus where it activates the expression of target genes (37). In particular, Hellstrom and coworkers showed that Dll4-Notch1 signaling regulates the formation of appropriate numbers of tip cells to control vessel sprouting and branching (38).

Briefly, VEGF binds its cognate receptor VEGFR2, and promotes Dll4 expression in the tip cells that form filopodial extensions sensing and responding to guidance signals (Fig. 6) (33). Dll4 expressed by the tip cells activates Notch1 in the adjacent stalk cells, where Notch1 impedes VEGFR2 expression, while induces VEGFR1 and Dll4 expression (35). VEGFR1 works as VEGF trap preventing VEGF-VEGFR2 binding (39). Therefore, stalk cells have high Notch signaling, while low VEGFR2 activation compared to tip cells; Dll4 expression is stronger in tip cells and weaker in stalk cells (33). Stalk cells restricted Jag1 ligand competes with Dll4 to avoid Notch1 activation, and favors tip cell selection (40). However, Fringe family of glycosyltransferases can add sugar modifications to Notch1, repressing Jag1 binding to Notch1 in favor of Dll4 ligand (40). In addition, macrophage-derived VEGF-C has been described to activate VEGFR3 in tip cells to reinforce Notch signaling and promote the conversion of tip in stalk cells (41). The sprout by the

tip cells is accompanied by BM breakdown and pericyte detachment to provide space to the filopodia invasion. This vessel destabilization is achieved by disruption of Ang-1 signaling via the Tie2 receptor by the antagonist Ang-2 (35). Stalk cells do not migrate like the tip cells, instead they proliferate and support the extension of sprouting vessels and the connection to the collateral vessels (33). The sprout continues till tip cell connects with adjacent vessels and undergo to anastomosis, which leads to the fusion of the contacting capillaries. Following, BM deposition, pericytes recruitment, endothelial cells polarization, and lumen formation events determine the formation of mature and functional vessels (35).

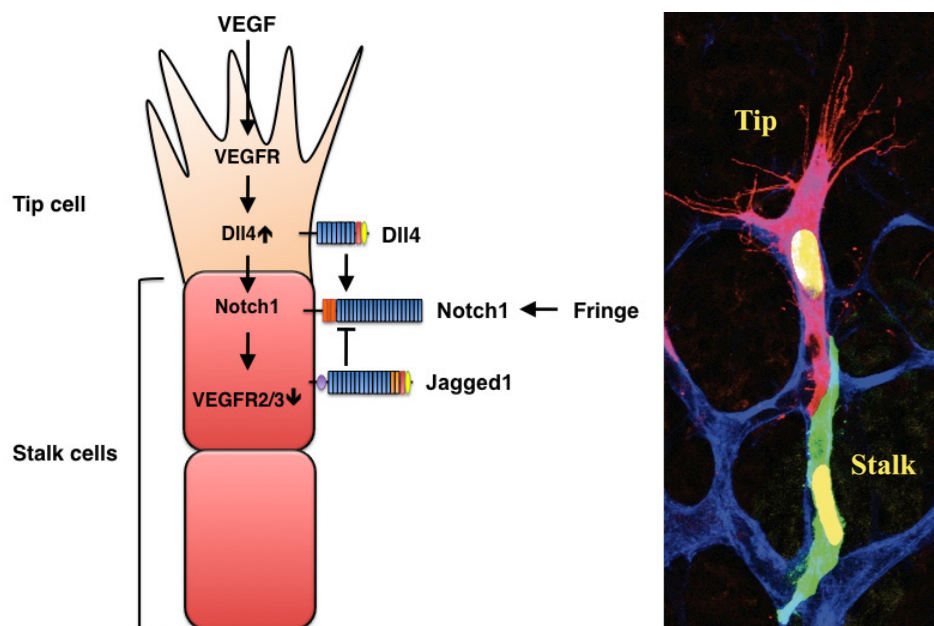


Figure 6 A) Dll4 and Jagged1 have opposite effects on sprouting angiogenesis. VEGF signaling triggers Dll4 expression in tip cells, and Dll4, in turn, activates Notch signaling in stalk cells, which reduces stalk-cell sensitivity to VEGF stimulation and, therefore suppresses the tip-cell phenotype. Contrary, Jagged1 antagonizes Dll4-mediated Notch activation in stalk cells to increase tip cell numbers and enhances vessel sprouting. The antagonistic activity of the two ligands is controlled by Fringe-dependent modulation of Notch signaling (adapted from Kume et al., 2012). B) Fluorescent laser scanning photomicrograph of an angiogenic sprout in retina (adapted from Benedito et al, 2013).

1.2.2 Intussusception angiogenesis

Intussusception angiogenesis (IA) means “growth within itself” and was first observed in the rapidly expanding lung capillary bed of neonatal rats and then identified in various organs such as heart, endometrium, eye, kidney, and yolk sac (42, 43). The chicken chorioallantoic membrane (CAM) is an organ assay suitable for prolonged videomicroscopy and allowed to characterize IA mechanism that consists of 4 phases: 1) protrusion of opposing capillary walls into the lumen and the formation of a contact zone between the endothelial cells 2) rearrangement of the intercellular junctions and central perforation of the endothelial bilayer 3) invasion of interstitial pillar core formed by supporting cells and deposition of matrix 4) enlargement in girth and fusion of the pillars (Fig. 7) (42, 44). The direction taken by the pillars delineates IA into three phases namely: 1) intussusceptive microvascular growth that result in increase capillary surface area 2) intussusceptive arborization that form the typical tree-like vascular arrangement 3) intussusceptive branching remodeling that remodels the vasculature to meet the local demand (44).

IA occurs during vascular development following vasculogenesis and sprouting, and in adult life both in physiological and pathological situations, for example exercised muscles and tumorigenesis, respectively (45, 46). It is believed that hemodynamic changes are crucial in IA (4). In fact, Djonov and coworkers showed that blood flow enhanced the formation of new pillars by IA (4). Blood flow within the vessels results in an increase of shear stress that can be laminar, thus acting tangentially to the endothelium surface, or oscillatory, i.e. turbulent (4).

Endothelial cells can sense changes in shear stress and transduce hemodynamic signals into biological ones (47). Endothelial cells respond by modifying the expression of some proteins, for example endothelial cell nitric oxide synthases (eNOS), adhesion molecules, and angiogenic factors (42). Laminar shear stress is in general associated with intussusception, while oscillatory with sprouting angiogenesis (4). Besides hemodynamic factors, computer simulations have emphasized that signaling pathways may also play a role in intussusception, in particular during the process that entails the pillar formation (44). However, so far the molecular mechanisms controlling intussusception are still poorly understood compared to sprouting, mostly due to a paucity of appropriate models (48).

In our group, we have recently demonstrated that over-expression of the matrix binding VEGF₁₆₄ at two different supra-physiologic doses in skeletal muscle by a cell-based gene transfer system, induces vascular enlargement with robust endothelial proliferation in the absence of migrating tip cells, followed by transluminal pillar formation and intussusceptive remodeling (48). The mechanisms underlying this vascular remodeling by vascular splitting, rather than sprouting, are under investigation. We have first analyzed the role of Notch1 signaling in intussusception, knowing that its alternate ‘salt and pepper’ activation is responsible of the proper number of tip and stalk cells in sprouting. Interestingly, we have observed that Notch1 is homogeneously expressed by contiguous endothelial cells during vascular remodeling induced by VEGF overexpression dose, assuming an “all-stalk” phenotype (Gianni-Barrera et al., manuscript in preparation). Based on these results, it is tempting to assume that the pattern of the same signaling may differ between sprouting and

intussusception as consequence of, for example, different VEGF doses and shapes of its gradient (13) (Gianni-Barrera et al., manuscript in preparation).

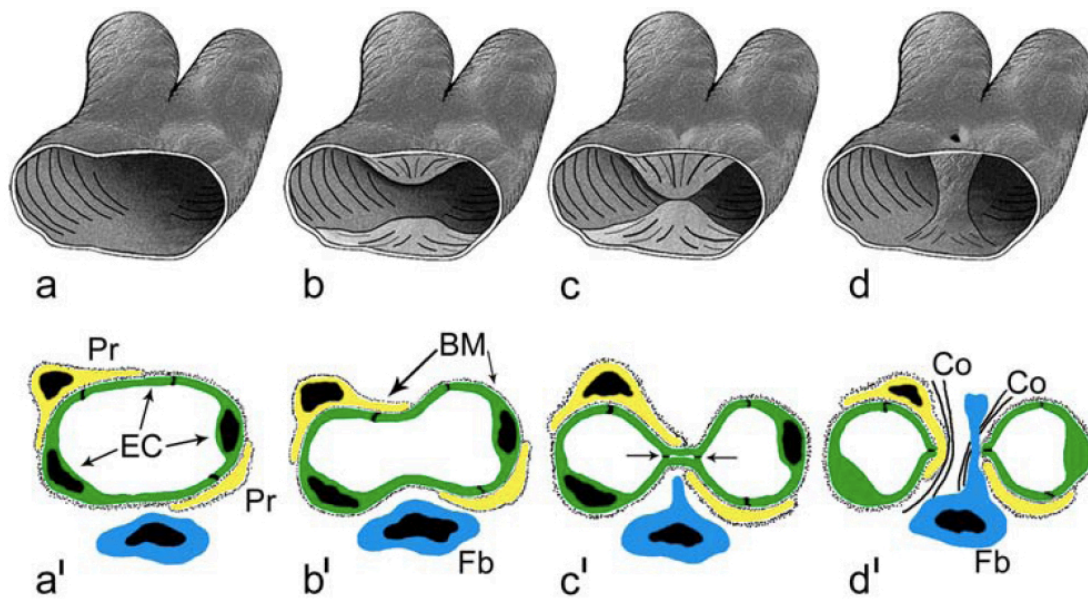


Figure 7 Mechanisms involved in pillar formation. Three-dimensional schema illustrating the steps in the formation of transluminal pillars during intussusceptive angiogenesis (a–d). The process starts with the protrusion of portions of the walls from opposite sides into the vessel lumen (a–b). After contact has been established, the endothelial bilayer becomes perforated centrally and a transluminal pillar is formed (c–d). Two-dimensional representation of the events depicted above (a'–d') (adapted from Makanya et al, 2009).

2. Mechanisms of vascular maturation and stabilization

2.1 Vascular maturation

To become functional, vessels newly formed must mature at the level of the vessel wall and as well as at the network level (35, 49). In regard to vessel wall, a fundamental feature of vessel maturation is the recruitment of mural cells, pericytes in capillaries and vascular smooth muscle cells in arteries and veins (Fig. 8). At the network level, vascular maturation means an optimal capillary remodeling into a hierarchically branched network that respond to local tissue needs (49).

2.2 Vascular stabilization

After maturation, vessels undergo to stabilization through the onset of blood flow, the integration of mural cells into the vascular wall, and the deposition of perivascular extracellular matrix, in particular the vascular basement membrane (33, 50). This phase defines the transition from an actively growing vascular bed to a quiescent, fully formed, and functional network that is independent of pro-angiogenic factor stimulus withdrawal (33). Hemodynamic changes play a critical role for determining the vessel fate, proved by the fact that decrease or cessation

of blood flow may cause vessel regression (51). However, there are strong evidences that support also an autonomous fate control achieved by vessels (33, 51). The tight juxtapositions of pericytes with endothelial cells, for example the occurrence of synapse-like peg pocket contacts, allow them signaling to the endothelium (Fig. 8) (50). These heterotypic interactions induce specific molecular events that control vascular stabilization by affecting basement membrane matrix synthesis and deposition, recognition of the ECM through differential integrin expression, and protection of the basement membrane matrix from metalloproteinase activity (52). However, nowadays, there is still conflicting literature in regard to the fact that pericytes per se prevent vessel regression. This dilemma may be due to problems with pericyte identification and heterogeneity in the pericyte population (50).

2.3 Pericytes: heterogeneous but unique cells

Pericytes are vascular smooth muscle lineage unique by their distribution and relationship with BM and by the type of contacts formed with the endothelial cells. In fact, differently from the vascular smooth muscle cells, pericytes are embedded within the endothelial BM to whose deposition they also contribute (53, 54). Moreover, pericytes signal to the endothelial cells in a paracrine manner, while vascular smooth muscle cells provide mechanical support to the endothelium wall in the microvessels (Fig. 8) (50, 51). The pericyte coverage of the abluminal vessel area of the endothelium is partial, ranging from around 10% to 50% according to type of the vascular bed. This difference reflects a variation in

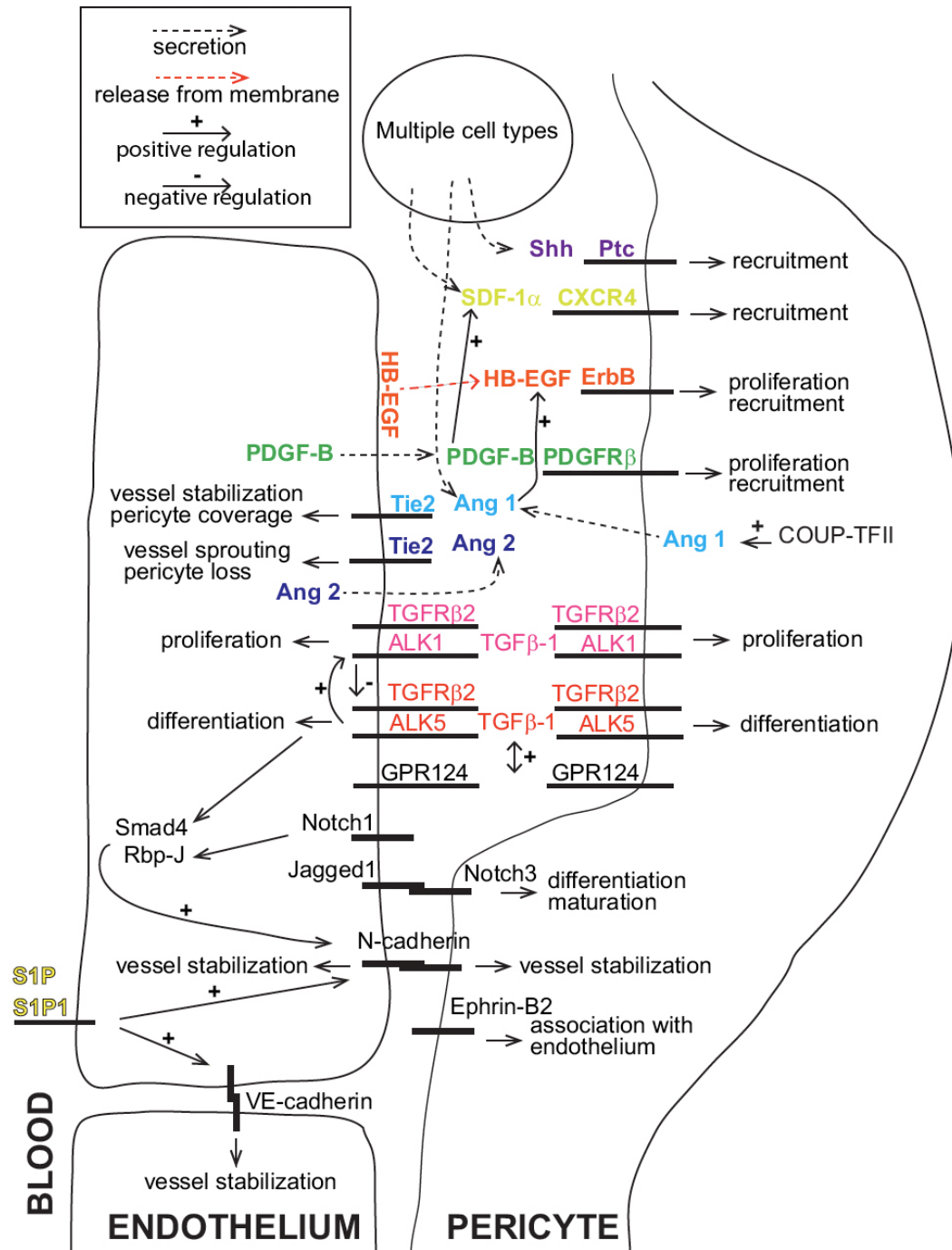


Figure 8 Signaling pathways mediating mural cell recruitment, differentiation, and endothelium-pericyte interaction to achieve vascular maturation and stabilization (adapted from Armulik et al 2011).

the pericyte relative frequency and morphology. The frequency of pericytes varies from 1:100 in skeletal muscles to 1:1 in the retina. The morphology of the pericyte/endothelial interface reflects the vessel function. For instance, pericytes of the central nervous system (CNS) are flattened or elongated, stellate-shaped

solitary cell with multiple cytoplasmic processes encircling the capillary endothelium, whereas those of mesangial kidney glomerulus, are rounded, compact, and contacting a minimal abluminal vessel, while making only focal attachments to the BM (53, 54). This morphological heterogeneity of pericytes is associated with diversity also at molecular levels, in fact, several markers are used to identify pericytes, and none of them, is absolutely specific for pericytes (50, 53, 54). Pericytes on normal capillaries typically express desmin, but not alpha smooth muscle actin (55). Similar to vascular smooth muscle cells, pericytes have different origins, in fact, pericytes that populate CNS and thymus are originated from ectoderm-derived neural crest, while those that reside in coelomic organs come from mesoderm-and mesothelium (53). In regard to cell plasticity, pericytes can differentiate to vascular smooth muscle cells, but not only. Several studies have recently proved that pericytes have multipotent stem cell features, because they are able to differentiate into osteoblasts, myofibers, adipocytes, and even neurons (56, 57).

Several works in development and adult models have demonstrated that Platelet Derived Growth Factor-BB and its receptor (PDGF-BB and PDGFR β , respectively) pathway has a key role in recruiting pericytes (53).

2.3.1 PDGF ligands and receptors

In 1979, Platelet Derived Growth Factor (PDGF) was described to stimulate the proliferation of fibroblasts, arterial smooth muscle cells, and glial cells. PDGF family includes PDGF-A, -B, -C and -D isoforms that share a conserved growth factor domain in the cysteine knot fold that is related to vascular endothelial

growth factors (VEGFs) as well, and is primarily responsible for recruiting receptors (58). Except the growth factor domain, there are significant sequence and domain variations among PDGFs. The tails of PDGF-A and PDGF-B are both rich in positively charged amino acids such as arginine and lysine, and are involved in retention and distribution by binding to heparin/heparan sulfate proteoglycans (59). Instead, PDGF-C and PDGF-D lack the tail sequences. PDGF folding structure forms homodimers or heterodimers, for example PDGF-BB and PDGF-AB (58). There are two types of RTKs for PDGFs, PDGFR α and PDGFR β , which have different expression patterns and physiological roles. Particularly strong expression of PDGFR α has been noticed in subtypes of mesenchymal progenitors in lung, skin, and intestine, and in oligodendrocyte progenitors. PDGFR β is expressed by perivascular mesenchymal cells likely representing vascular mural cell (vascular smooth muscle cells and pericytes) progenitors (60). PDGF signaling through PDGFRs utilizes the general strategy for RTKs, which involves ligand-induced receptor dimerization, and the subsequent receptor conformational changes that are coupled to the activation of intracellular tyrosine kinase domain (58).

2.3.1.1 PDGF-BB/PDGFR β signaling in embryonic vascular development

The physiological function of this PDGF-BB/PDGFR β signaling was assessed with a large number of genetic studies in mice. *Pdgfb* and *pdgfrb* knockout mice showed a lack of pericytes, endothelial hyperplasia, abnormal junctions, and excessive luminal membrane folds (Fig. 9). Similar results were obtained upon endothelium specific ablation of *pdgfb*, suggesting that PDGF-BB expressed by endothelial cells

is necessary for mural cell recruitment. In addition, the deletion of the retention motif of pdgfb to ECM, caused pericytes to detach from the endothelium wall, revealing that PDGF-BB has a short-range action and its diffusion in the tissue is regulated by binding to ECM (61). Therefore, similarly to what previously discussed with VEGF, the spatial distribution of PDGF-BB defines its biological activity. Taken together, these findings suggested a model in which PDGF-BB secreted from endothelial cells interacts with heparan sulfate at the endothelial surface or in the periendothelial matrix (60). This would lead to local deposits of PDGF-BB, which, in turn, are critical to enroll pericytes and achieve a correct vessel coating (60, 61).

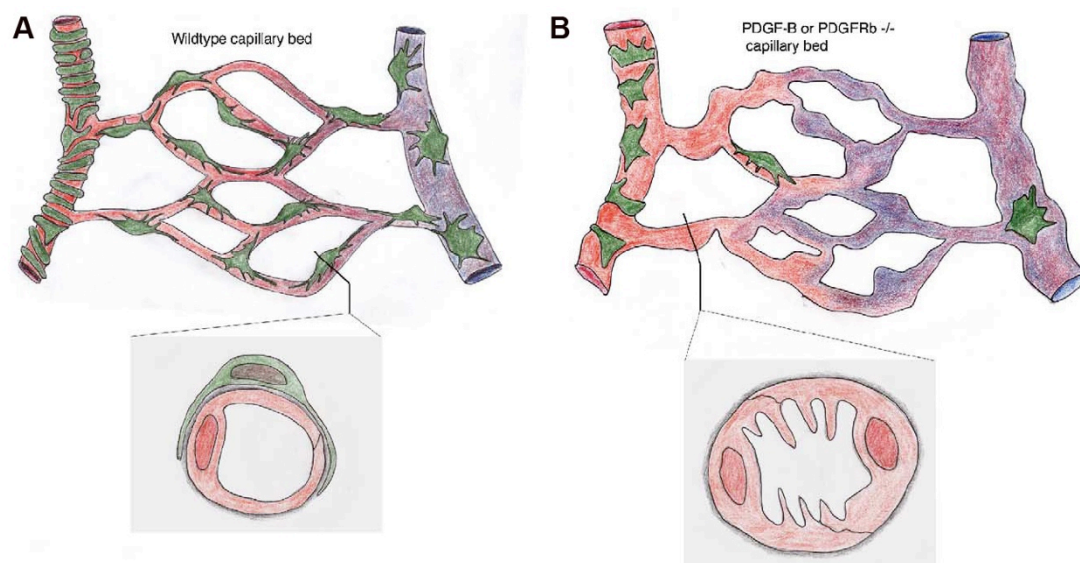


Figure 9 Consequences of pericyte deficiency in the pdgfb or pdgfrb deficient state causes very few pericytes (green) recruited into the capillary bed, but also a shortage of mural cells around the arterioles and venules. Moreover, the pericyte-deficient microvascular bed has an irregular capillary diameter. At the ultrastructural level, this correlated with endothelial hyperplasia and an oversized, folded luminal membrane. Functionally this microvascular bed is compromised and there are signs of decreased flow and increased hypoxia in the surrounding tissue, as illustrated by the irregular distribution of oxygenated (red) versus oxygen-depleted (blue) blood (adapted from Betsholtz et al, 2004).

2.4 Pericyte-endothelium paracrine signals

Vascular maturation and stabilization requires the interaction between endothelial cells and pericytes, as suggested by the anatomical relationship of these cells. Several paracrine signals determine pericyte-endothelium crosstalk, for example via specific RTK signaling (Fig. 8) (53).

2.4.1 *TGF- β family and its receptors*

Tumor-secreted factor- β (TGFB1-3) is a member of a large family of evolutionary conserved secreted cytokines, which includes also activins, inhibins, nodals, anti-mullerian hormone (AMH), and bone morphogenetic proteins (BMPs) (2). Signaling by these cytokines converges to five type II and seven type I serine/threonine kinase receptors located at the plasmamembrane, and two main Small Mother Against Decapentaplegic (SMAD) transcription factors, which have a pivotal role in intracellular signaling (Fig. 10) (2, 62). The type I receptor, named activin receptor-like kinases (ALKs), form heterodimer with type II receptors and act downstream of them. Besides, accessory receptors, i.e. endoglin and betaglycan, have been identified to regulate the access of TGF- β family members to the cognate receptors. TGF- β family members work in a highly contextual manner with pleiotropic effects due to the fact that TGF- β receptors are expressed by several types of cells like, for example, endothelial cells and mural cells (pericytes and smooth muscle cells) (62). Experiments with null mice for different members of TGF- β signaling have provided evidences that TGF- β signaling is essential for regulation of vasculogenesis and angiogenesis (63).

Moreover, studies in human corroborated the importance of TGF- β signaling in vascular function. In fact, mutations in TGF- β family genes, which lead to missregulated TGF- β signaling, result in vascular pathologies, such as arteriovenous malformations (AVMs), aneurysms, hypertension, atherosclerosis, and cardiovascular disease (2).

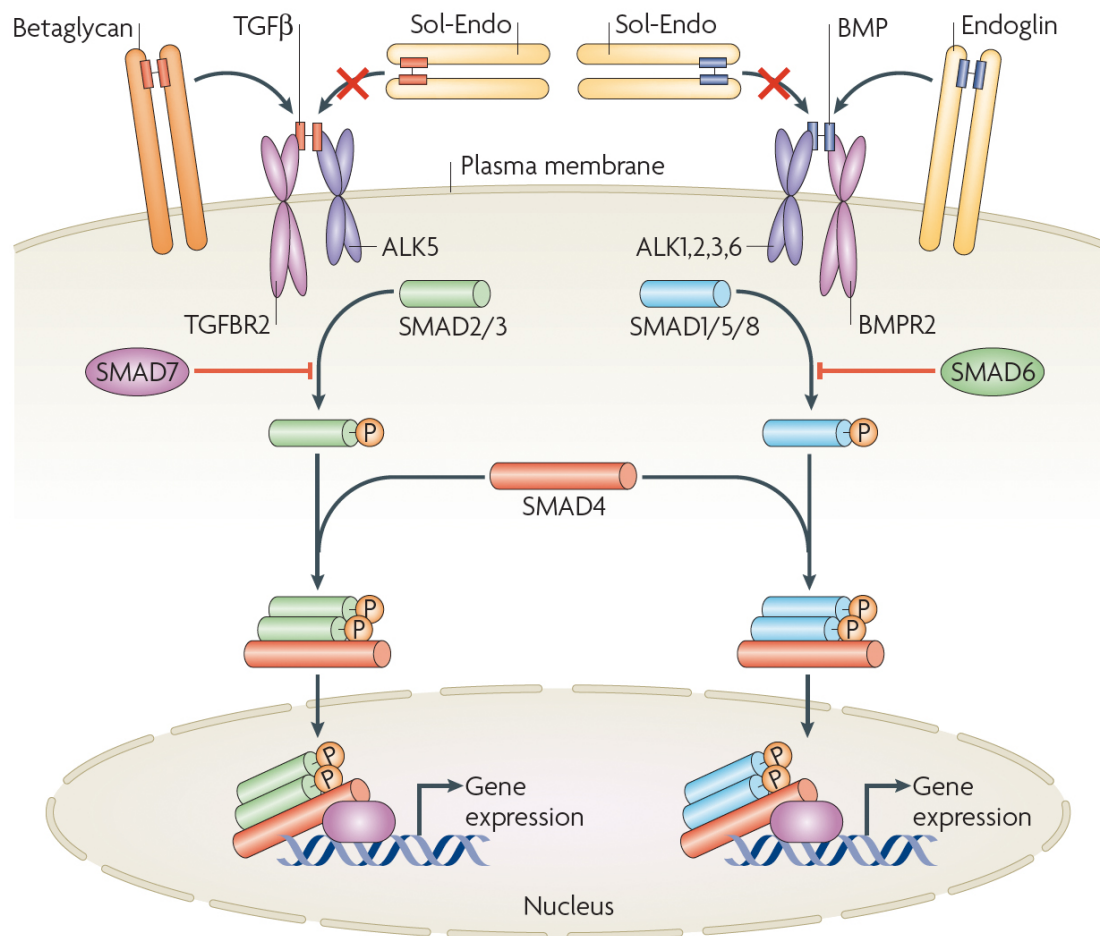


Figure 10 Signal transduction by TGF- β family members. TGF- β and BMP dimers induce heteromeric complex formation between specific type II and type I receptors. The type II receptors then transphosphorylate the type I receptors, leading to their activation. Subsequently, the type I receptor propagates the signal into the cell by phosphorylating receptor-regulated (R)-Smads, which form heteromeric complexes with Smad4 (common (Co)-Smad) and translocate in the nucleus where by interacting with other transcription factors regulate gene transcriptional responses (canonical Smad signaling pathway) (adapted from ten Dijke et al, 2007).

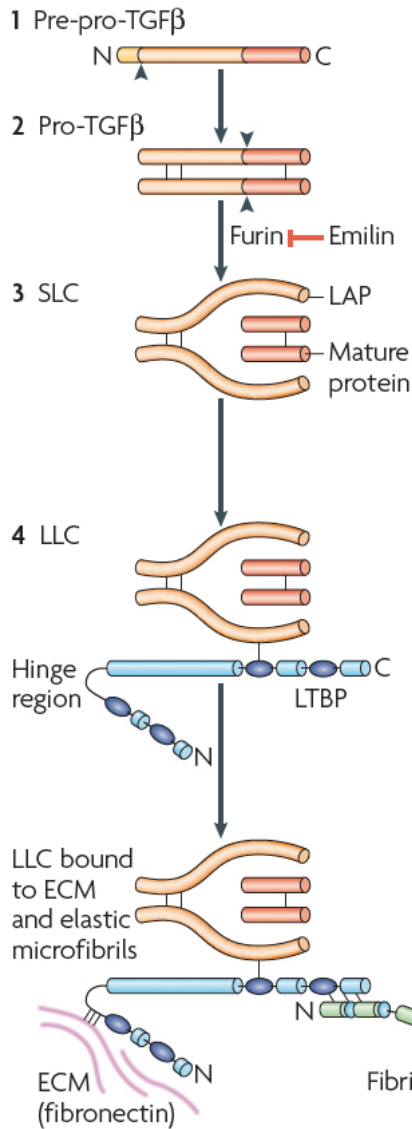
2.4.1.1 TGF- β activation

ECM has a crucial role not only for physical support for cells and tissues, but also as an information-rich structure by and through which cells receive and transmit signals, mainly via integrin that allow to the cells to adhere to ECM and growth factors (GF). TGF- β signaling is an example of how integrin, ECM, and GF function are linked (Fig. 11) (64). The prototypic family member TGF- β is secreted as an inactive latent dimeric precursor consisting of TGF- β and a latency associated peptide (LAP) to form the small latent complex (SLC). The SLC associates with the large latent TGF- β binding protein (LTBP) by covalent attachment to form the large latent complex, LLC. LLC is anchored to ECM through the N-terminal and C-terminal of LTBP by covalent and non-covalent bounds, respectively (62). TGF- β gets activated by proteolytic cleavage of LAP and LTBP by thrombospondin, plasmin, reactive oxygen species, acidic microenvironment, matrix metalloproteinases (MMP2 and 9), and β 6 integrin (65). Notably, the inactivation of genes that encode putative activators of TGF- β causes phenotypes that resemble mice deficient in TGF- β signaling components, suggesting that the extracellular activation of TGF- β is key step to achieve TGF- β signaling in vivo (62).

2.4.1.2 TGF- β /TGF β R signaling in endothelial cells

Several divergent and contradictory responses of endothelial cells to TGF- β have been reported (66). This discrepancy is due to a number of factors which significantly alter how endothelial cells react to TGF- β , like for example cellular density, TGF- β concentration, duration of treatment, presence of serum components, surrounding matrix, micro/macrovessel origin of endothelial cells

a Synthesis and secretion



b Activation and receptor binding

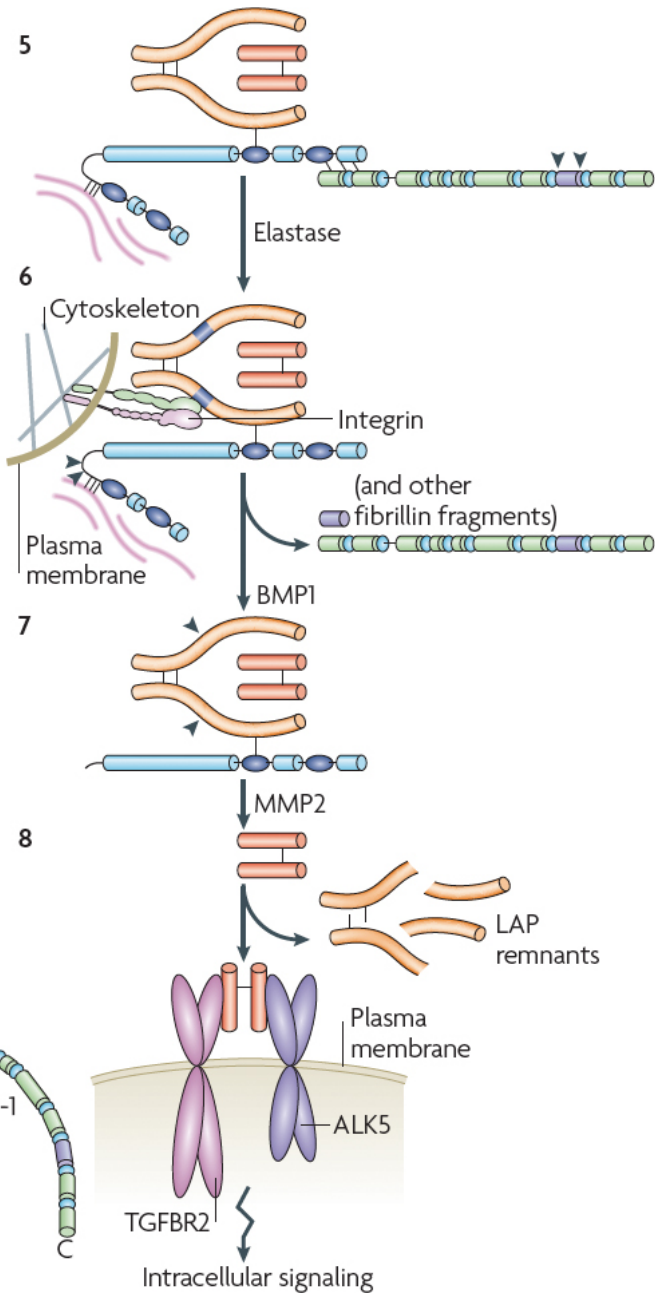


Figure 11 Regulation of TGF- β bioavailability. TGF- β and LAP are proteolytically separated, and after processing, TGF- β remains non-covalently associated with LAP to form the small latent TGF- β complex (SLC) (1-3). LAP and LTBP are joined by disulfide bonds and create the large latent TGF- β complex (LLC)(4). The LLC is covalently linked to the ECM through an isopeptide bond by the N-terminus of LTBP, and to the N-terminal region of fibrillin-1 via non-covalent interaction by the C-terminal region of LTBP (4). LAP can be activated through binding of $\alpha\beta 6$ and $\alpha\beta 8$ integrins to the RGD sequence in LAP. The mechanism is unclear, but interaction with the RGD domain of LAP may induce a conformational change that leads to liberation or exposure of TGF- β (6). The hinge domain (black arrowheads) of LTBP is a protease sensitive region that allows LLC to be proteolytically released from the EC. Bone morphogenetic protein-1 (BMP-1) can cleave two sites in the hinge region of LTBP, which results in the release of LLC (7). Matrix metalloprotease-2 (MMP-2) (and other proteases) can cleave LAP to release the mature TGF- β (8). Mature TGF- β can then bind to its cognate receptors, TGFR2 and ALK5 (adapted from ten Dijke et al 2007).

and also species derivation. However, today it is well accepted that the inhibitory effects of TGF- β on endothelial cells migration and proliferation are mediated by the TGF- β /ALK5/Smad2/3 signaling pathway.

In contrast, TGF- β signaling via the TGF- β /ALK1/Smad1/5 leads to proliferation and migration. The bioavailability of active TGF- β is crucial, because low extracellular TGF- β doses induce ALK1 signaling, while high levels trigger ALK5 (63). In the endothelial cells, the biological activity of TGF- β signaling can be modulated by presence or absence of other mediators (66). For instance, VE-cadherin deficient endothelial cells caused a loss of TGF- β -induced inhibitory effects on both cell migration and proliferation (67). In addition TGF- β interacts with other key pathways, such as VEGF, by shifting VEGF signaling from prosurvival to proapoptotic (68). TGF- β cooperates also with Notch to regulate N-cadherin expression, an adhesion molecule that determines heterotypic contacts between endothelium and mural cells (69).

2.4.1.3 TGF- β /TGF β R signaling in mural cells

Several *in vitro* and *in vivo* studies have demonstrated that TGF- β signaling is necessary not only for endothelium behavior, but also for mural cell differentiation and function (63). In fact, co-culture of endothelial cells and 10T1/2 mesenchymal cell line (pericyte-like cells) showed impaired endothelium and pericyte assembly, defective mural cell differentiation, increased apoptosis of endothelial cells, and reduced capillary-like structures formation when TGF- β signaling was abrogated (70, 71). In line with this, genetic studies in mice revealed impaired mural cell differentiation and recruitment, and enlarged and tortuous

vessels, by deleting specific components of TGF- β signaling (66). Notably, in order to signal via TGF- β /TGF β R, endothelial cells and pericytes require a juxtaposition and communication that allow to activate TGF- β , for example through gap junctions (72, 73).

2.4.2 Tie receptors and their Ang-1 and Ang-2 ligands

Tunica internal endothelial cell kinase 1 and 2 (Tie1 and 2) receptors are single transmembrane molecules that have an extracellular ligand-binding domain and split intracellular Tyr kinase domain. Tie2 is constitutively expressed in endothelial cells, while Tie1 is strongly regulated. The Tie receptors are expressed also by circulating haematopoietic cells, in particular by a population named tumor associate macrophages (TEM) (74). Ang sequence includes an N-terminal Ang-specific superclustering domain, which contains Cys molecules followed by a coiled-coil domain, a linker peptide and a carboxy-terminal fibrinogen-homology domain (Fig. 12). The fibrinogen-homology domain mediates receptor binding, whereas the coiled-coil domain is required for dimerization or oligomerization. The linker peptide allows Ang-1 to be sequestered into the ECM (75). Ang-1 and Ang-2 bind Tie2 with similar affinities and in the same site. Differently from Tie2, Ang ligands have distinct expression pattern. Ang-1 is expressed by periendothelial cells, fibroblasts, and other types of non-vascular normal and tumour cells, and is present in the blood of healthy people, but is upregulated in angiogenesis. Instead, Ang-2 is expressed by endothelial cells only upon stimuli like hypoxia, shear stress, and VEGF, or in some pathological conditions. Ang-2 can

be stored in specific vesicles named Weibel-Palade bodies that are secreted upon thrombin or vasopressin stimulation (74).

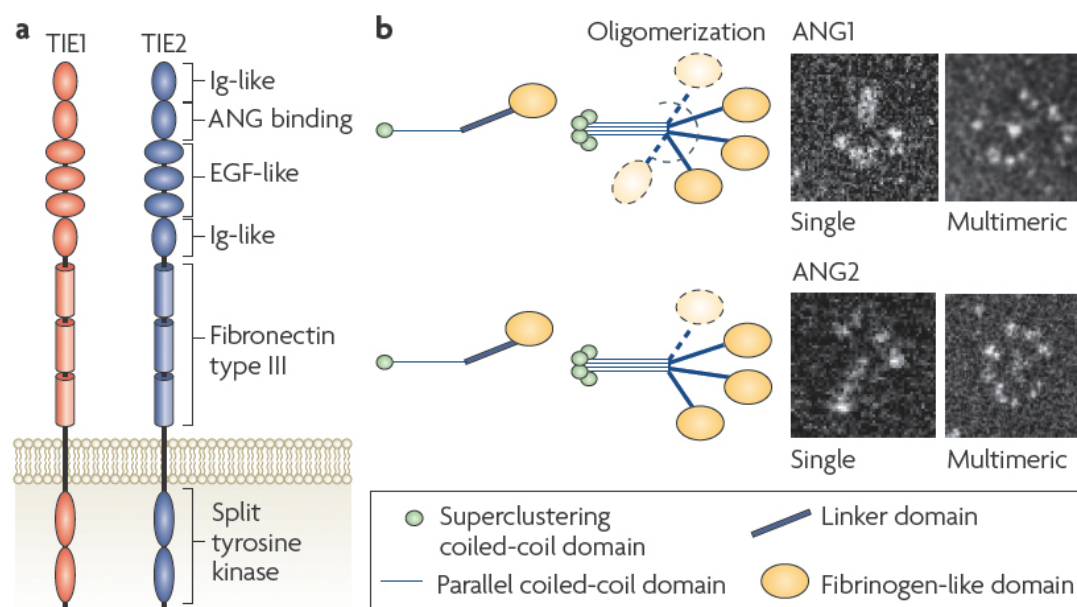


Figure 12 Structural properties of the Tie receptors and the angiopoietin ligands. Tie receptors are single membrane receptor Tyr kinases that consist of an amino-terminal angiopoietin (Ang)-binding domain and a carboxy-terminal split Tyr kinase domain. The Ang ligands are soluble secreted proteins that consist of an N-terminal coiled-coil domain and a C-terminal fibrinogen-like domain. The molecules oligomerize through the parallel coiled-coil domain, which contains additional coiled-coil domain sequences that supercluster in the end of the N-terminal domain. Tie2-receptor binding occurs through the fibrinogen-like domain. The electron microscopic images show variable oligomeric three-dimensional structures of recombinant Ang-1 and Ang-2 using the rotary shadowing technique (adapted from Augustin et al, 2009).

2.4.2.1 Angs/Tie signaling in embryonic vascular development

Genetic studies in mice allowed understanding the biological significance of Angs/Tie signaling in vascular development. Ang-1 and Tie2 global gene depletion prevented the development of the primary capillary plexus and the existing vessels appeared dilated and showed a poor connection of endothelial cells with ECM and pericytes (75). The deletion of Tie1 and Ang-2 gene was compatible with embryonic development, despite some vascular defects were noticed (74). Ang-2 overexpression gave rise to a phenotype which recalled the effects observed in

Ang-1 and Tie2 null mice, while Ang-1 overexpression displayed a highly organized vascular architecture with a drastic permeability reduction (75-77). These results suggested that Angs/Tie2 signaling is important in vascular development and Ang-1 and Ang-2 likely act as antagonists (74).

2.4.2.2 Angs/Tie signaling activation

Further *in vitro* and *in vivo* studies defined the role of Tie2 and its ligands in adult angiogenesis. It is now clear that the competition of Ang ligands to Tie2 receptor induces opposite effects on vessels. Upon pro-angiogenic stimuli, Ang-2 destabilizes quiescent vasculature causing the mural cell detachment (74). Ang-1 assembles on endothelial cells distinct Tie2 signaling according to their status, quiescent or activated. This differential action is favored by two mechanisms of Ang-1 presentation to Tie2 receptor, i.e. trans (cell to cell) or cis (ECM to cell). When cells are quiescent, trans-endothelial cell exposure of Ang-1 to Tie2 leads cell survival and cell-cell adhesion. Instead, the cis presentation of Ang-1 anchors Tie2 to ECM, and causes the activation of focal adhesion kinase (FAK). The activated FAK induce endothelial cell to migrate, proliferate, and form highly organized and branched vessel network that undergo maturation (78). Ang-1 induces endothelial cells to proliferate circumferentially, rather by sprouting, via Apelin signaling, at least during a critical developmental period (74, 79). Apelin is a protein secreted by endothelial cells under the activation of Tie2, and plays a role in the regulation of caliber size of blood vessel through its cognate receptor APJ, which is also expressed on endothelial cells (80). In addition, some publications support the idea that Ang-1 recruits, directly or indirectly, pericytes to the area of

vessels newly induced, however, this point is controversial (35, 53). It is more likely that Ang-1 promotes pericyte-endothelium adhesion by tightening cell junctions that reduce vascular permeability (35).

2.4.3 Eph receptors and their Ephrin ligands

The erythropoietin-producing hepatocellular (Eph) receptor family constitutes the largest family of tyrosine kinase receptors in mammals, including 14 members (81). The correspondent ligands, the ephrins, are divided in A-subclass, which are linked to the cell membrane by a glycosylphosphatidylinositol (GPI), and B-subclass, which are transmembrane protein with a short cytoplasmatic region (Fig. 13). The receptors are also categorized in subclass A (9) and B (5), based on their sequence similarity and ligand affinity. Despite this subdivision, some promiscuity of receptor-ligand binding occurs between the two subclasses and within the same subclass (82). Differently from the other RTK pathways, Ephrin/Eph interaction activates a bidirectional signaling, i.e. the ligand binding induces forward signaling through phosphotyrosine-mediated pathway, but the ligand can also signal to the host cell by reverse signaling. Since both receptor and ligand are membrane bound, this signaling requires cell-cell contact. In addition, Eph receptors are activated only when they are bound by clustered, membrane-anchored ephrin ligands. Eph signaling is initiated by autophosphorylation followed by the recruitment of adaptor protein that triggers phosphorylation of downstream substrates to regulate cytoskeleton, mitogenesis, and cell-substrate interaction (adhesion) (81). Instead, B Ephrins do not possess intrinsic catalytic activity, therefore, they recruit other proteins that phosphorylate specific tyrosine

residues in their intracytoplasmic domain to regulate cytoskeleton dynamics and motility (82). It has been shown that B Ephrins can control cell morphology and motility also independently of Eph-receptor bindings (83).

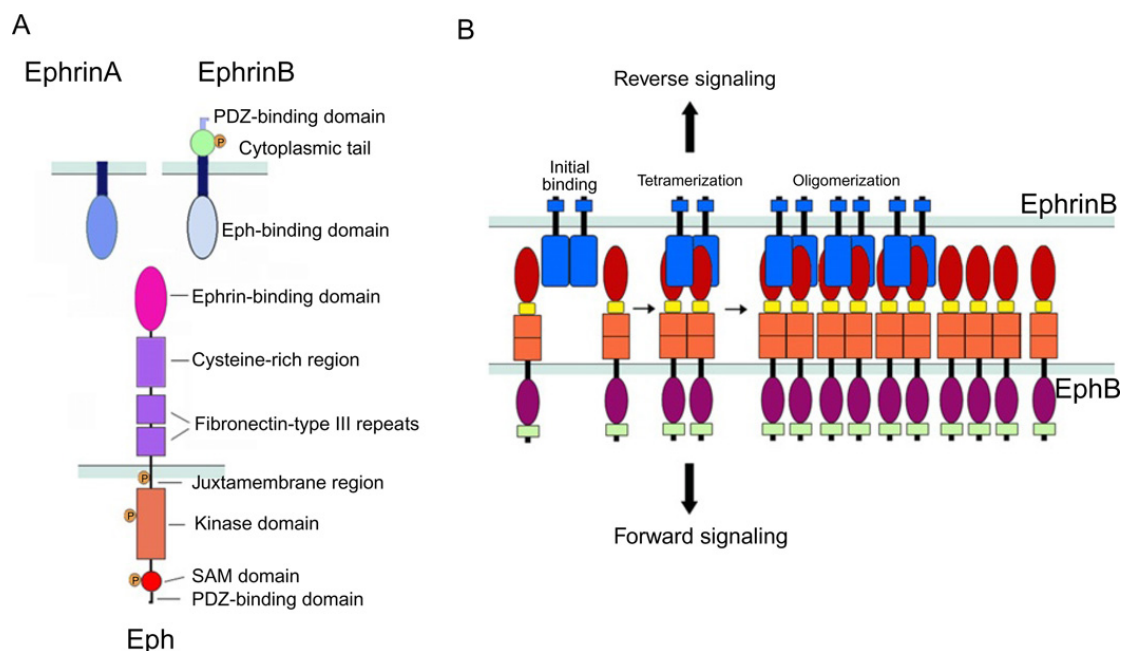


Figure 13 (A) Schematic representation of the domain structure and binding interfaces of Ephrins and Eph receptors. EphrinA ligands are attached to the cell surface through a glycosylphosphatidylinositol (GPI)-anchor; the extracellular domain contains an Eph receptor-binding domain that is connected to the transmembrane segment. EphrinB ligands are transmembrane proteins with an extracellular Eph receptor-binding domain linked to a transmembrane segment, which is followed by a short intracellular domain. The Eph receptors consist of an extracellular domain composed of an Ephrin-binding domain, a cysteine-rich segment that contains an epidermal growth factor (EGF)-like motif, and two fibronectin-type III domains; and a cytoplasmic region that contains a juxtamembrane region, the kinase domain, a sterile a-motif (SAM), and a binding site for PDZ-containing proteins. (B) Representation of initial binding of cell surface Eph and Ephrin molecules to form heterotetramers, which initiate signaling, and subsequent oligomerization to form large receptor/ligand clusters that expand laterally through hemophilic interactions between Eph receptors (adapted from Salvucci et al, 2012).

2.4.3.1 Vascular distribution of EphB4 receptor and EphrinB2 ligand

EphrinB2/EphB4 is one the most specific Ephrin ligand/Eph receptor binding because EphB4 essentially recognizes only EphrinB2 (81). EphB4 receptor and EphrinB2 ligand are expressed by endothelial cells and determine the artery and vein specification during development based on a segregation mechanism regulated by EphrinB2/EphB4 interaction (84, 85). Expression of EphrinB2 and

EphB4 is not limited to arterial/vein boundaries, instead is extended to capillaries in the adult (81). Pericytes and smooth muscle cells also express EphrinB2 in embryonic and adult vasculature (84, 86-88). Despite the complexity of EphrinB2/EphB4 signaling, it has been demonstrated that it plays a crucial role in regulating embryonic and adult angiogenesis (81).

2.4.3.2 EphrinB2/EphB4 signaling in embryonic vascular development

Genetic experiments with mice showed that the global deletion of either EphrinB2 or EphB4 caused detrimental effects on vascular system that blocked at the primitive capillary plexus, did not remodel, and mice died at midgestation (84, 89). In addition, endothelial-cell-specific EphrinB2 knockout as well as mutant lacking the cytoplasmic domain of EphrinB2 recapitulated the vascular phenotypes of the ephrinB2^{-/-} null mice (90, 91). Similarly, the overexpression of EphrinB2 in the endothelium prevented the normal embryonic vascular development, although mice were viable (92). Taken together, these results suggested that EphrinB2 reverse and EphB4 forward signaling may be required for proper morphogenesis and patterning of the vascular system, and in particular that EphrinB2 signal may have dosage-dependent function in endothelial cells (91). Interestingly, also mural-cell-specific EphrinB2 knockout mice presented hemorrhaging vasculature and died. In this case, mural cells were recruited to the endothelium wall, but were scattered and resulted in incomplete vessel coverage (88).

2.4.3.3 EphrinB2/EphB4 signaling in physiological and pathological angiogenesis

Besides in vascular development, EphrinB2/EphB4 signaling acts in physiological and pathological processes, which have been mostly addressed in retina sprouting and tumor. Interestingly, EphrinB2 was found to be highly expressed in tip cells where its reverse signaling regulates VEGFR2 internalization that determines the formation of sprouting. In tumor, the function of EphrinB2/EphB4 signaling is more complex given that certain tumor cells express EphB4 (81). In cancer such as breast and squamous cell carcinoma, the activation of EphB4 by EphrinB2 ligand decreases tumor growth by preventing endothelial cell proliferation and normalizing vasculature (93, 94). Conversely, in other cancers such as bladder and melanoma tumor, the activation of EphB4 induces tumor migration and survival (95, 96). A possible explanation for this contradictory results, it might be the difference in concentration or clustering of EphB4 and EphrinB2, or the loss of receptor and ligand dependent functions (81).

2.5 Accessory cells in angiogenesis

Bone marrow-derived cells, predominantly with haematopoietic features, have been described to participate to angiogenesis (97). The expression of chemotactic signals can recruit bone marrow-derived precursors that differentiate into endothelial and mural cells and assemble new vessels (97-99). Instead, other cells of the haematopoietic lineage can be enrolled, maintained in a perivascular position, and favor angiogenesis in a paracrine fashion (97). In the latter situation,

different bone marrow-derived myeloid cell subsets have been discovered, ranging from physiological to pathological processes (100).

In adult neovascularization, bone-marrow derived CXC-motif chemokine receptor-4 (CXCR4) cells can be retained in the perivascular area to promote angiogenesis, recruited by the ligand stromal-derived factor-1 (SDF-1) that is expressed by fibroblast and smooth muscle cells in response to VEGF (101). The VEGF withdrawal causes the loss of CXCR4⁺ cells and angiogenesis termination.

In vascularization newly induced in adult skeletal muscle, Neuropilin-1 (NP-1)⁺ and CD11b⁺ monocytes, defined NEM, have been described to be enrolled through the receptor NP-1, and promote vessel stabilization by secreting growth factors such as TGF- β and Ang-1, without being incorporated into the vessels (102).

Similarly, a subpopulation of circulating Tie2-expressing monocytes (TEM), known as TEM, homes to perivascular regions to induce functional tumor vasculature in a paracrine manner (103). Interestingly, the selective elimination of TEM impairs angiogenesis and induces tumor regression in mice. Moreover, Fantin and coworkers have described embryonic macrophages resembling TEM phenotype, which act as chaperones of tip cell fusion during sprouting (104).

3. Therapeutic angiogenesis

3.1 Peripheral arterial disease

Cardiovascular disease defines a group of disorders that affect the heart and blood vessels, and leads cause of deaths worldwide. Heart-related pathologies include coronary heart disease (heart attacks), congenital heart disease, rheumatic heart disease, and heart failure. The impairment of vasculature in the rest of the body can cause cerebrovascular disease (stroke), raised blood pressure (hypertension), and peripheral artery disease (definition from World Health Organization).

Peripheral arterial disease (PAD) refers to ischemia of the limbs secondary to atherosclerotic occlusion that is the accumulation of lipids, inflammatory cells, and fibrous material in the inner layer of arterial wall (105). Nowadays, there are no effective pharmacological treatments to cure ischemic tissue. Nevertheless, it is possible to prevent the progression of this disease with lifestyle related changes, i.e. avoid smoking, sedentary life, and poor diet. In second place, pharmacological drugs help to reduce cardiovascular risk factors and relieve the ischemic symptoms (106). Angioplasty or surgical bypass can be applied as revascularization strategies that, however, are not always feasible and may have poor long-term results (107). PAD often follows an aggressive clinical course culminating in critical limb ischemia (CLI) that causes an irreversible tissue loss (105).

3.2 Angiogenic therapy

In the last decades, therapeutic angiogenesis have been considered an effective strategy to induce the growth of new vessels to recover oxygen and nutrients supply in ischemic tissue, by delivering pro-angiogenic factors that have key role in the natural process of angiogenesis (108). Three delivery systems have been developed and tested in clinical trials to treat PAD related diseases: protein, gene, and cell therapy (106). In addition, tissue engineering has started to focus on the development of strategies to induce the growth of blood vessels. The results of these studies could have clinical implications in the treatment of ischemic conditions, but also allow overcoming problems associated to the vascularization of engineered tissues (109, 110).

The protein therapy is based on the administration of recombinant protein, and induces direct effects, however, has very short half-life in ischemic tissue (106).

Gene therapy via non-viral and viral vectors consists in carrying a gene construct encoding a therapeutic protein into the target cells (111). The use of non-viral vectors is not enough effective due the low efficiency uptake of DNA naked plasmid by target cells (108). Gene therapy via viral vector, for example with adenoviral vectors (Ad), presents higher efficacy compared to the use of DNA naked (111). However, Ads have limits about safety and duration of the transgene expression caused by immune response. Contrary, adeno-associated vectors (AAV) appear to be suitable candidates for gene therapy approaches, because, for example, they do not display relevant immunogenicity, they transduce cells at

high efficiency, and express the transgene for long period of time due to their tropism for postmitotic tissue (112).

Cell therapy has been developed based on the concept that hematopoietic stem cells and endothelial cells derived from common precursors, i.e. hemangioblasts (113). During embryonic development, hemangioblasts differentiate to hematopoietic stem cells that migrate to liver and then to bone marrow where they reside during adult life (105). Instead, other hemangioblasts originate angioblasts that form blood vessels *de novo* (vasculogenesis) (113). Despite this divergent differentiation, it was demonstrated that bone marrow derived cells could differentiate into endothelium-like and form new vessels (99). The use of bone marrow derived cells in clinical trials in the treatment of PAD is gaining the momentum, however, there are still several open questions about this approach. On one hand, it is still to define the effective cell populations, isolation, and processing methods, and, on the other hand, it is not clear whether implanted bone marrow derived cells favor neovascularization in ischemic tissue in a paracrine manner or/and they are directly incorporated into the vessels (105).

Tissue engineering (TE) has recently contributed to vascular biology research to build vascular networks with promising results for the future. Biocompatible and biodegradable scaffolds can be biochemically functionalized to be gradually degraded by host cells, for example by incorporation of RGD sequences, and enable a controlled release of angiogenic factors. Another strategy adopted by TE is the combination of cells with biomaterials, i.e. seeding stem and progenitor cells on scaffolds. In these circumstances, cells live in 3D environment that mimics the *in vivo* situation, and trigger cell signaling, differentiation, and migration, as

well as dynamic interaction among cells. These events may be favored by developing scaffolds with optimal biophysical and biomechanical properties, such as mechanical strength and biodegradability (110).

3.2.1 The issues with VEGF for therapeutic angiogenesis

VEGF is one of the master regulators of angiogenesis, and therapeutic angiogenesis has been long focused on developing VEGF-based approaches, which unfortunately, have not fulfilled the expectations yet (107, 112, 114). The failures in clinical trials are mainly due to concerns about dose and duration of VEGF expression (115).

As observed in development and postnatal life, VEGF activity in vessel growth has a very narrow therapeutic window in vivo, such that low doses have no or little angiogenic effects, whereas higher doses rapidly become unsafe, inducing vessels that frequently present morphological and functional abnormalities (116). In fact, the decrease of 50% of VEGF expression in development precluded vascular hierarchical remodeling and caused embryonic lethality (16). In clinical trials, VEGF doses released by single injections of recombinant protein or naked plasmid DNA were too low to induce any relevant angiogenic effects (108, 112). On the other hand, increased VEGF expression in embryonic vasculogenesis resulted in altered development of vessels with large lumens (117). Consistently, uncontrolled VEGF expression by retrovirally transduced myoblasts caused the formation of vascular tumors, called hemangiomas, in skeletal muscle (118, 119). The overexpression of VEGF by adenoviral vectors injected into the skin, fat, heart, and skeletal muscle of mice, caused enlarged, thin-walled, pericyte-poor vessels, as well as multi-

lumenized glomeruloid structures that resembled hemangiomas malformations (120, 121). Finally, the injection of a VEGF encoding plasmid in infarcted rat hearts induced angioma growth (122, 123).

Taking advantage of a myoblast-based gene delivery transfer system (described in section 3.3), our group has previously carefully investigated the dose-dependent effects of VEGF delivery in both normal and ischemic skeletal muscle (124, 125). The results showed that VEGF induces normal or aberrant angiogenesis depending on its amount in the microenvironment around each producing cell, and not the total dose (Fig. 14) (124). In fact, decreasing the total number of VEGF expressed by polyclonal myoblasts did not prevent the formation of abnormal vessels, due to the presence in the ECM of hot spots of high VEGF expression (124) (126). Instead, the implantation of monoclonal myoblast populations expressing homogeneous VEGF doses, revealed a threshold between normal and aberrant angiogenesis. Clonal populations expressing low to medium VEGF levels below the threshold induced normal, pericyte-covered, and stable vessels, while myoblasts expressing high VEGF doses yielded smooth muscle cells-invested hemangiomas, which regressed after VEGF withdrawal (124). Moreover, studies in a murine model of hind limb ischemia showed that either low and high VEGF levels did not have clinical benefit, while medium VEGF doses did (125). Taken together, these results highlight that VEGF has a narrow therapeutic window in term of dosage and explain the previous difficulty to identify a manageable therapeutic window of VEGF dosage in preclinical and clinical studies (124, 125).

The duration of VEGF expression is also crucial to achieve therapeutic angiogenesis since long lasting expression causes aberrant angiogenesis, whereas

VEGF stimulus withdrawal before four weeks causes vascular regression (116). In a transgenic system, the cessation of VEGF stimulus in the short term i.e. 2weeks, caused the vessels to regress, while the longer expression up to 4 weeks, led to vascular persistence (127). Injection of inducible VEGF-AAVs or VEGF-expressing myoblasts in skeletal muscles confirmed 4 weeks as the minimal window of time of VEGF sustained delivery required to generate stable vessels (124, 128).

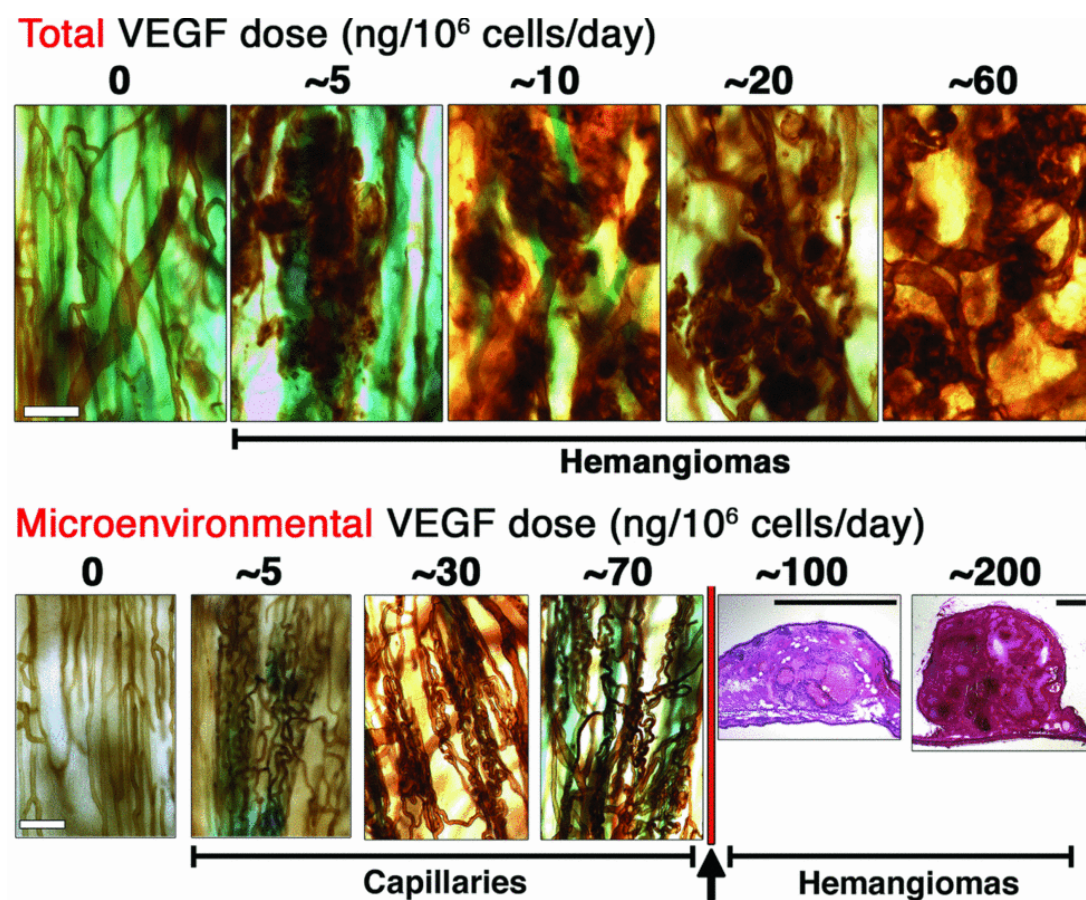


Figure 14 Microenvironmental VEGF concentration, not total dose, determines a threshold between normal and aberrant angiogenesis. Histological analysis performed by lectin staining on whole mount ear tissue previously injected with genetically modified myoblasts. Reducing the total amount of VEGF dose does not prevent the formation of abnormal vascular growth, as indicated by growth of morphologically abnormal, bulbous vascular structures induced by different polyclonal myoblast populations expressing heterogeneous VEGF levels. Conversely, the microenvironmental level of VEGF produced by monoclonal myoblast populations determines a threshold between the growth of normal capillaries and hemangiomas (adapted from Ozawa et al, 2004).

Based on these considerations, we can assume that the use of VEGF as single factor in gene-delivery based therapy, needs the design of tools that allow controlling VEGF expression in term of dosage and timing in order to be clinically successful (108).

3.3 Myoblast-based gene transfer system

Myoblast based delivery system is a cell-based approach that uses engineered muscle precursor cells as vehicle to deliver angiogenic growth factors *in vivo*. This approach comprises three main steps:

- 1) isolation of precursor myoblasts;
- 2) myoblast retroviral-transduction, purification, and *in vitro* characterization;
- 3) myoblast injection into skeletal tissue.

Myoblasts are obtained by digesting skeletal muscle harvested from neonatal mice, and eliminating contaminations by other cell types, such as fibroblasts (129). For transduction, high-titer retroviral supernatants are obtained from the helper-free, ecotropic Phoenix packaging cell line, which is previously transfected with a plasmid containing the transgene (130). Pure myoblasts are transduced by four sequential rounds of infection, typically resulting in a transduction efficiency of 99% (129). The insertion of the transgene into a bicistronic construct together with the sequence of a non-functional surface marker allows purifying specific populations by FACS sorting, for instance, clonal cells that express homogenous microenvironmental level of the gene of interest. Sorted myoblast populations are expanded and characterized for the expression of the transgene by ELISA,

and then injected intramuscularly into skeletal muscle where they fuse with the resident adult muscle fibers and express the transgene (131).

In vivo gene transfer by implantation of retrovirally transduced myoblasts, presents different advantages compared to other gene delivery systems, for example the gene of interest can be expressed over a long period of time, large and multiple gene products can be inserted (up to 6 kb), and additional genes can be introduced by re-infecting the cells with retroviral constructs carrying other genes of interest. Moreover, this cell-based approach is relatively rapid, inexpensive, and easy to handle method. Taken together, these features could have encouraged to use retrovirally infected myoblasts for clinical applications, taking advantage of the possibility of using autologous cells, and therefore even preventing immune response (129). Unfortunately, this is not achievable because of the risk that the retroviral integration into the recipient cells leads to malignant transformation (108, 132).

Nevertheless, this cell-based *ex-vivo* approach has unique properties that let to investigate cellular and molecular mechanisms underlying adult vascularization newly formed by delivering specific angiogenesis factors whose expression can be controlled in terms of dosage and timing (48). Gaining our knowledge in these mechanisms may lead to identify novel candidates to apply for therapeutic angiogenesis.

Aims of the thesis

Aims of the thesis

In order to harness the biological potential of VEGF to achieve therapeutic angiogenesis it is necessary to overcome specific issues related to dosage and timing of its expression, which are challenging to address with the currently available clinical vectors for gene delivery, such as plasmid DNA, adenoviral and adeno-associated viral vectors.

Recent research has focused on alternative approaches to overcome the limits of VEGF-based gene therapy. An attractive strategy is the sustained delivery of recombinant protein factors through biodegradable natural polymers, which avoids the genetic modification of target cells and in which the dose and duration of VEGF release may be controlled by engineering of the biomaterial properties (Sacchi et al., manuscript in preparation). A challenge for this approach remains the need to sustain factor release for at least 4 weeks in order to achieve vascular stabilization. On the other hand, we have recently developed a high-throughput technology to determine the VEGF level of expression of genetically-modified progenitors in single live cells by Fluorescence Activated Cell Sorting (FACS) and to rapidly purify populations homogeneously expressing a specific therapeutic level, so that controlled microenvironmental VEGF doses can be delivered without the need to isolate clonal populations (131, 133-136). A limitation of this approach lies in the safety concerns related to the use of integrating viral vectors. In fact, retroviral vectors can lead to malignant cell transformation by insertional mutagenesis and stimulation of proto-oncogenes, as discussed in section 3.3. An

equally effective and safer alternative is represented by lentiviral vectors, which do not display preferential integration in transcriptionally active start-sites and therefore have been shown to possess a very low oncogenic potential (137, 138).

While these approaches seek to translate current biological concepts into clinically applicable strategies, a more detailed understanding of the cellular and molecular mechanisms by which exogenous VEGF overexpression at therapeutic doses regulates the growth of new vessels would provide novel and possibly more specific molecular targets for therapeutic angiogenesis. In fact, blood vessel growth is a highly orchestrated process that requires the coordinated interplay of multiple factors and cell types, where VEGF is the initiator of the cascade of events (139). Therefore, identifying and targeting the mechanisms of vascular morphogenesis and stabilization by VEGF dose is key to refine VEGF-based therapeutic strategies through the development of combined therapy (116).

We previously found that murine VEGF₁₆₄ can induce the formation of normal vessels coated by pericytes, or hemangioma-like structures invested by smooth muscle cells, depending strictly on its level of expression in the microenvironment around each producing cell *in vivo*, and not on the total dose delivered to the tissue (124). Furthermore, our group recently showed that balanced co-delivery of PDGF-BB and VEGF from a single bicistronic construct could prevent pericyte loss from vascular structures induced by VEGF over-expression at uncontrolled levels and switch the formation of aberrant angioma-like structures into normal and mature micro-vascular networks (140). Therefore, PDGF-BB-recruited pericytes, responsible for the proper maturation of nascent vasculature, can provide crucial signals to normalize aberrant angiogenesis induced by VEGF. However, the role of

paracrine signals between pericytes and endothelium during the transition from normal to aberrant angiogenesis are poorly understood. Therefore, the first part of this thesis aims at identifying the pericyte-derived molecular signals that control the switch between normal and aberrant angiogenesis by VEGF.

Rapid vascular stabilization is also a key target to achieve therapeutic angiogenesis, as short-term expression of growth factors is desirable to ensure safety, but VEGF requires at least 4 weeks of sustained delivery to achieve vascular stabilization and avoid regression of newly induced vessels (124, 127, 128). Several molecular and cellular pathways contribute to vascular stabilization (52). However, it is unknown whether VEGF dose controls also vascular stabilization, as previously shown for the switch from normal to aberrant angiogenesis. Therefore, the second aim of this thesis is to define whether the stabilization of newly formed vessels is regulated by the dose of VEGF over-expression in a therapeutic setting and to investigate the underlying cellular and molecular mechanisms.

These experiments are expected to identify novel cellular or molecular candidates to provide specific therapeutic effects, such as triggering normalization and stabilization of vessels newly induced by exogenous VEGF overexpression, in order to improve both the safety and efficacy of VEGF-based therapeutic angiogenesis.

References

1. G. L. Semenza, Vasculogenesis, angiogenesis, and arteriogenesis: mechanisms of blood vessel formation and remodeling. *Journal of cellular biochemistry* **102**, 840 (Nov 1, 2007).
2. E. Pardali, M. J. Goumans, P. ten Dijke, Signaling by members of the TGF-beta family in vascular morphogenesis and disease. *Trends in cell biology* **20**, 556 (Sep, 2010).
3. P. Carmeliet, R. K. Jain, Principles and mechanisms of vessel normalization for cancer and other angiogenic diseases. *Nature reviews. Drug discovery* **10**, 417 (Jun, 2011).
4. B. Styp-Rekowska, R. Hlushchuk, A. R. Pries, V. Djonov, Intussusceptive angiogenesis: pillars against the blood flow. *Acta physiologica* **202**, 213 (Jul, 2011).
5. R. Munoz-Chapuli, A. R. Quesada, M. Angel Medina, Angiogenesis and signal transduction in endothelial cells. *Cellular and molecular life sciences : CMLS* **61**, 2224 (Sep, 2004).
6. M. Shibuya, Structure and function of VEGF/VEGF-receptor system involved in angiogenesis. *Cell structure and function* **26**, 25 (Feb, 2001).
7. D. R. Senger et al., Tumor cells secrete a vascular permeability factor that promotes accumulation of ascites fluid. *Science* **219**, 983 (Feb 25, 1983).
8. N. Ferrara, VEGF and the quest for tumour angiogenesis factors. *Nature reviews. Cancer* **2**, 795 (Oct, 2002).

9. K. Holmes, O. L. Roberts, A. M. Thomas, M. J. Cross, Vascular endothelial growth factor receptor-2: structure, function, intracellular signalling and therapeutic inhibition. *Cellular signalling* **19**, 2003 (Oct, 2007).
10. N. Ferrara, Vascular endothelial growth factor: basic science and clinical progress. *Endocrine reviews* **25**, 581 (Aug, 2004).
11. J. E. Park, G. A. Keller, N. Ferrara, The vascular endothelial growth factor (VEGF) isoforms: differential deposition into the subepithelial extracellular matrix and bioactivity of extracellular matrix-bound VEGF. *Molecular biology of the cell* **4**, 1317 (Dec, 1993).
12. C. Ruhrberg, Growing and shaping the vascular tree: multiple roles for VEGF. *BioEssays : news and reviews in molecular, cellular and developmental biology* **25**, 1052 (Nov, 2003).
13. R. Gianni-Barrera, M. Trani, S. Reginato, A. Banfi, To sprout or to split? VEGF, Notch and vascular morphogenesis. *Biochemical Society transactions* **39**, 1644 (Dec, 2011).
14. J. Grunstein, J. J. Masbad, R. Hickey, F. Giordano, R. S. Johnson, Isoforms of vascular endothelial growth factor act in a coordinate fashion To recruit and expand tumor vasculature. *Molecular and cellular biology* **20**, 7282 (Oct, 2000).
15. C. Ruhrberg et al., Spatially restricted patterning cues provided by heparin-binding VEGF-A control blood vessel branching morphogenesis. *Genes & development* **16**, 2684 (Oct 15, 2002).
16. P. Carmeliet et al., Abnormal blood vessel development and lethality in embryos lacking a single VEGF allele. *Nature* **380**, 435 (Apr 4, 1996).

17. L. Miquerol, B. L. Langille, A. Nagy, Embryonic development is disrupted by modest increases in vascular endothelial growth factor gene expression. *Development* **127**, 3941 (Sep, 2000).
18. J. Yao et al., Expression of a functional VEGFR-1 in tumor cells is a major determinant of anti-PlGF antibodies efficacy. *Proceedings of the National Academy of Sciences of the United States of America* **108**, 11590 (Jul 12, 2011).
19. S. P. Herbert, D. Y. Stainier, Molecular control of endothelial cell behaviour during blood vessel morphogenesis. *Nature reviews. Molecular cell biology* **12**, 551 (Sep, 2011).
20. B. Barleon et al., Migration of human monocytes in response to vascular endothelial growth factor (VEGF) is mediated via the VEGF receptor flt-1. *Blood* **87**, 3336 (Apr 15, 1996).
21. S. Djordjevic, P. C. Driscoll, Targeting VEGF signalling via the neuropilin co-receptor. *Drug discovery today* **18**, 447 (May, 2013).
22. R. P. Kruger, J. Aurandt, K. L. Guan, Semaphorins command cells to move. *Nature reviews. Molecular cell biology* **6**, 789 (Oct, 2005).
23. I. C. Zachary, P. Frankel, I. M. Evans, C. Pellet-Many, The role of neuropilins in cell signalling. *Biochemical Society transactions* **37**, 1171 (Dec, 2009).
24. C. A. Staton, I. Kumar, M. W. Reed, N. J. Brown, Neuropilins in physiological and pathological angiogenesis. *The Journal of pathology* **212**, 237 (Jul, 2007).
25. G. Serini et al., Class 3 semaphorins control vascular morphogenesis by inhibiting integrin function. *Nature* **424**, 391 (Jul 24, 2003).

26. E. Geretti, A. Shimizu, M. Klagsbrun, Neuropilin structure governs VEGF and semaphorin binding and regulates angiogenesis. *Angiogenesis* **11**, 31 (2008).
27. A. Vacca et al., Loss of inhibitory semaphorin 3A (SEMA3A) autocrine loops in bone marrow endothelial cells of patients with multiple myeloma. *Blood* **108**, 1661 (Sep 1, 2006).
28. F. Maione et al., Semaphorin 3A overcomes cancer hypoxia and metastatic dissemination induced by antiangiogenic treatment in mice. *The Journal of clinical investigation* **122**, 1832 (May 1, 2012).
29. G. Chakraborty, S. Kumar, R. Mishra, T. V. Patil, G. C. Kundu, Semaphorin 3A suppresses tumor growth and metastasis in mice melanoma model. *PloS one* **7**, e33633 (2012).
30. F. Maione et al., Semaphorin 3A is an endogenous angiogenesis inhibitor that blocks tumor growth and normalizes tumor vasculature in transgenic mouse models. *The Journal of clinical investigation* **119**, 3356 (Nov, 2009).
31. M. Narazaki, G. Tosato, Ligand-induced internalization selects use of common receptor neuropilin-1 by VEGF₁₆₅ and semaphorin3A. *Blood* **107**, 3892 (May 15, 2006).
32. K. Norrby, Angiogenesis: new aspects relating to its initiation and control. *APMIS : acta pathologica, microbiologica, et immunologica Scandinavica* **105**, 417 (Jun, 1997).
33. R. H. Adams, K. Alitalo, Molecular regulation of angiogenesis and lymphangiogenesis. *Nature reviews. Molecular cell biology* **8**, 464 (Jun, 2007).

34. H. Gerhardt *et al.*, VEGF guides angiogenic sprouting utilizing endothelial tip cell filopodia. *The Journal of cell biology* **161**, 1163 (Jun 23, 2003).
35. M. Potente, H. Gerhardt, P. Carmeliet, Basic and therapeutic aspects of angiogenesis. *Cell* **146**, 873 (Sep 16, 2011).
36. T. Kume, Ligand-dependent Notch signaling in vascular formation. *Advances in experimental medicine and biology* **727**, 210 (2012).
37. C. Roca, R. H. Adams, Regulation of vascular morphogenesis by Notch signaling. *Genes & development* **21**, 2511 (Oct 15, 2007).
38. M. Hellstrom *et al.*, Dll4 signalling through Notch1 regulates formation of tip cells during angiogenesis. *Nature* **445**, 776 (Feb 15, 2007).
39. N. C. Kappas *et al.*, The VEGF receptor Flt-1 spatially modulates Flk-1 signaling and blood vessel branching. *The Journal of cell biology* **181**, 847 (Jun 2, 2008).
40. R. Benedito *et al.*, The notch ligands Dll4 and Jagged1 have opposing effects on angiogenesis. *Cell* **137**, 1124 (Jun 12, 2009).
41. T. Tammela *et al.*, VEGFR-3 controls tip to stalk conversion at vessel fusion sites by reinforcing Notch signalling. *Nature cell biology* **13**, 1202 (Oct, 2011).
42. V. Djonov, O. Baum, P. H. Burri, Vascular remodeling by intussusceptive angiogenesis. *Cell and tissue research* **314**, 107 (Oct, 2003).
43. J. H. Caduff, L. C. Fischer, P. H. Burri, Scanning electron microscope study of the developing microvasculature in the postnatal rat lung. *The Anatomical record* **216**, 154 (Oct, 1986).
44. H. Kurz, P. H. Burri, V. G. Djonov, Angiogenesis and vascular remodeling by intussusception: from form to function. *News in physiological sciences : an*

international journal of physiology produced jointly by the International Union of Physiological Sciences and the American Physiological Society **18**, 65 (Apr, 2003).

45. A. N. Makanya, R. Hlushchuk, V. G. Djonov, Intussusceptive angiogenesis and its role in vascular morphogenesis, patterning, and remodeling. *Angiogenesis* **12**, 113 (2009).
46. R. Hlushchuk *et al.*, Tumor recovery by angiogenic switch from sprouting to intussusceptive angiogenesis after treatment with PTK787/ZK222584 or ionizing radiation. *The American journal of pathology* **173**, 1173 (Oct, 2008).
47. L. Loufrani, D. Henrion, Role of the cytoskeleton in flow (shear stress)-induced dilation and remodeling in resistance arteries. *Medical & biological engineering & computing* **46**, 451 (May, 2008).
48. R. Gianni-Barrera *et al.*, VEGF over-expression in skeletal muscle induces angiogenesis by intussusception rather than sprouting. *Angiogenesis* **16**, 123 (Jan, 2013).
49. R. K. Jain, Molecular regulation of vessel maturation. *Nature medicine* **9**, 685 (Jun, 2003).
50. D. von Tell, A. Armulik, C. Betsholtz, Pericytes and vascular stability. *Experimental cell research* **312**, 623 (Mar 10, 2006).
51. M. Murakami, Signaling required for blood vessel maintenance: molecular basis and pathological manifestations. *International journal of vascular medicine* **2012**, 293641 (2012).
52. A. N. Stratman, G. E. Davis, Endothelial cell-pericyte interactions stimulate basement membrane matrix assembly: influence on vascular tube

- remodeling, maturation, and stabilization. *Microscopy and microanalysis : the official journal of Microscopy Society of America, Microbeam Analysis Society, Microscopical Society of Canada* **18**, 68 (Feb, 2012).
53. A. Armulik, G. Genove, C. Betsholtz, Pericytes: developmental, physiological, and pathological perspectives, problems, and promises. *Developmental cell* **21**, 193 (Aug 16, 2011).
 54. A. Armulik, A. Abramsson, C. Betsholtz, Endothelial/pericyte interactions. *Circulation research* **97**, 512 (Sep 16, 2005).
 55. D. Ribatti, B. Nico, E. Crivellato, The role of pericytes in angiogenesis. *The International journal of developmental biology* **55**, 261 (2011).
 56. P. Dore-Duffy, A. Katychew, X. Wang, E. Van Buren, CNS microvascular pericytes exhibit multipotential stem cell activity. *Journal of cerebral blood flow and metabolism : official journal of the International Society of Cerebral Blood Flow and Metabolism* **26**, 613 (May, 2006).
 57. M. Crisan et al., A perivascular origin for mesenchymal stem cells in multiple human organs. *Cell stem cell* **3**, 301 (Sep 11, 2008).
 58. P. H. Chen, X. Chen, X. He, Platelet-derived growth factors and their receptors: Structural and functional perspectives. *Biochimica et biophysica acta*, (Nov 5, 2012).
 59. M. Andersson, A. Ostman, B. Westermark, C. H. Heldin, Characterization of the retention motif in the C-terminal part of the long splice form of platelet-derived growth factor A-chain. *The Journal of biological chemistry* **269**, 926 (Jan 14, 1994).

60. J. Andrae, R. Gallini, C. Betsholtz, Role of platelet-derived growth factors in physiology and medicine. *Genes & development* **22**, 1276 (May 15, 2008).
61. C. Betsholtz, Insight into the physiological functions of PDGF through genetic studies in mice. *Cytokine & growth factor reviews* **15**, 215 (Aug, 2004).
62. P. ten Dijke, H. M. Arthur, Extracellular control of TGFbeta signalling in vascular development and disease. *Nature reviews. Molecular cell biology* **8**, 857 (Nov, 2007).
63. E. Pardali, P. Ten Dijke, TGFbeta signaling and cardiovascular diseases. *International journal of biological sciences* **8**, 195 (2012).
64. J. S. Munger, D. Sheppard, Cross talk among TGF-beta signaling pathways, integrins, and the extracellular matrix. *Cold Spring Harbor perspectives in biology* **3**, a005017 (Nov, 2011).
65. J. P. Annes, J. S. Munger, D. B. Rifkin, Making sense of latent TGFbeta activation. *Journal of cell science* **116**, 217 (Jan 15, 2003).
66. V. V. Orlova, Z. Liu, M. J. Goumans, P. ten Dijke, Controlling angiogenesis by two unique TGF-beta type I receptor signaling pathways. *Histology and histopathology* **26**, 1219 (Sep, 2011).
67. N. Rudini et al., VE-cadherin is a critical endothelial regulator of TGF-beta signalling. *The EMBO journal* **27**, 993 (Apr 9, 2008).
68. G. Ferrari et al., TGF-beta1 induces endothelial cell apoptosis by shifting VEGF activation of p38(MAPK) from the prosurvival p38beta to proapoptotic p38alpha. *Molecular cancer research : MCR* **10**, 605 (May, 2012).

69. F. Li *et al.*, Endothelial Smad4 maintains cerebrovascular integrity by activating N-cadherin through cooperation with Notch. *Developmental cell* **20**, 291 (Mar 15, 2011).
70. D. C. Darland, P. A. D'Amore, TGF beta is required for the formation of capillary-like structures in three-dimensional cocultures of 10T1/2 and endothelial cells. *Angiogenesis* **4**, 11 (2001).
71. T. E. Walshe *et al.*, TGF-beta is required for vascular barrier function, endothelial survival and homeostasis of the adult microvasculature. *PLoS one* **4**, e5149 (2009).
72. K. K. Hirschi, S. A. Rohovsky, P. A. D'Amore, PDGF, TGF-beta, and heterotypic cell-cell interactions mediate endothelial cell-induced recruitment of 10T1/2 cells and their differentiation to a smooth muscle fate. *The Journal of cell biology* **141**, 805 (May 4, 1998).
73. A. Antonelli-Orlidge, K. B. Saunders, S. R. Smith, P. A. D'Amore, An activated form of transforming growth factor beta is produced by cocultures of endothelial cells and pericytes. *Proceedings of the National Academy of Sciences of the United States of America* **86**, 4544 (Jun, 1989).
74. H. G. Augustin, G. Y. Koh, G. Thurston, K. Alitalo, Control of vascular morphogenesis and homeostasis through the angiopoietin-Tie system. *Nature reviews. Molecular cell biology* **10**, 165 (Mar, 2009).
75. S. Tsigkos, M. Koutsilieris, A. Papapetropoulos, Angiopoietins in angiogenesis and beyond. *Expert opinion on investigational drugs* **12**, 933 (Jun, 2003).

76. G. Thurston *et al.*, Leakage-resistant blood vessels in mice transgenically overexpressing angiopoietin-1. *Science* **286**, 2511 (Dec 24, 1999).
77. A. Uemura *et al.*, Recombinant angiopoietin-1 restores higher-order architecture of growing blood vessels in mice in the absence of mural cells. *The Journal of clinical investigation* **110**, 1619 (Dec, 2002).
78. S. Fukuhara *et al.*, Angiopoietin-1/Tie2 receptor signaling in vascular quiescence and angiogenesis. *Histology and histopathology* **25**, 387 (Mar, 2010).
79. G. Thurston *et al.*, Angiopoietin 1 causes vessel enlargement, without angiogenic sprouting, during a critical developmental period. *Development* **132**, 3317 (Jul, 2005).
80. H. Kidoya *et al.*, Spatial and temporal role of the apelin/APJ system in the caliber size regulation of blood vessels during angiogenesis. *The EMBO journal* **27**, 522 (Feb 6, 2008).
81. O. Salvucci, G. Tosato, Essential roles of EphB receptors and EphrinB ligands in endothelial cell function and angiogenesis. *Advances in cancer research* **114**, 21 (2012).
82. K. Kullander, R. Klein, Mechanisms and functions of Eph and ephrin signalling. *Nature reviews. Molecular cell biology* **3**, 475 (Jul, 2002).
83. M. L. Bochenek, S. Dickinson, J. W. Astin, R. H. Adams, C. D. Nobes, Ephrin-B2 regulates endothelial cell morphology and motility independently of Eph-receptor binding. *Journal of cell science* **123**, 1235 (Apr 15, 2010).
84. R. H. Adams *et al.*, Roles of ephrinB ligands and EphB receptors in cardiovascular development: demarcation of arterial/venous domains,

- vascular morphogenesis, and sprouting angiogenesis. *Genes & development* **13**, 295 (Feb 1, 1999).
85. S. P. Herbert *et al.*, Arterial-venous segregation by selective cell sprouting: an alternative mode of blood vessel formation. *Science* **326**, 294 (Oct 9, 2009).
 86. N. W. Gale *et al.*, Ephrin-B2 selectively marks arterial vessels and neovascularization sites in the adult, with expression in both endothelial and smooth-muscle cells. *Developmental biology* **230**, 151 (Feb 15, 2001).
 87. D. Shin *et al.*, Expression of ephrinB2 identifies a stable genetic difference between arterial and venous vascular smooth muscle as well as endothelial cells, and marks subsets of microvessels at sites of adult neovascularization. *Developmental biology* **230**, 139 (Feb 15, 2001).
 88. S. S. Foo *et al.*, Ephrin-B2 controls cell motility and adhesion during blood-vessel-wall assembly. *Cell* **124**, 161 (Jan 13, 2006).
 89. H. U. Wang, Z. F. Chen, D. J. Anderson, Molecular distinction and angiogenic interaction between embryonic arteries and veins revealed by ephrin-B2 and its receptor Eph-B4. *Cell* **93**, 741 (May 29, 1998).
 90. S. S. Gerety, D. J. Anderson, Cardiovascular ephrinB2 function is essential for embryonic angiogenesis. *Development* **129**, 1397 (Mar, 2002).
 91. Y. Wang *et al.*, Ephrin-B2 controls VEGF-induced angiogenesis and lymphangiogenesis. *Nature* **465**, 483 (May 27, 2010).
 92. M. Luxey, J. Laussu, T. Jungas, A. Davy, Generation of transgenic mice overexpressing EfnB2 in endothelial cells. *Genesis* **49**, 811 (Oct, 2011).

93. M. Kimura *et al.*, Soluble form of ephrinB2 inhibits xenograft growth of squamous cell carcinoma of the head and neck. *International journal of oncology* **34**, 321 (Feb, 2009).
94. N. K. Noren, G. Foos, C. A. Hauser, E. B. Pasquale, The EphB4 receptor suppresses breast cancer cell tumorigenicity through an Abl-Crk pathway. *Nature cell biology* **8**, 815 (Aug, 2006).
95. G. Xia *et al.*, EphB4 receptor tyrosine kinase is expressed in bladder cancer and provides signals for cell survival. *Oncogene* **25**, 769 (Feb 2, 2006).
96. N. Y. Yang, E. B. Pasquale, L. B. Owen, I. M. Ethell, The EphB4 receptor-tyrosine kinase promotes the migration of melanoma cells through Rho-mediated actin cytoskeleton reorganization. *The Journal of biological chemistry* **281**, 32574 (Oct 27, 2006).
97. N. Takakura, Role of intimate interactions between endothelial cells and the surrounding accessory cells in the maturation of blood vessels. *Journal of thrombosis and haemostasis : JTH* **9 Suppl 1**, 144 (Jul, 2011).
98. I. Rajantie *et al.*, Adult bone marrow-derived cells recruited during angiogenesis comprise precursors for periendothelial vascular mural cells. *Blood* **104**, 2084 (Oct 1, 2004).
99. T. Asahara *et al.*, Bone marrow origin of endothelial progenitor cells responsible for postnatal vasculogenesis in physiological and pathological neovascularization. *Circulation research* **85**, 221 (Aug 6, 1999).
100. S. Nucera, D. Biziato, M. De Palma, The interplay between macrophages and angiogenesis in development, tissue injury and regeneration. *The International journal of developmental biology* **55**, 495 (2011).

101. M. Grunewald et al., VEGF-induced adult neovascularization: recruitment, retention, and role of accessory cells. *Cell* **124**, 175 (Jan 13, 2006).
102. S. Zacchigna et al., Bone marrow cells recruited through the neuropilin-1 receptor promote arterial formation at the sites of adult neoangiogenesis in mice. *The Journal of clinical investigation* **118**, 2062 (Jun, 2008).
103. R. Mazziere et al., Targeting the ANG2/TIE2 axis inhibits tumor growth and metastasis by impairing angiogenesis and disabling rebounds of proangiogenic myeloid cells. *Cancer cell* **19**, 512 (Apr 12, 2011).
104. A. Fantin et al., NRP1 acts cell autonomously in endothelium to promote tip cell function during sprouting angiogenesis. *Blood* **121**, 2352 (Mar 21, 2013).
105. Z. Raval, D. W. Losordo, Cell therapy of peripheral arterial disease: from experimental findings to clinical trials. *Circulation research* **112**, 1288 (Apr 26, 2013).
106. G. Dragneva, P. Korpisalo, S. Yla-Herttuala, Promoting blood vessel growth in ischemic diseases: challenges in translating preclinical potential into clinical success. *Disease models & mechanisms* **6**, 312 (Mar, 2013).
107. B. H. Annex, Therapeutic angiogenesis for critical limb ischaemia. *Nature reviews. Cardiology*, (May 14, 2013).
108. S. Yla-Herttuala, K. Alitalo, Gene transfer as a tool to induce therapeutic vascular growth. *Nature medicine* **9**, 694 (Jun, 2003).
109. S. Soker, M. Machado, A. Atala, Systems for therapeutic angiogenesis in tissue engineering. *World journal of urology* **18**, 10 (Feb, 2000).
110. H. Bae et al., Building vascular networks. *Science translational medicine* **4**, 160ps23 (Nov 14, 2012).

111. P. Korpisalo, S. Yla-Herttuala, Stimulation of functional vessel growth by gene therapy. *Integrative biology : quantitative biosciences from nano to macro* **2**, 102 (Mar, 2010).
112. M. Giacca, S. Zacchigna, VEGF gene therapy: therapeutic angiogenesis in the clinic and beyond. *Gene therapy* **19**, 622 (Jun, 2012).
113. D. W. Losordo, S. Dimmeler, Therapeutic angiogenesis and vasculogenesis for ischemic disease: part II: cell-based therapies. *Circulation* **109**, 2692 (Jun 8, 2004).
114. H. Karvinen, S. Yla-Herttuala, New aspects in vascular gene therapy. *Current opinion in pharmacology* **10**, 208 (Apr, 2010).
115. S. Yla-Herttuala, J. E. Markkanen, T. T. Rissanen, Gene therapy for ischemic cardiovascular diseases: some lessons learned from the first clinical trials. *Trends in cardiovascular medicine* **14**, 295 (Nov, 2004).
116. S. Reginato, R. Gianni-Barrera, A. Banfi, Taming of the wild vessel: promoting vessel stabilization for safe therapeutic angiogenesis. *Biochemical Society transactions* **39**, 1654 (Dec, 2011).
117. C. J. Drake, C. D. Little, Exogenous vascular endothelial growth factor induces malformed and hyperfused vessels during embryonic neovascularization. *Proceedings of the National Academy of Sciences of the United States of America* **92**, 7657 (Aug 15, 1995).
118. M. L. Springer, A. S. Chen, P. E. Kraft, M. Bednarski, H. M. Blau, VEGF gene delivery to muscle: potential role for vasculogenesis in adults. *Molecular cell* **2**, 549 (Nov, 1998).

119. R. J. Lee et al., VEGF gene delivery to myocardium: deleterious effects of unregulated expression. *Circulation* **102**, 898 (Aug 22, 2000).
120. A. Pettersson et al., Heterogeneity of the angiogenic response induced in different normal adult tissues by vascular permeability factor/vascular endothelial growth factor. *Laboratory investigation; a journal of technical methods and pathology* **80**, 99 (Jan, 2000).
121. C. Sundberg et al., Glomeruloid microvascular proliferation follows adenoviral vascular permeability factor/vascular endothelial growth factor-164 gene delivery. *The American journal of pathology* **158**, 1145 (Mar, 2001).
122. J. M. Isner et al., Clinical evidence of angiogenesis after arterial gene transfer of phVEGF165 in patient with ischaemic limb. *Lancet* **348**, 370 (Aug 10, 1996).
123. E. R. Schwarz et al., Evaluation of the effects of intramyocardial injection of DNA expressing vascular endothelial growth factor (VEGF) in a myocardial infarction model in the rat--angiogenesis and angioma formation. *Journal of the American College of Cardiology* **35**, 1323 (Apr, 2000).
124. C. R. Ozawa et al., Microenvironmental VEGF concentration, not total dose, determines a threshold between normal and aberrant angiogenesis. *The Journal of clinical investigation* **113**, 516 (Feb, 2004).
125. G. von Degenfeld et al., Microenvironmental VEGF distribution is critical for stable and functional vessel growth in ischemia. *FASEB journal : official publication of the Federation of American Societies for Experimental Biology* **20**, 2657 (Dec, 2006).

126. A. Banfi, G. von Degenfeld, H. M. Blau, Critical role of microenvironmental factors in angiogenesis. *Current atherosclerosis reports* **7**, 227 (May, 2005).
127. Y. Dor et al., Conditional switching of VEGF provides new insights into adult neovascularization and pro-angiogenic therapy. *The EMBO journal* **21**, 1939 (Apr 15, 2002).
128. S. Tafuro et al., Inducible adeno-associated virus vectors promote functional angiogenesis in adult organisms via regulated vascular endothelial growth factor expression. *Cardiovascular research* **83**, 663 (Sep 1, 2009).
129. G. von Degenfeld, A. Banfi, M. L. Springer, H. M. Blau, Myoblast-mediated gene transfer for therapeutic angiogenesis and arteriogenesis. *British journal of pharmacology* **140**, 620 (Oct, 2003).
130. W. S. Pear, G. P. Nolan, M. L. Scott, D. Baltimore, Production of high-titer helper-free retroviruses by transient transfection. *Proceedings of the National Academy of Sciences of the United States of America* **90**, 8392 (Sep 15, 1993).
131. H. Misteli et al., High-throughput flow cytometry purification of transduced progenitors expressing defined levels of vascular endothelial growth factor induces controlled angiogenesis in vivo. *Stem cells* **28**, 611 (Mar 31, 2010).
132. S. Hacein-Bey-Abina et al., A serious adverse event after successful gene therapy for X-linked severe combined immunodeficiency. *The New England journal of medicine* **348**, 255 (Jan 16, 2003).

133. T. Wolff et al., FACS-purified myoblasts producing controlled VEGF levels induce safe and stable angiogenesis in chronic hind limb ischemia. *Journal of cellular and molecular medicine* **16**, 107 (Jan, 2012).
134. U. Helmrich et al., Generation of human adult mesenchymal stromal/stem cells expressing defined xenogenic vascular endothelial growth factor levels by optimized transduction and flow cytometry purification. *Tissue engineering. Part C, Methods* **18**, 283 (Apr, 2012).
135. A. Marsano et al., The effect of controlled expression of VEGF by transduced myoblasts in a cardiac patch on vascularization in a mouse model of myocardial infarction. *Biomaterials* **34**, 393 (Jan, 2013).
136. L. F. Melly et al., Controlled angiogenesis in the heart by cell-based expression of specific vascular endothelial growth factor levels. *Human gene therapy methods* **23**, 346 (Oct, 2012).
137. E. Montini et al., Hematopoietic stem cell gene transfer in a tumor-prone mouse model uncovers low genotoxicity of lentiviral vector integration. *Nature biotechnology* **24**, 687 (Jun, 2006).
138. M. Giacca, S. Zacchigna, Virus-mediated gene delivery for human gene therapy. *Journal of controlled release : official journal of the Controlled Release Society* **161**, 377 (Jul 20, 2012).
139. A. Alfranca, VEGF therapy: a timely retreat. *Cardiovascular research* **83**, 611 (Sep 1, 2009).
140. A. Banfi et al., Therapeutic angiogenesis due to balanced single-vector delivery of VEGF and PDGF-BB. *FASEB journal : official publication of the*

Federation of American Societies for Experimental Biology **26**, 2486 (Jun, 2012).

EphrinB2/EphB4 signaling controls the switch between normal and aberrant angiogenesis by increasing VEGF doses

Elena Groppa MSc¹, Veronica Sacchi MSc¹, Marianna Trani PhD¹, Michael Heberer MD¹ and Andrea Banfi MD¹

¹Cell and Gene Therapy, Department of Biomedicine and Department of Surgery, Basel University Hospital, Basel, Switzerland

Introduction

Peripheral artery disease due to atherosclerosis is a common clinical problem that does not have any effective medical treatment yet (1). Over the past two decades, in order to halt the vessel obstruction process, the cardiovascular research has identified in therapeutic angiogenesis a promising approach to restore blood flow in ischemic tissues, by stimulating the formation of new vessels through release of growth factors (2). Several strategies based on the administration of one pro-angiogenic factor have enhanced vascularization and tissue recovery in preclinical settings, however, they have not been approved during clinical trials because of safety and/or efficacy concerns (3). The failure of these single factor-based therapies has uncovered the issue whether the delivery of one factor alone is safe and effective to produce therapeutic angiogenesis (4).

Vascular Endothelial Growth Factor A₁₆₄ (VEGF) is the master regulator of angiogenesis, being able to promote the activation of the angiogenic process that is followed by a maturation phase with the recruitment of mural cells via regulation of additional factors, such as platelet derived growth factor-BB (PDGF-BB) (5). Based on this, most clinical trials for pro-angiogenic gene therapy have been done by using VEGF, however, they have not been successful because of VEGF-induced side effects, among which uncontrolled vessel growth (3, 6). Taking advantage of a highly controlled cell-based delivery platform, we have previously demonstrated that the activity of VEGF overexpression in skeletal muscle is tightly mediated by its micro-environmental dosage, forming either normal capillaries wrapped by pericytes at low levels, or angioma-like structures covered by smooth muscle cells at high ones (7). Interestingly, VEGF and PDGF-BB co-expression completely prevents VEGF-induced aberrant angiogenesis, promoting a network of homogeneous capillaries covered by pericytes. Vice versa, endogenous PDGF-BB blockade reverts VEGF-induced angiogenesis from normal to aberrant vessels (8). These results clearly reveal the key role of PDGF-BB in normalizing VEGF-induced angiogenesis by recruiting pericytes, which interact with endothelial cells by activating a variety of paracrine signals to achieve vessel maturation. However, it is completely unknown which pericyte-endothelium specific pathway, or combination of signals, may be responsible of the normalization of vessels newly induced by VEGF overexpression in skeletal muscle. Identifying and targeting these pathways could allow overcoming some limitations related to the use of VEGF as a single factor in gene-delivery approaches for therapeutic angiogenesis (6).

Genetic studies in mouse demonstrated that a group of receptor tyrosine kinases (RTK) with their cognate ligands, is crucial in the endothelium-pericyte interaction during the development of the embryonic vasculature, among which there are transforming growth factor beta-1 receptor (TGF β R)/TGF- β 1, Tie2/Angiopoietin-1 (Ang-1), and EphB4/EphrinB2 (9). Besides the vascular development, these pathways regulate adult angiogenesis (10, 11). TGF- β 1 is synthesized by, and can signal to, both endothelial and mural (pericytes and smooth muscle cells) cells, and it can trigger different, even opposite, effects according to the activation of its two receptors, activin receptor-like kinase (Alk)-1 and Alk-5 (9). Alk-1 activation promotes cell proliferation and migration, whereas Alk-5 prompts cell differentiation and quiescence (12). Similarly, the Tie2 receptor expressed by the endothelium, acts either in the activation or maturation phase of the angiogenic process by binding Ang-2 secreted by endothelial cells, or Ang-1 produced by pericytes, respectively (11, 13). EphrinB2/EphB4 signaling is bidirectional such that EphrinB2 ligand triggers reverse signaling, while EphB4 receptor activates the forward one. The expression of EphrinB2 ligand and EphB4 receptor defines arterial and venous specification in vascular development, respectively, but it also extends to area of postnatal neovascularization (14). Besides, expression of EphrinB2 by mural cells controls the association to EphB4-expressing endothelial cells (15, 16).

In the present study, we asked whether TGF- β 1/TGF β R, Ang-1/Tie2, and EphrinB2/EphB4 signaling pathways are responsible of the normalization of VEGF-induced angiogenesis by PDGF-BB-recruited pericytes. To address this question, we took advantage of a highly controlled gene transfer platform we previously

developed (17, 18), to investigate whether the inhibition of these pathways by soluble blockers, can switch VEGF-induced aberrant angiogenesis to normal. We discovered EphrinB2/EphB4 signaling to control angiogenesis induced by VEGF overexpression.

MATERIALS AND METHODS

Generation of retroviral vectors

The cDNA sequences of human latency associated peptide (LAP) and extracellular region of murine Tie2 conjugated to Fc (sTie2Fc) were kindly provided by collaborations and generated as previously described (19, 20). The cDNA of human soluble EphB4 was polymerase chain reaction (PCR) cloned from a full-length cDNA clone (ImaGenes GmbH, Berlin, Germany) using primers FW 5'-ATA GTCGAC ATGGAGCTCCGGGTGCTGCT-3' and RV 5'-T GCGGCCGC TCA CTGCTCCCCGCCAGCCCTCGCTCTCAT-3', as previously performed (21). The cDNA sequence of each soluble receptor was inserted into Sall/NotI restriction sites of pAMFG in a bicistronic construct with a truncated rabbit CD4 surface marker joined through an internal ribosomal entry sequence (ICD4), producing pAMFG.LAP.ICD4, pAMFG.sTie2Fc.ICD4, and pAMFG.sEphB4.ICD4. All generated plasmids were verified by sequencing.

Cell culture

Primary myoblasts isolated from C57BL/6 mice were previously infected to express specific VEGF microenvironmental doses, as previously described (17). In this study, we used a low VEGF-expressing myoblast clone (V Low clone ~ 60 VEGF

ng/10⁶ cells/day), and empty myoblasts (Ctrl). We infected V Low and Ctrl cells at high efficiency with pAMFG.LAP.ICD4, pAMFG.sTie2Fc.ICD4, pAMFG.sEphB4.ICD4, or pAMFG.ICD4 retroviruses. Briefly, myoblasts were incubated with fresh viral supernatants, supplemented with 8 µl/ml polybrene (Sigma-Aldrich, St. Louis, MO) for 15 min at 37°C, and centrifuged in a microplate carrier at 1,100 g for 30 min at room temperature. Transduced cell populations were FACS-sorted based on the staining of non-functional surface marker CD4, as following reported. For specific experiments a clone expressing high levels of VEGF was used (V High clone ~ 120 VEGF ng/10⁶ cells/day). All myoblasts were cultured in 5% CO₂ on collagen-coated dishes, with a growth medium consisting of 40% F10, 40% Dulbecco's modified Eagle's medium (DMEM) low glucose, 20% fetal bovine serum (FBS), 1% penicillin (P) and streptomycin (S) supplemented with 2.5 ng/ml FGF-2, as previously described (22).

Flow cytometric analysis and cell sorting

We assessed the expression of the truncated version of CD4 by individual transduced cells by staining the myoblasts with an antibody against rabbit CD4 directly conjugated to FITC (clone MCA799F, AbD Serotec). The staining was performed using 0.4 µg of antibody/10⁶ cells in 200 µl (1:50 dilution) of phosphate-buffered saline (PBS) with 5% BSA for 20 min in ice. Data were acquired using a FACS Calibur flow cytometer (Becton, Dickinson and Company) and analyzed using FlowJo software (Tree Star, Ashland, OR). Cell sorting was performed with a BD Influx cell sorter (Becton, Dickinson and Company).

Implantation of myoblasts into mice

To avoid an immunological response to transduced myoblasts, cells were implanted into 6- to 8-week-old immunodeficient SCID CB.17 mice (Charles River Laboratories, Wilmington, MA). Animals were treated in accordance with Swiss Federal guidelines for animal welfare, and the study protocol was approved by the Veterinary Office of the Canton of Basel-Stadt (Basel, Switzerland). Myoblasts were dissociated in trypsin and resuspended in sterile PBS with 0.5% BSA. According to the experiment, 10^6 cells in 10 μ l were implanted into the posterior auricular muscle, midway up the dorsal aspect of the external ear, or into the tibialis anterior (TA) and gastrocnemius (GC) muscles in the calf.

To perform gain of function of EphB4 signaling, mice were intraperitoneally injected with EphrinB2-Fc or control-Fc (R&D) at the concentration 1 mg/kg, twice weekly starting 3 days before the myoblast injection (23). Animals were sacrificed and samples collected and processed as following described.

Quantitative Real-Time PCR

For RNA extraction from the total tissue, TA and GC muscles previously injected with transgenic myoblasts were freshly harvested and disrupted using a Qiagen Tissue Lyser (Qiagen) in 1 ml of PBS+ 1% Trizol (Invitrogen). RNA was extracted according to manufacturer's instruction. RNA from total muscles was reverse transcribed into cDNA with the Omniscript Reverse Transcription kit (Qiagen) at 37 °C for 60 minutes. Quantitative Real-Time PCR (qRT-PCR) was performed on an ABI 7300 Real-Time PCR system (Applied Biosystems).

Expression of genes of interest was determined using commercial TaqMan gene expression assays (Applied Biosystems). The cycling parameters were: 50°C for 2 minutes, followed by 95°C for 10 minutes and 40 cycles of denaturation at 95°C for 15 seconds and annealing/extension at 60°C for 1 minute. Reactions were performed in triplicate for each template, averaged, and normalized to expression of the GAPDH housekeeping gene.

Tissue staining

The entire vascular network of the ear could be visualized following intravascular staining with a biotinylated *Lycopersicon esculentum* lectin (50 µg in 100 µl, Vector Laboratories). Mice were anesthetized and lectin was injected intravenously for 4 minutes. Then, the tissues were fixed by vascular perfusion of 1% paraformaldehyde and 0.5% glutaraldehyde in PBS pH 7.4 for 3 minutes and PBS for 1 minute. Ears were removed, bisected in the plane of the cartilage, and stained with X-gal staining buffer (1 mg/ml 5-bromo-4-chloro-3-indoyl-β-D-galactoside, 5 mM potassium ferricyanide, 5 mM potassium ferrocyanide, 0.02% Nonidet P-40, 0.01% sodium deoxycholate, 1 mM MgCl₂ in PBS pH 7.4). Tissues were stained using avidin-biotin complex-diaminobenzidine histochemistry (Vector Laboratories), dehydrated through an alcohol series, cleared with toluene and whole-mounted on glass slides with Permount embedding medium (Fisher Scientific). All images were taken with a 20X objective on an Olympus BX61 microscope (Olympus, Volketswil, Switzerland).

For tissue sections, mice were anesthetized and the tissues were fixed by vascular perfusion of 1 % paraformaldehyde in PBS pH 7.4 for 3 min under 120

mm/Hg of pressure. TA and GC muscles were collected and embedded in tissue freezing medium (OCT) compound (Sakura Finetek, Torrance, CA), frozen in isopentane, and cryosectioned. Tissue sections were then stained with X-gal (20 μ m sections) or with hematoxylin & eosin (10 μ m sections). The following primary antibodies and dilutions were used: rat monoclonal anti-mouse CD31 (clone MEC 13.3; BD Biosciences) at 1:100; mouse monoclonal antimouse alpha-smooth muscle actin (α -SMA) (clone 1A4; MP Biomedicals, Irvine, CA) at 1:400; rabbit polyclonal anti-NG2 (Chemicon, Temecula, CA) at 1:200; rabbit anti-Ki67 (Abcam, Cambridge, UK) at 1:100. Fluorescently labeled secondary antibodies (Invitrogen, Carlsbad, CA) were used at 1:200. Sections were then washed 3 times in PBS and mounted with Faramount Aqueous Mounting Medium (Dako), and images were acquired using both Olympus BX61 microscope (Olympus, Volketswil, Switzerland) and Zeiss LSM 710 confocal microscope (Carl Zeiss, Feldbach, Switzerland).

To study vessel perfusion, fluorescein isothiocyanate (FITC)-labeled *Lycopersicon esculentum* lectin (50 μ g in 50 μ l; Vector Laboratories) was injected into the femoral vein and allowed to circulate for 4 minutes before perfusion of fixative.

Vessel analysis

Vessel diameters were measured in whole mounts of ears stained with intravascular *L. esculentum* lectin perfusion, and leg tissue sections stained with fluorescently labeled antibodies against endothelium (CD31), pericyte (NG2), and smooth muscle cell (α -SMA). Briefly, vessel diameters were measured by overlaying captured microscopic images with a square grid. Squares were

randomly chosen, and the diameter of each vessel (if any) in the center of selected squares was measured. To avoid selection bias, we systematically measured the shortest diameter in the selected vascular segment. We analyzed from 3 to 5 fields from each of 6 analyzed ears per group ($n = 6$) and from 3 to 10 fields from each of 3 analyzed legs per group ($n = 3$). All images were taken with a 20X objective on an Olympus BX61 microscope (Olympus, Volketswil, Switzerland) and analyses were performed with Cell Sense software (Olympus, Volketswil, Switzerland).

Qualitative analysis of vascular morphology in immunofluorescence images was performed on all vascular structures visible in at least 3 fields/section with a 40X objective on a Carl Zeiss LSM710 3-laser scanning confocal microscope (Carl Zeiss, Feldbach, Switzerland) in at least 5 sections/muscle, cut at 150 μm of distance from each other, in 3 muscles/group.

Ki67 positive endothelial cells were quantified from the total amount of endothelial cells (300–800 total endothelial cells were counted per condition and per time-point) in up to 3 vascular enlargements visible in each of 3–5 fields in each area of effect. At least five areas with a clear angiogenic effect were analyzed per group.

Statistical analysis

Data are presented as mean \pm standard error. The significance of differences was evaluated using analysis of variance (ANOVA) followed by the Bonferroni test (for multiple comparisons), or using a Mann Whitney test (for single comparisons); $P < 0.05$ was considered statistically significant.

RESULTS

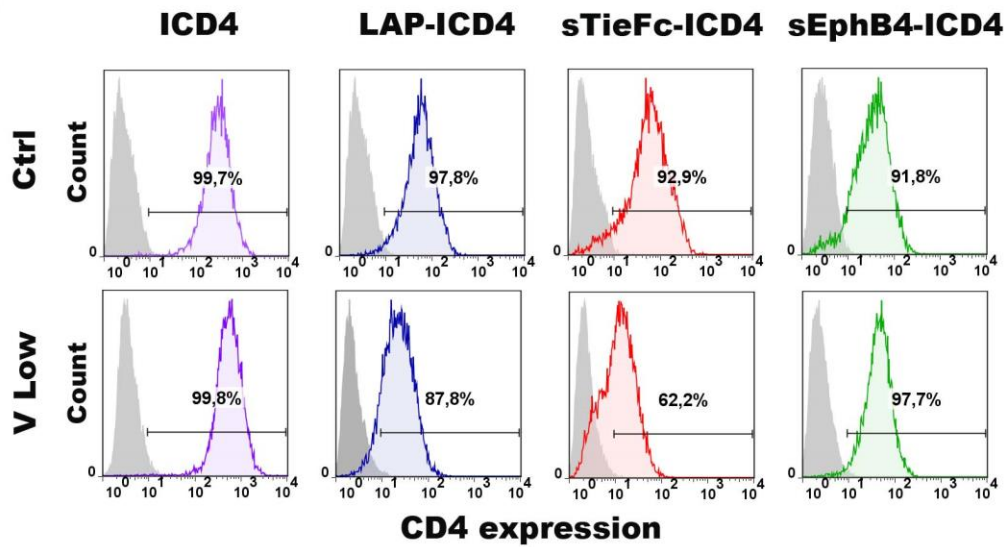
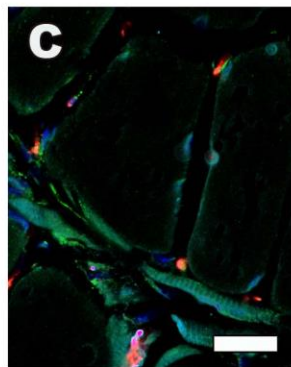
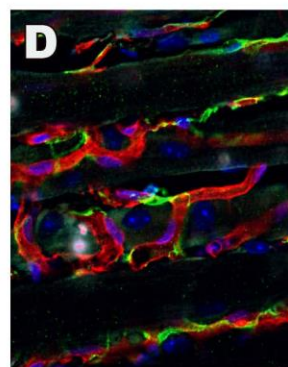
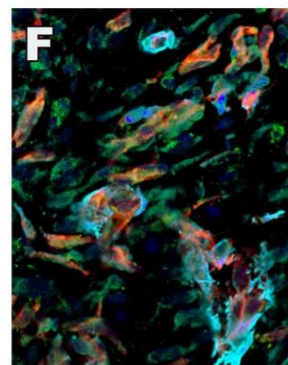
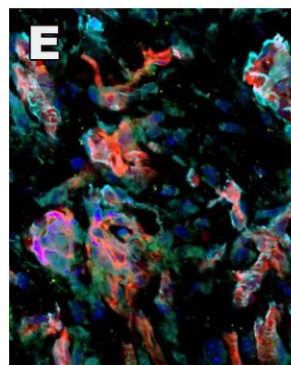
Triple blockade of TGF- β 1/TGF β R, Ang-1/Tie2, and EphrinB2/EphB4 paracrine signals reverts VEGF-induced normal angiogenesis to aberrant

To investigate by which mechanisms the endothelium-pericyte crosstalk achieves the normalization of vessels newly induced by VEGF, we took advantage of our myoblast-based gene delivery platform. From our pool of myoblast clones, we selected one population that expresses specific low VEGF levels (V Low = 68 ± 9 ng/ 10^6 cells/day) that form normal angiogenesis (17, 24). cDNA sequences encoding LAP, sTie2Fc, and sEphB4 soluble receptors of TGF- β 1, Angs, and EphrinB2, respectively, were inserted into a bicistronic construct together with a FACS-quantifiable surface marker (trCD4) (Fig. 1A), and retroviral vectors were produced (17). V Low myoblast clone and empty myoblasts were retro-transduced and the following groups were generated: V Low-CD4 (V Low), V Low LAP-CD4 (V Low LAP), V Low sTie2Fc-CD4 (V Low sTie2-Fc), V Low sEphB4-CD4 (V Low sEphB4), Ctrl LAP-CD4 (Ctrl LAP), Ctrl sTie2Fc-CD4 (Ctrl sTie2-Fc), and Ctrl sEphB4-CD4 (Ctrl sEphB4). After transduction, cell were sorted based on the expression of CD4 surface marker, and FACS analysis proved the generation of CD4 highly positive myoblasts as depicted in Fig. 1B. Moreover, enzyme-linked immune sorbent assay (ELISA) confirmed previous VEGF expression values, excluding any effect by the transduction procedure on the exogenous VEGF expression by V Low cells (V Low = 64 ± 3 , V Low LAP = 64 ± 6 , V Low sTie2-Fc = 79 ± 4 , V Low sEphB4 = 62 ± 5 ng/ 10^6 cells/day) (17) (24).

We firstly verified whether endogenous PDGF-BB-mediated pericyte recruitment normalizes low VEGF-induced angiogenesis at least through one of the TGF- β 1/TGF β R, Ang-1/Tie2, and EphrinB2/EphB4 signaling pathways, by implanting a pool of blocker expressing-V Low myoblast clones into the tibialis anterior (TA) and gastrocnemius lateralis (GC) muscles in the hind limb of adult SCID mice. As control, we injected myoblasts expressing only the blockers (Ctrl 3b). By 14 days after cell injection, control myoblasts did not perturb either the preexisting vasculature or skeletal muscle tissue, as shown in Fig. 1C. Instead, the expression of the three soluble receptors switched angiogenesis by low VEGF doses from normal to aberrant, forming vessels with enlarged and irregular diameter and covered by a patchy layer of α -SMA⁺ mural cells, similar to the classic angioma-like structures previously detected at high VEGF levels (Fig. 1D-F) (7).

Taken together, these results indicate that the TGF- β 1/TGF β R, Ang-1/Tie2, and EphrinB2/EphB4 signaling pathways together are crucial for the normalization of VEGF-newly induced capillaries by PDGF-BB endogenous-mediated pericyte recruitment.

Figure 1 Triple blockade of specific pericyte-endothelium paracrine signals switches VEGF-induced angiogenesis from normal to aberrant. A) Retroviral constructs used to generate myoblast populations expressing soluble blocker and CD4 truncated surface marker. B) Generation of CD4 highly positive myoblasts by retroviral infection and FACS-based isolation. C-F) Immunofluorescence staining of endothelium (CD31, in red), pericyte (NG2, in green), and smooth muscle cell (α -SMA, in cyan) on frozen sections of leg skeletal muscles of mice injected with myoblasts expressing the three blockers alone (Ctrl 3b), or with VEGF (V Low 3b), or VEGF alone (V Low), and sacrificed at 14 days after cell injection. C) Ctrl 3b did not affect skeletal tissue vasculature. D-F) Triple blockade switched normal angiogenesis induced by low VEGF levels to aberrant. Size bars= 25 μ m.

A**pAMFG-blocker****B****Ctrl 3b****V Low****V Low 3b****DAPI CD31 NG2 αSMA**

Blockade of EphrinB2/EphB4 signaling pathway, but not of TGF- β 1/TGF β R and Ang-1/Tie2, switches VEGF-induced angiogenesis from normal to aberrant

In order to understand whether TGF- β 1/TGF β R, Ang-1/Tie2, and EphrinB2/EphB4 pathways contribute together or alone to the switch of angiogenesis induced by low VEGF doses from normal to aberrant, we injected the three blocker-secreting V Low myoblast populations alone into TA and GC muscles. By 2 weeks after myoblast implantation, normal angiogenesis newly induced by V Low was not affected either by TGF- β 1/TGF β R or Ang-1/Tie2 signaling inhibition, in fact, we observed capillaries homogeneous in size and morphology tightly covered by NG2⁺/ α -SMA⁻ pericytes, similarly to control vessels (Fig. 2A, B, and C). Instead, EphrinB2/EphB4 signaling blockade displayed a mixture of normal and aberrant new vessels at low VEGF doses (Fig. 2D-F). Closed to area of normal capillaries, we observed glomeruloid bodies with a mantel of NG2⁺/ α -SMA⁺ mural cells, and irregularly enlarged structures lacking NG2⁺/ α -SMA⁻ pericytes and wrapped, instead, by long protrusions of NG2⁻/ α -SMA⁺ mural cells, resembling the aberrant phenotype generated by high VEGF doses (7). Pericytes covering normal capillaries induced by low VEGF doses become embedded within a capillary basement membrane (BM), as indicated by laminin staining that wraps NG2⁺ cells (Fig. 3J and M). Instead, the exclusion of NG2⁻/ α -SMA⁺ cells from the BM suggested that endothelium wall of abnormal vessels caused by V Low sEphB4 cells was covered by proper smooth muscle cells (Fig. 3K, L, N, and O) (9).

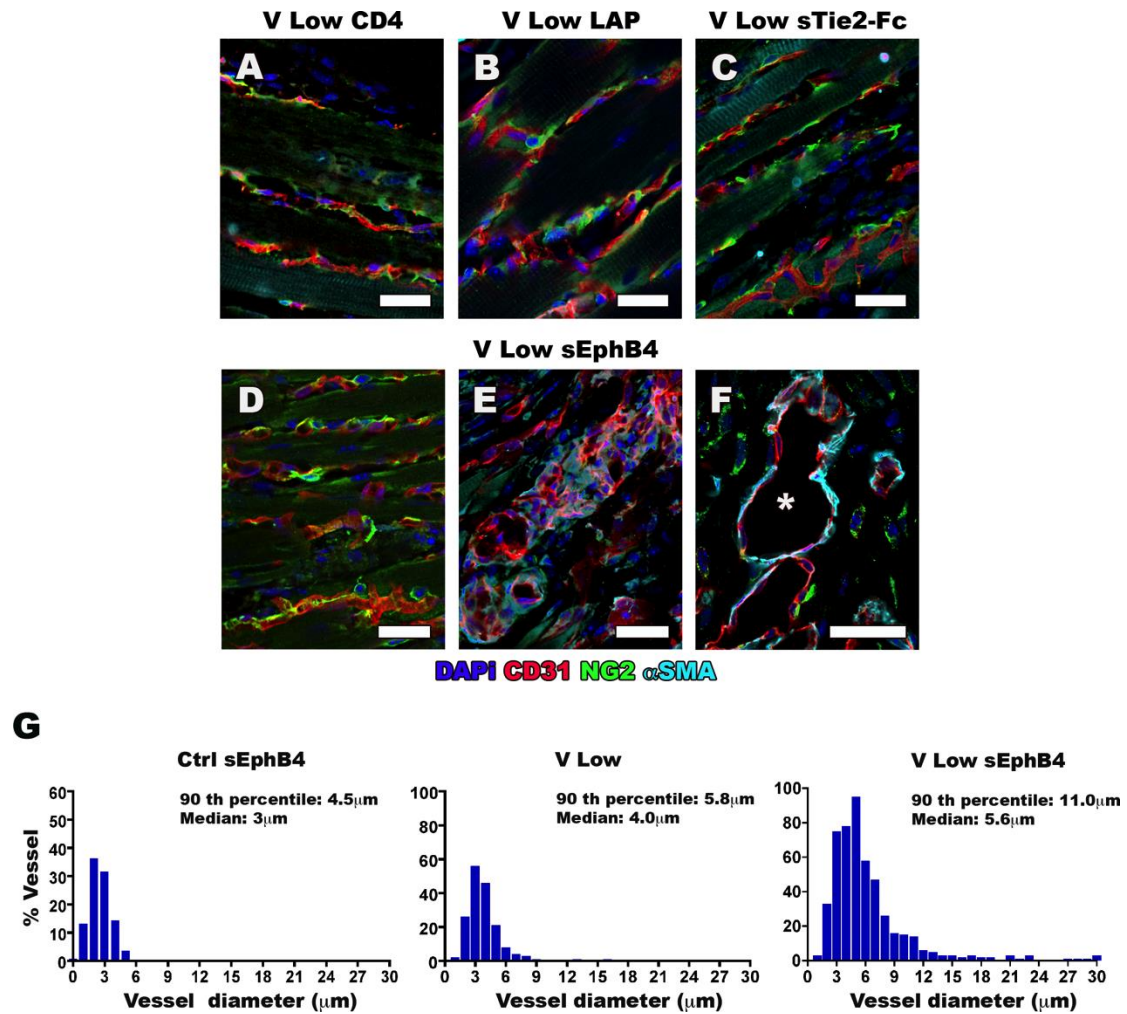


Figure 2 EphrinB2/EphB4 signaling blockade, but not TGF- β 1/TGF β R and Ang-1/Tie2, affects normal angiogenesis by low VEGF doses. A-F Immunofluorescence staining of endothelium (CD31, in red), pericyte (NG2, in green), and smooth muscle cell (α -SMA, in cyan) on frozen sections of leg skeletal muscles of mice injected with myoblasts expressing low VEGF doses alone (V Low), or with LAP (V Low LAP), sTie2-Fc (V Low sTie2-Fc), sEphB4 (V Low sEphB4) blocker, and sacrificed at 14 days post cell injection. Neither TGF- β 1/TGF β R nor Ang-1/Tie2 pathway blockade impaired normal angiogenesis by low VEGF doses (A-C), instead, EphrinB2/EphB4 pathway inhibition induced a mixture of normal and aberrant vessels (D-F). Size bars= 25 μ m. G) Vascular diameter distribution was quantified on immunostained cryosections from leg skeletal muscles collected at 14 days post implantation of Ctrl sEphB4, V Low, and V Low sEphB4 myoblasts. n= 3 legs per group.

Quantification of vascular diameter distribution showed that vessels in areas implanted with control Ctrl sEphB4 cells were uniformly distributed around a median of 3.0 μ m and 90th percentile of 4.5 μ m. Similarly, V Low cells induced a homogeneous population of vascular enlargements with a median of 4.0 μ m and 90th percentile of 5.8 μ m. Instead, V Low sEphB4 myoblasts caused a significantly higher degree of vascular diameter reflected by a heterogeneous distribution

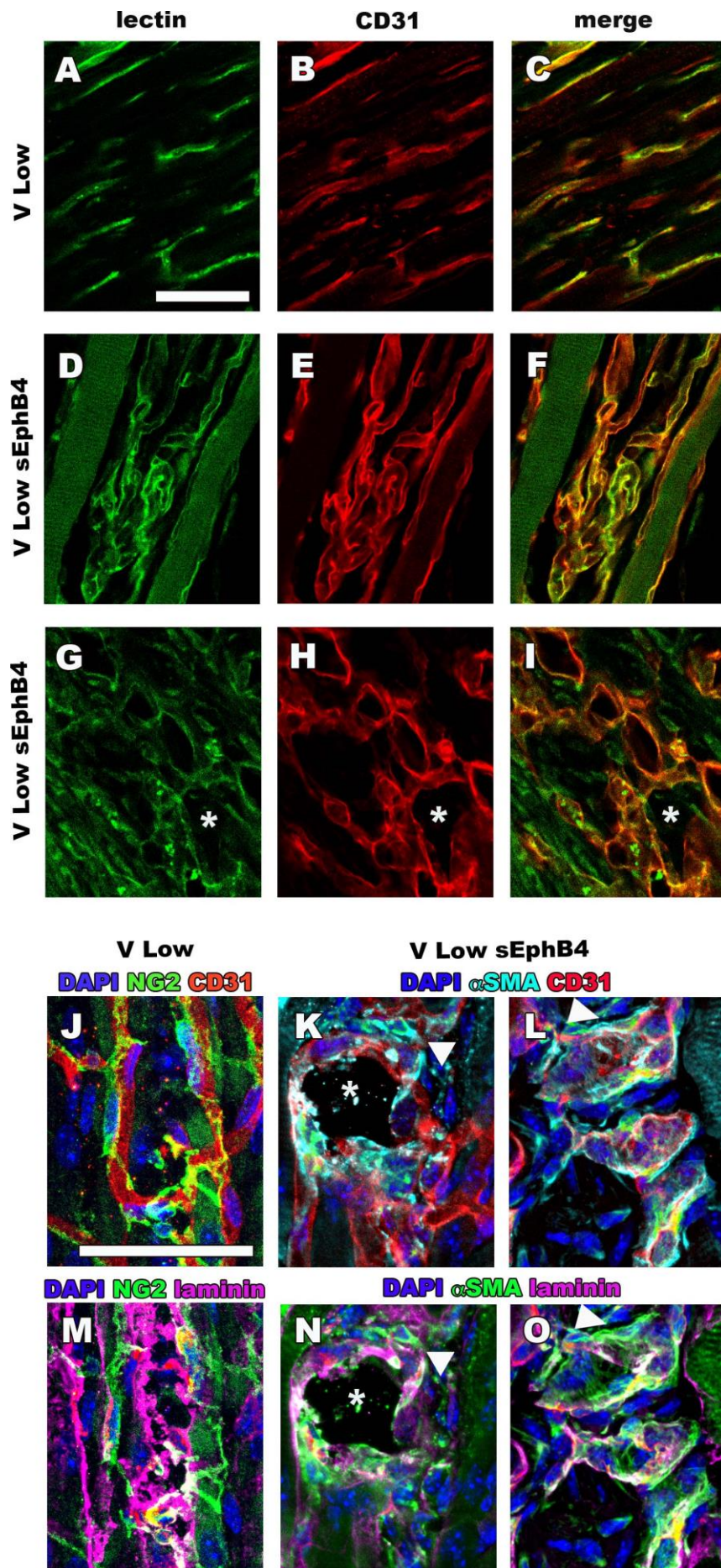


Figure 3 Aberrant vessels newly induced by V Low sEphB4 cells are functionally connected to the circulation and covered by smooth muscle cells. A-I) Mice received intravenous injections of FITC-lectin 2 weeks after implantation of V Low and V Low sEphB4 myoblast clones. Frozen sections were immunostained for the endothelial marker CD31 (red) and perfused structures were visualized by FITC-lectin (green). J-O) Immunofluorescence staining of endothelium (CD31), pericytes (NG2), smooth muscle cell (α -SMA), nuclei (dapi), and basement membrane (laminin) on frozen sections of leg skeletal muscles of mice injected with myoblasts expressing low VEGF doses alone or together with sEphB4 blocker, and sacrificed at 14 days after cell injection. Low VEGF levels caused vascular normal capillaries covered by NG2⁺ pericytes embedded into basement membrane (J and M), whereas the co-expression of sEphB4 blocker induced vascular enlargements which were associated with α -SMA⁺ smooth muscle cells external to it (white arrowheads) (K, L, N, and O). Size bars= 25 μ m.

with a median of 5.6 μ m and 90th percentile of 11.0 μ m (average diameter: Ctrl sEphB4 = 3.1 ± 0.03 μ m, V Low = 4.3 ± 0.1 μ m, and V Low sEphB4 = 6.7 ± 0.2 μ m; $P < 0.001$) (Fig. 2G).

Intravascular staining by FITC-labeled tomato lectin, which binds to the luminal endothelial wall of vessels, co-localized with endothelium staining (CD31), indicating that aberrant capillaries caused by V Low sEphB4 cell injection, were functionally perfused (Fig. 3D-I), in line with the observations made on angioma-like structures induced by high VEGF doses (25).

To investigate the evolution of abnormal angiogenesis by co-expression of low VEGF doses and sEphB4 blocker, we injected V Low, V Low sEphB4, and Ctrl sEphB4 myoblasts into posterior auricular (ear), and TA and GC muscles of SCID mice, and collected the tissues at 4 weeks post myoblast implantation. We noticed the persistence of aberrant angiogenesis by V Low sEphB4 myoblasts by histological staining on both ears and leg tissue sections, compared to control tissues injected with V Low cells (Fig. 4A-H). Co-expression of low VEGF levels and sEphB4 soluble receptor displayed enlarged vessels and disorganized multi-lumen capillaries covered by NG2⁺/ α -SMA⁺ mural cells (Fig. 4C and D). Quantification of vessel diameter distribution on whole mount ears stained with lectin (Fig. 4E-H), confirmed the formation of a significant number of enlarged vessels by V Low

sEphB4 cells, as indicated by the tail of Gaussian curve with a 90th percentile of 15.7 μm compared to V Low, which led to a 90th percentile of 7.6 μm (average diameter: Ctrl sEphB4 = $5.2 \pm 0.1 \mu\text{m}$, V Low = $5.5 \pm 0.1 \mu\text{m}$, and V Low sEphB4 = $8.9 \pm 0.4 \mu\text{m}$; $P < 0.001$) (Fig. 4E-I).

Taken together, these results suggest that EphrinB2/EphB4 pathway, but not TGF- β 1/TGF β R and Ang-1/Tie2, is pivotal for pericyte-endothelium crosstalk for forming normal capillaries upon delivery of low VEGF doses.

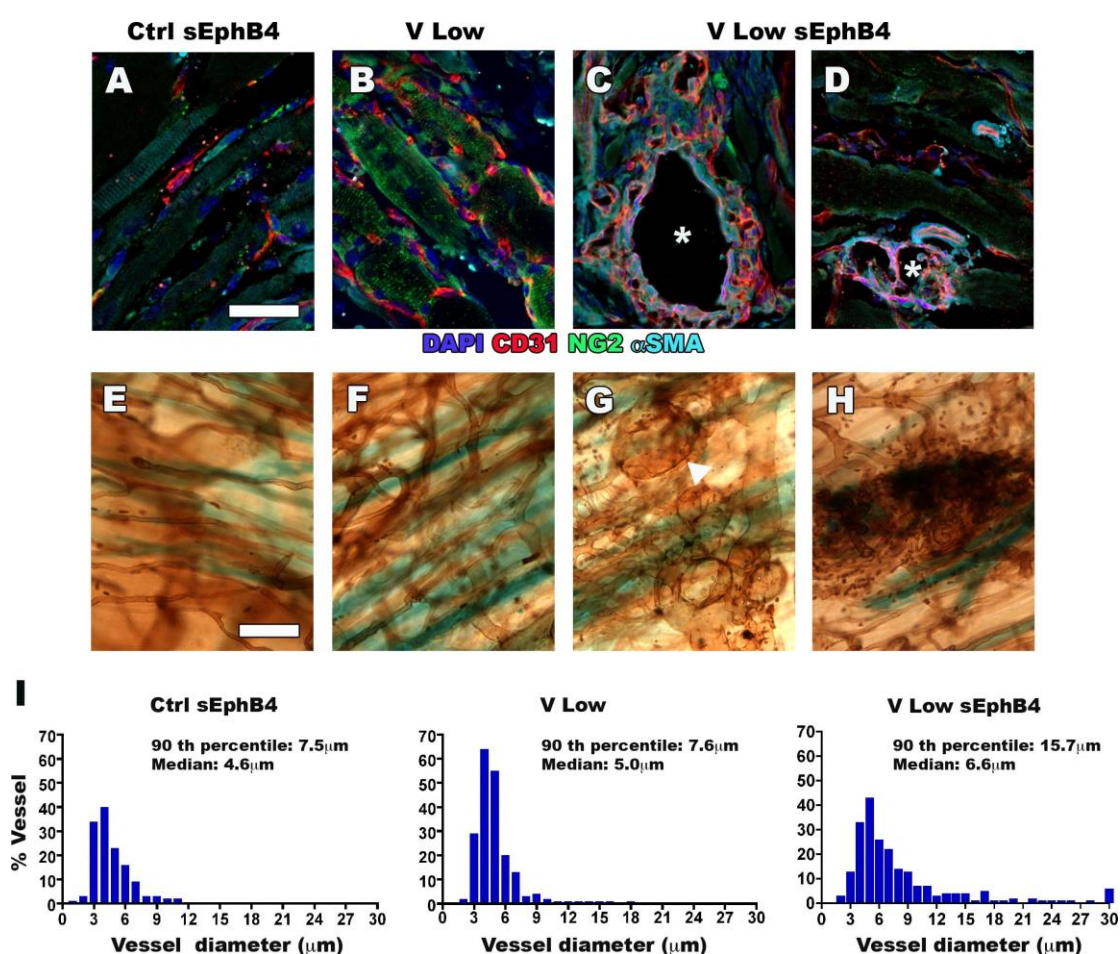


Figure 4 Persistence of abnormal angiogenesis induced by EphrinB2/EphB4 signaling blockade upon implantation of low VEGF doses. A-D) Immunofluorescence staining of endothelium (CD31, in red), pericytes (NG2, in green), and smooth muscle cell (α -SMA, in cyan) on frozen sections of leg skeletal muscles of mice injected with myoblasts expressing sEphB4 (Ctrl sEphB4), low VEGF doses alone (V Low), or with sEphB4 (V Low sEphB4), and sacrificed at 28 days post cell implantation. Size bars= 25 μm . E-I). Blood vessels were visualized in whole-mount preparations after intravascular lectin perfusion (in brown) at 28 days. Quantification of vessel diameter distribution performed on ear skeletal muscle implanted with each cell population.

EphrinB2/EphB4 pathway blockade affects vascular remodeling of VEGF-induced angiogenesis

We sought to verify if EphrinB2/EphB4 pathway blockade affects vascular remodeling of angiogenesis newly induced by low VEGF levels. For this purpose, analyses on vascular morphology were conducted at early time points, i.e. 3, 4, and 7 days after the injection of myoblasts expressing VEGF alone or together with sEphB4 blocker. In regard to vascular remodeling, we have recently demonstrated that angiogenesis by VEGF overexpression in adult skeletal muscle, occurs via intussusception, which starts by vessel enlargement and proceeds with the formation of pillars that fuse together and divide longitudinally the affected vascular segment to form new capillaries. The initial vascular enlargement is crucial in intussusception and its degree is proportional to VEGF dose (24).

By 3 days after cell injection, NG2⁺ pericytes were recruited to the area of vascular structures newly formed by low VEGF doses both in absence or presence of sEphB4 soluble receptor (Fig. 5A and B). In agreement with this, gene expression analysis in muscles implanted with V Low or V Low sEphB4 myoblasts showed similar regulation of endogenous PDGF-BB, which recruits mural cells (Fig. 5C) (10). However, careful examination of the histological staining revealed that upon co-expression of low VEGF doses and sEphB4 blocker, few NG2⁺/α-SMA⁺ mural cells covered the endothelium wall of enlarged structures newly induced, whereas only NG2⁺/α-SMA⁻ pericytes were observed in tissue injected with V Low alone (Fig. 5A-B).

By 4 days after cell injection, quantification of vessel diameter distribution indicated that both V Low and V Low sEphB4 formed vessel populations heterogeneous in size, however, the co-expression of sEphB4 blocker significantly enhanced the degree of vascular enlargement. In fact, V Low injection cells displayed a vascular diameter distribution with a median of 7.4 μm and 90th percentile of 12.3 μm , whereas, V Low sEphB4 led to a median of 9.3 μm and 90th percentile of 16.4 μm (average diameter: V Low = $8.0 \pm 0.2 \mu\text{m}$ and V Low sEphB4 = $10.8 \pm 0.3 \mu\text{m}$; $P < 0.0001$) (Fig. 5D, E, and F). Diameter quantification of vessels formed by high levels of VEGF doses (V High), generated a Gaussian curve with a 90th percentile of 15.3 μm , suggesting that V High and V Low sEphB4 similarly increased the degree of vascular enlargement compared to V Low (Supplementary Fig. 1). The divergent effect by V Low and V Low sEphB4 cells on diameter distribution of the vascular structures newly formed, was registered also at 3 and 7 days post cell injection, with V Low sEphB4 leading an increase of the degree of vascular enlargement (Supplementary Fig. 2).

After 7 days post myoblast implantation, low VEGF doses alone gave rise to a network of homogenous and mature capillaries (Fig. 5G and H), whereas, the co-expression of sEphB4 soluble receptor yielded an heterogeneous vascular phenotype characterized by the presence of normal angiogenesis, but also mural cell-naked capillaries, and aberrant structures covered by NG2⁺/ α -SMA⁺ or NG2⁺/ α -SMA⁺ cells (Fig. 5I-L). The latter disparate mural phenotype was deeper investigated in combination with a staining for basement membrane, which suggested a pericytic identity for the NG2⁺ cells embedded into the basement

membrane, while defined smooth muscle cells the α -SMA⁺ cells external to this layer (Fig. 5M and N).

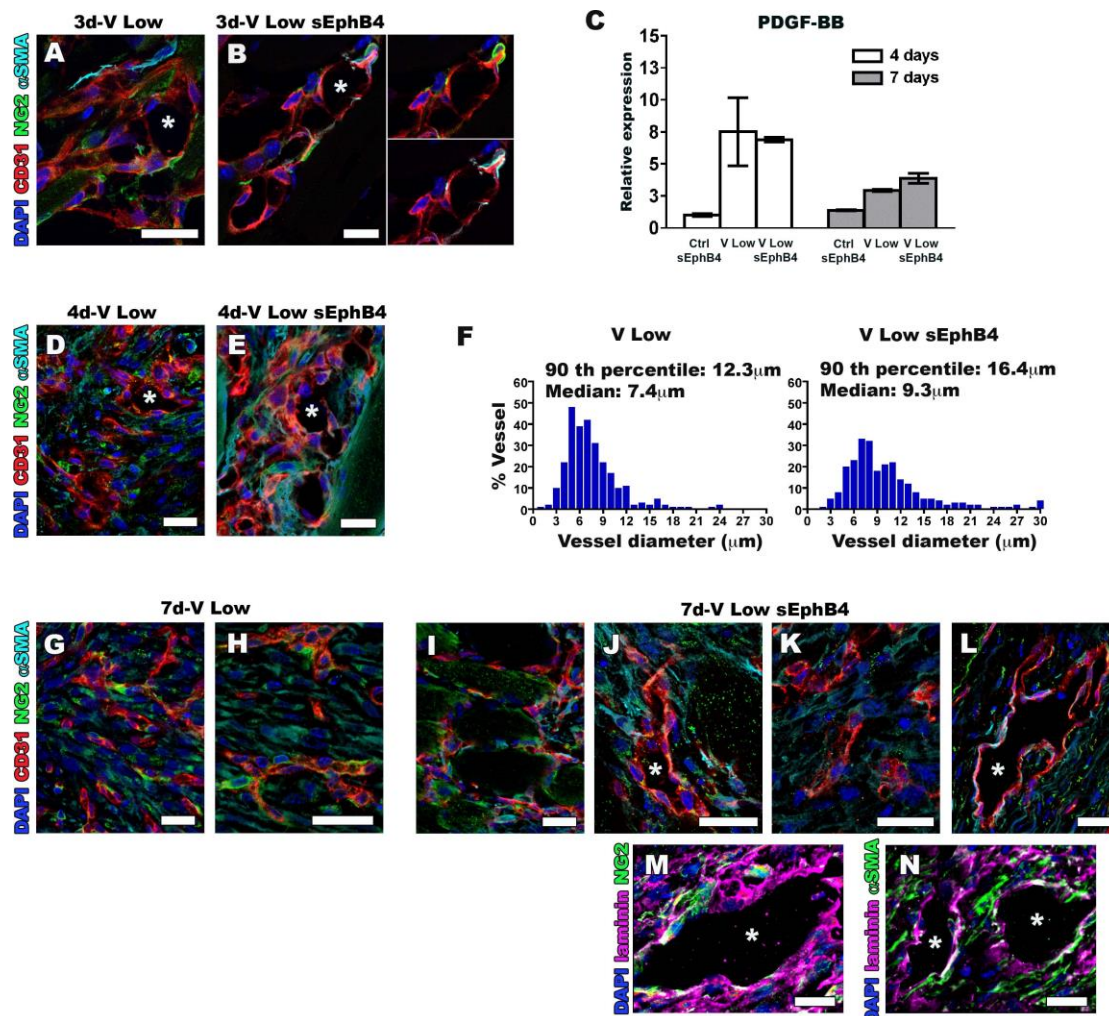


Figure 5 EphrinB2/EphB4 signaling blockade impairs vascular remodeling in hind limb muscles implanted with low VEGF doses. Immunofluorescence staining of endothelium (CD31, in red), pericytes (NG2, in green), smooth muscle cell (α -SMA, in cyan), and basement membrane (laminin, violet) on frozen sections of leg skeletal muscles of mice injected with V Low and V Low sEphB4. A-B) At 3 days post cell injection, normal NG2⁺/ α -SMA⁻ pericytes were recruited to vascular structures induced by V Low, while NG2⁺/ α -SMA⁺ mural cells were observed in those generated by V Low sEphB4. C) Analysis of PDGF-BB endogenous expression was conducted on total RNA extracted from TA and GC muscles harvested at 4 and 7 days after implantation of Ctrl sEphB4, V Low, and V Low sEphB4. F) Quantification of vessel diameter distribution on immunofluorescence labeled cryosections (D-E) from skeletal muscles injected with V Low and V Low sEphB4 and collected at 4 days post cell injection. G-N) By 7 days after myoblast injection, V Low cells induced the formation of remodeled normal vascular network, whereas, V Low sEphB4 formed a mixture of NG2⁺/ α -SMA⁻ pericyte covered-normal capillaries, naked-vessels, and NG2⁺/ α -SMA⁺ smooth muscle cell-coated angioma structures. Size bars= 25 μ m.

Taken together, these results indicate that EphrinB2/EphB4 pathway blockade does not prevent the recruitment of pericytes by endogenous PDGF-BB. Nevertheless, the expression of sEphB4 blocker affects the mural coverage of

vessels newly formed by low VEGF levels, causing the loss of NG2⁺/α-SMA⁻ pericytes replaced by NG2⁺/α-SMA⁺ and NG2⁻/α-SMA⁺ cells, and increases the degree of vascular enlargement during intussusception remodeling, as observed in angiogenesis induced by high VEGF doses.

Aberrant vessels caused by co-expression of low VEGF doses and sEphB4 blocker, are associated with endothelial cell proliferation

In intussusception angiogenesis induced by VEGF overexpression, the initial vascular enlargement is associated with endothelium proliferation that depends on VEGF signaling (24). Therefore, we verified if EphrinB2/EphB4 pathway inhibition affects vascular enlargement upon delivery of low VEGF levels by influencing cell proliferation.

After 4 days post cell injection, the number of Ki67-positive cells indicated that the structures induced by both V Low and V Low sEphB4 myoblasts, had 50% of endothelium actively proliferating as shown by the Fig. 6 (A, C, and E). At 7 days post myoblast implantation, endothelial cells in the normal vascular network newly induced by low VEGF levels drastically decreased down to 8% (Fig. 6B and E). Similarly, the endothelial cells in the normal capillaries generated by V Low sEphB4 cells become quiescent (5%), while the endothelium of the aberrant vascular structures continued to proliferate (50%) (Fig. 6D and E).

Comparison of gene expression analysis performed on total skeletal muscles showed a significant difference of endogenous VEGF expression in tissues injected with control myoblasts (Ctrl sEphB4) compared to V Low and V Low

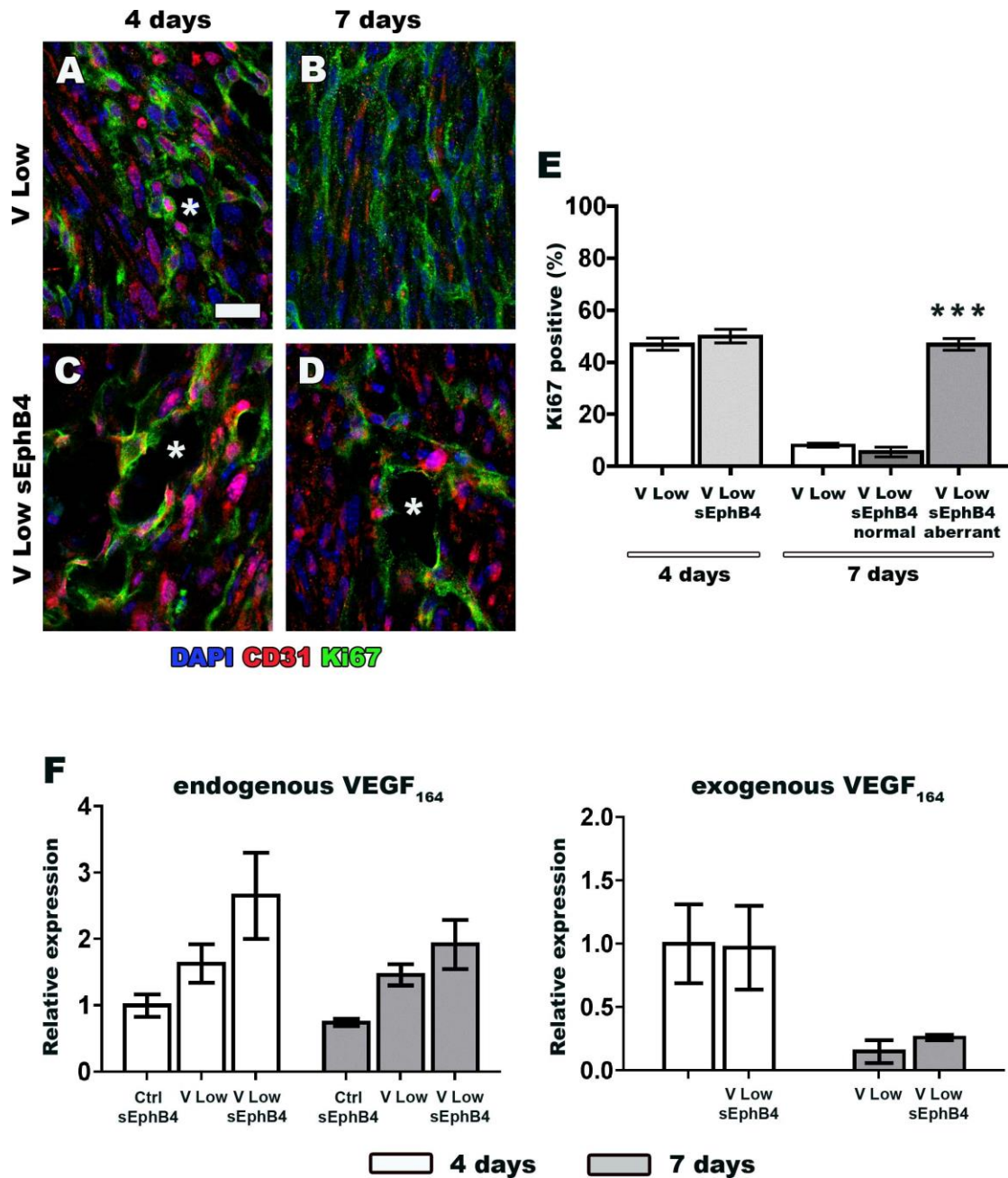


Figure 6 Endothelial cells of aberrant structures induced by V Low sEphB4 cells continue proliferate. A-D) Immunostaining with antibodies for endothelium (CD31, in green), proliferating cells (Ki67, in red), and with nuclei (DAPI, in blue) was performed on cryosections of skeletal muscles harvested at 4 and 7 days after implantation of V Low and V Low sEphB4 myoblasts. E) The percentage of proliferating endothelial cells was quantified in areas of effect, *** $P < 0.0001$, V Low vs V Low sEphB4 aberrant (*); $n = 3$ muscles per group, per time-point; size bars=25 μm . F) Expression of exogenous and endogenous VEGF was analyzed from total RNA extracted from TA and GC muscles harvested at 4 and 7 days after implantation with Ctrl sEphB4, V Low, and V Low sEphB4 myoblasts.

sEphB4, which instead did not diverge (Fig. 6F). The latter groups did not display any difference also in regard to exogenous VEGF expression (Fig. 6F).

Taken together, these results indicate that vascular enlargements observed by 4 days after the injection of V Low and V Low sEphB4 myoblasts, are characterized by similar endothelium proliferation. However, 7 days post cell implantation, cell proliferation percentage is higher in aberrant vessels generated by V Low sEphB4 compared to the one found in normal capillaries formed either by V Low or V Low sEphB4. Notably, this difference in cell proliferation is not dependent on VEGF dose.

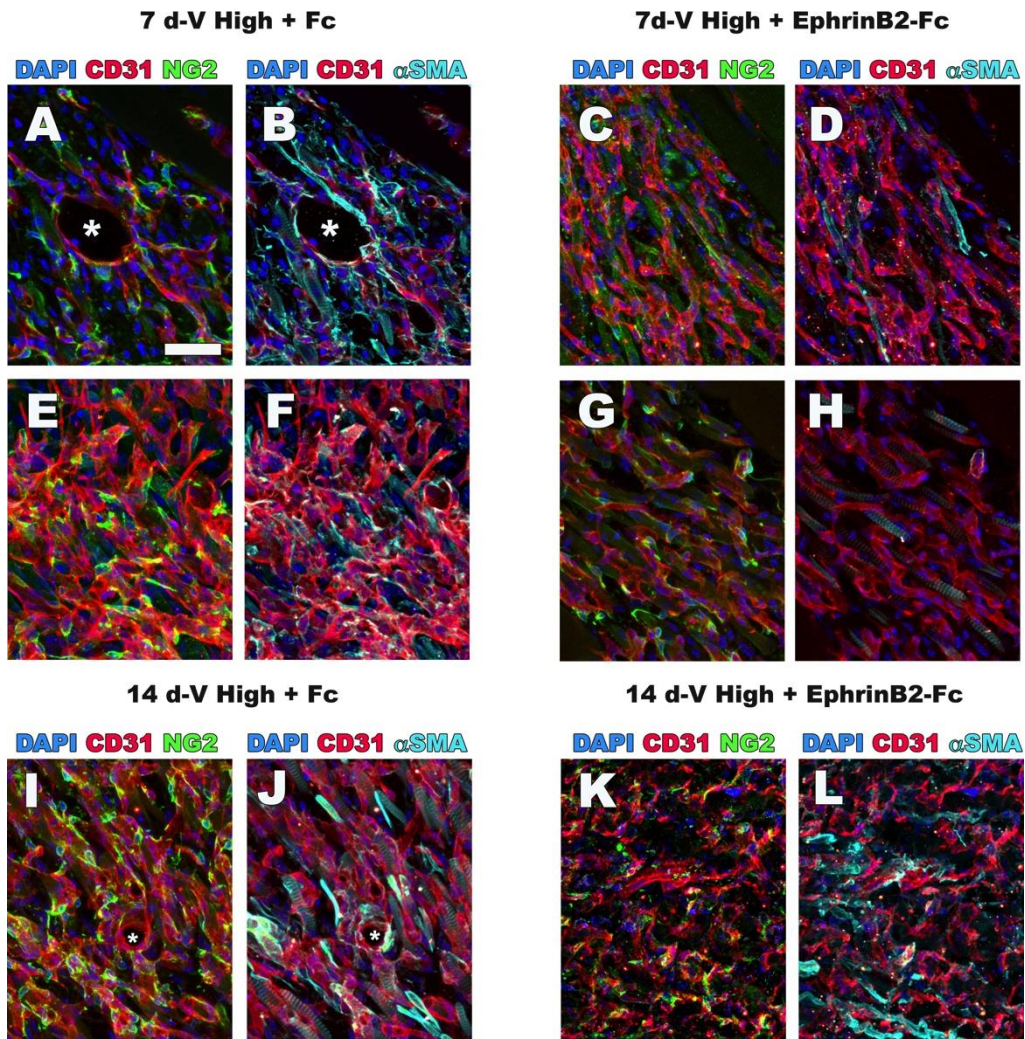
Activation of EphB4 signaling reverts aberrant angiogenesis induced by high VEGF doses to normal

To test the role of EphrinB2/EphB4 signaling in normalizing VEGF-induced angiogenesis, we verified whether the gain of function (GOF) of EphB4 signaling could revert aberrant angiogenesis by high VEGF levels to normal. For this purpose, we injected V High clone in TA and GC muscles of adult SCID mice, and treated systemically the animals with EphrinB2-Fc or Fc by intraperitoneal injection. The presence of Fc makes EphrinB2 able to form a dimer and therefore, activate EphB4 receptor (26). We collected the samples at 7 and 14 days after myoblast implantation and performed histological analysis. At both time points, high VEGF doses induced enlarged and tortuous capillaries, and angioma-like structures covered by NG2⁺/α-SMA⁺ smooth muscles cells, as expected (Fig. 7A, B, E, F, I, and J). Interestingly, GOF of EphB4 signaling caused V High clone to form a remodeled network of smaller diameter vessels covered by pericytes (Fig. 7C, D, G, H, K, and L). These observations were reflected by the quantification of vessel diameter distribution at 7 and 14 days post myoblast injection (Fig. 7M and N). In

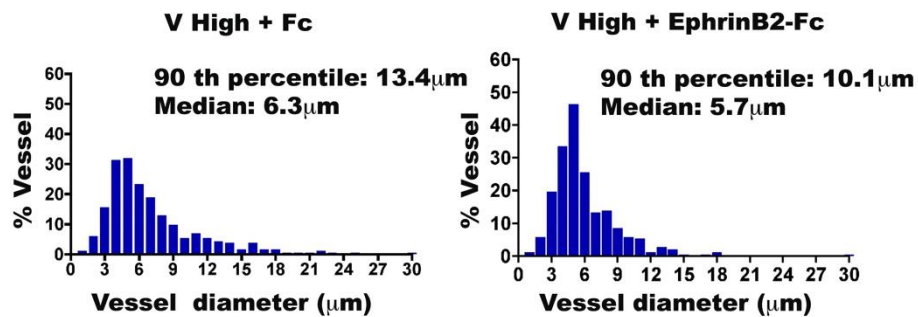
fact, by 7 days, the injection of V High together with Fc treatment yielded an heterogeneous vascular distribution with a median of 6.3 μm and 90th percentile of 13.4 μm , whereas V High combined with EphrinB2-Fc administration displayed a median of 5.7 μm and 90th percentile of 10.1 μm (Fig. 7M) (average diameter: V High + Fc = $7.7 \pm 0.2 \mu\text{m}$ and V High + EphrinB2-Fc = $6.5 \pm 0.2 \mu\text{m}$; $P < 0.0001$). The difference between the two conditions was striking at 14 days post cell injection, when we observed a heterogeneous vascular distribution upon V High cell injection and Fc treatment, characterized by a median of 6.7 μm and 90th percentile of 13.8 μm (Fig. 7N). Conversely, high VEGF levels injected into skeletal muscles of mice treated with EphrinB2-Fc, produced a vasculature with homogeneous diameter distribution (Fig. 7N), such that we found a median of 4.7 μm and 90th percentile of 7.9 μm (average diameter: V High + Fc = $8.1 \pm 0.2 \mu\text{m}$ and V High + EphrinB2-Fc = $5.4 \pm 0.2 \mu\text{m}$; $P < 0.0001$).

The normal vascular phenotype induced by GOF of EphB4 signaling could be due to regression of aberrant vessels. This was excluded by analyzing laminin staining that did not show any empty sleeve of vascular basement membrane, which serves as historical record of preexisting vessels (Fig. S3)(27).

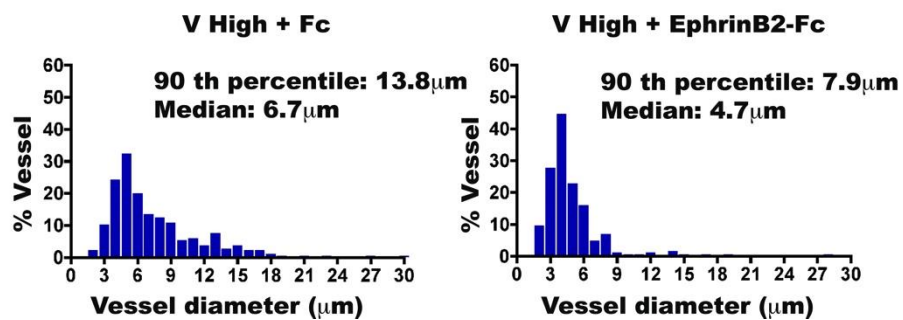
Figure 7 Gain of function of EphB4 signaling switches aberrant angiogenesis induced by high VEGF doses to normal. A-L) Vessels induced by implantation of V High cells in skeletal muscles of SCID mice treated with Fc or EphrinB2-Fc, were immunostained with antibodies against endothelium (CD31, in red), pericytes (NG2, in green), smooth muscle cells (α -SMA, cyan), and nuclei (DAPI, in blu) on frozen sections. Asterisks (*) indicate the lumen of an angioma-like structure devoid of pericytes and covered by smooth muscle cells. Size bars= 25 μm . M-N) The distribution of vessel diameters was quantified on immunofluorescence labeled cryosections.



M 7 days



N 14 days



DISCUSSION

In this work we tested the role of three specific endothelium-pericyte paracrine signals, i.e. TGF- β 1/TGF β R, Ang-1/Tie2, and EphrinB2/EphB4, in the transition from normal to aberrant angiogenesis by increasing VEGF doses. We discovered that neither TGF- β 1/TGF β R nor Ang-1/Tie2 affected normal vessels newly formed by low VEGF doses, whereas, EphrinB2/EphB4 signaling inhibition displayed angioma-like structures similar to the ones previously observed by expression of high VEGF doses (7).

TGF- β 1 has been described to regulate vessel formation by inhibiting sprouting angiogenesis (28, 29), while there are no evidences that support its activity in intussusception angiogenesis, which is the mode of vessels growth by VEGF overexpression in skeletal muscle (24). Moreover, the regulation of TGF- β 1 bioavailability is mediated by extracellular matrix remodeling (30) that occurs in sprouting (31), but is not so crucial in intussusception, as suggested by the differential gene and protein expression in the two mechanisms (32). These considerations lead us to speculate that TGF- β 1/TGF β R signaling does not act during intussusception, therefore, it does not regulate pericyte-endothelium crosstalk in angiogenesis induced by VEGF overexpression in skeletal muscle.

Ang-1/Tie2 signaling blockade did not reveal any mural cell coverage impairment, consistently with other works that demonstrated that neither Tie2 receptor nor Ang-1 ligand are required for pericyte enrollment to the endothelium (9). The capacity of Ang-1 to form enlarged blood vessels without inducing sprouting (33) suggests that this signaling could have a role in

intussusception. Nevertheless, our results did not show any vascular morphology impairment by sTie2-Fc soluble blocker. A likely explanation is that cell plasticity to Ang-1 is tissue and age-dependent, because Ang-1-induced effects were observed to occur in a critical developmental window (33). In line with this, the release of Ang-1 alone does not affect vasculature *per se* in adult tissue (34, 35). It is also plausible that in our system a redundancy of signaling overcomes Ang-1/Tie2 pathway blockade and preserves normal angiogenesis by low VEGF doses.

Contrary to the previous signaling pathways, we observed that the inhibition of EphrinB2/EphB4 pathway affected angiogenesis induced by low VEGF doses, producing a mixture of normal and aberrant capillaries. This disparate phenotype may be explained by our blocking strategy, since we did not completely silence the specific signaling, while we injected soluble blocker-expressing polyclonal myoblast populations in the skeletal tissue.

Our analyses converged to the conclusion that EphrinB2/EphB4 pathway blockade affects vascular remodeling of angiogenesis newly induced by low VEGF levels, at the level of vascular enlargement and mural coverage.

We tested whether there was a correlation between the increased degree of vascular enlargement caused by V Low sEphB4 compared to V Low and cell proliferation. Our data indicated that, by 4 days after cell injection, similar number of proliferating endothelial cells were present in the structures newly induced by co-expression of low VEGF levels and sEphB4 blocker compared to low VEGF alone, despite different vascular diameter distributions. Similar results were previously observed by comparing vessel diameter distribution and cell proliferation between V Low and V High (24). To deeply understand if there is an

association between vessel diameter and cell proliferation during vascular induction, we will verify whether endothelial cells start to proliferate earlier or proliferate faster in presence of sEphB4 blocker compared to V Low alone by 3 and 4 days post cell injection. Conversely, we registered an increase of endothelium proliferation in aberrant vessels newly formed by V Low and sEphB4 blocker compared to the normal capillary network caused by V Low alone at 7 days after cell injection. It is plausible that EphrinB2/EphB4 signaling inhibition triggers cell proliferation, since the activation of EphB4 receptor was described to inhibit cells proliferation in endothelial cells (23, 36).

Besides cell proliferation, endothelium motility and adhesion, which can be regulated by EphrinB2/EphB4 signaling, could induce an increase of the degree of vascular enlargement in presence of low VEGF doses and sEphB4 blocker compared to low VEGF alone (14).

Nevertheless, taken together our results on vascular diameter distribution lead us to speculate that while pillar formation occurs in presence of low VEGF levels, some mature pillars may fail to complete in the presence of an excessive diameter caused by EphrinB2/EphB4 pathway blockade, as previously caused by high VEGF doses (24).

In regard to mural coverage, at 3 days post cell implantation, EphrinB2/EphB4 signaling blockade did not interfere with mural cell recruitment, consistently with the results of Foo and coworkers, who showed that the number of mural cell-specific knockout of EphrinB2 recruited to the vasculature was comparable to control tissues, although they were scattered (15). Nevertheless, mural cells were not the classical identified NG2-positive pericytes, instead we

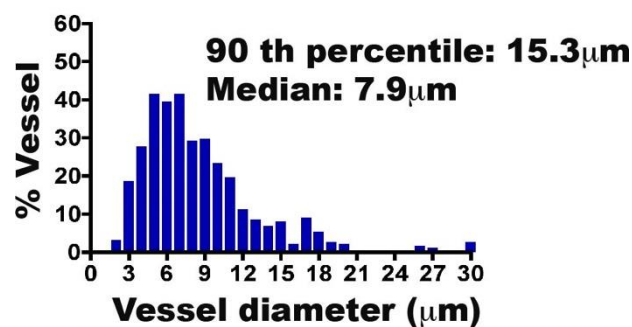
detected NG2 and α -SMA double positive cells. We hypothesize that EphrinB2 reverse signaling to mural cells, might cause differentiation from NG2-pericyte to α -SMA-positive smooth muscle cells. NG2 is associated to cytoskeleton components, while EphrinB2/EphB4 signaling coordinates cytoskeleton dynamics (14, 37), therefore EphrinB2/EphB4 signaling blockade may cause cytoskeleton changes that affect NG2 distribution and presentation. However, it is also possible that the growth of aberrant structures by itself impairs mural cell phenotype and promotes the differentiation to smooth muscles cells.

Contrary to the loss of function, the stimulation of EphB4 signaling reverted aberrant angiogenesis by high VEGF doses to normal, yielding the formation of remodeled capillary network. This is consistent with the results of Kimura and coworkers who showed that the activation of EphB4 receptor by EphrinB2 ligand induced the reduction of tumor growth through vascular normalization leading to mature narrow vessels (23). EphrinB2 normalizes high VEGF-induced angiogenesis likely by interfering with VEGF signaling, for example by reducing proliferation of endothelial cells induced by VEGF mainly through Ras/MAPK pathway, as described by Kim and coworkers (36).

In conclusion, our results show that EphrinB2/EphB4 signaling controls the switch between normal and aberrant angiogenesis by increasing VEGF doses, in particular EphrinB2 ligand can normalize VEGF-induced aberrant vessels. Therefore, in prospective of therapeutic angiogenesis approaches, EphrinB2 ligand could be co-delivered together with VEGF to target both vascular induction and maturation, thereby overcoming some limitations related to the use of VEGF as a single factor in gene-delivery.

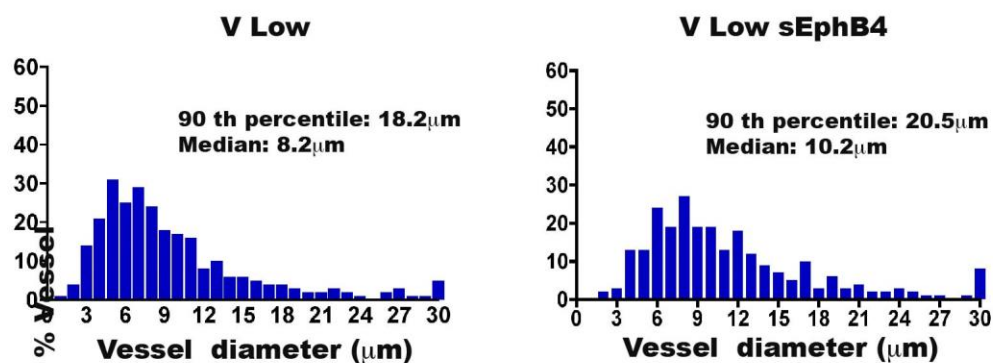
Supplementary Information

V High

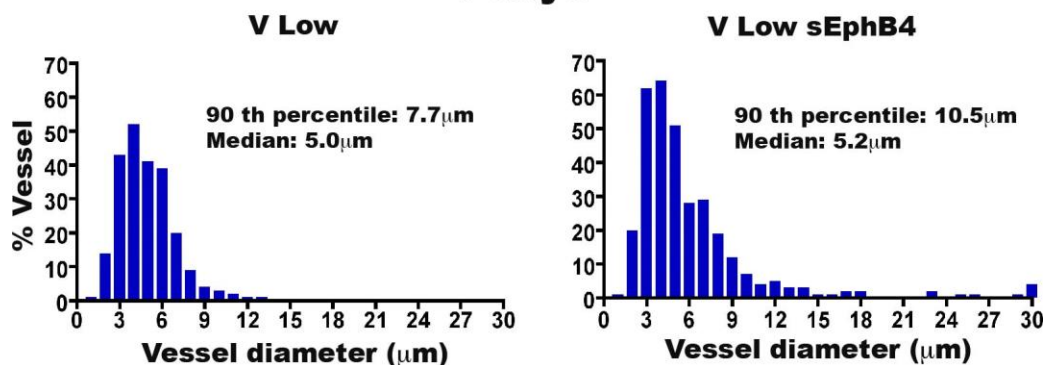


Suppl. Figure 1 Vascular diameter distribution quantified on immunostained cryosections of leg skeletal muscle of mice injected with high VEGF doses in leg skeletal muscles and sacrificed at 4 days post cell injection.

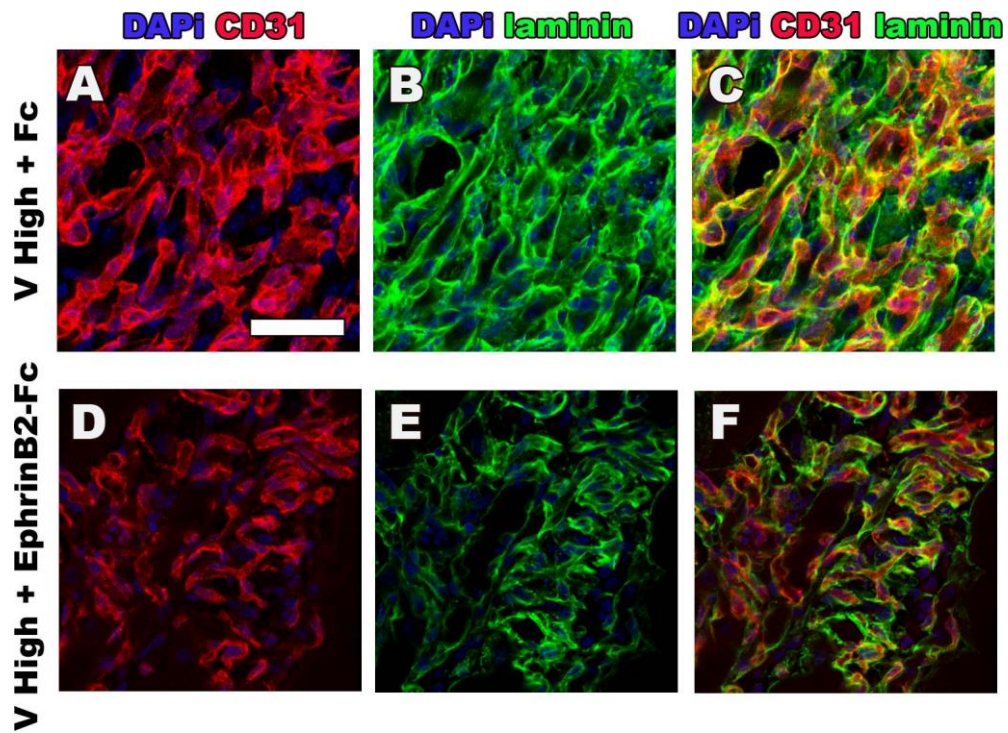
3 days



7 days



Suppl. Figure 2 Vascular diameter distribution quantified on immunostained sections from leg skeletal muscles of mice injected with low VEGF doses with or without co-expression of sEphB4 blocker, and sacrificed at 3 and 7 days after cell injection.



Suppl. Figure 3 **No vascular regression upon gain of function of EphB4 signaling.** Immunostaining for endothelium (CD31, in red), basement membrane (laminin, in green), and with nuclei (DAPI, in blue) was performed on cryosections of leg skeletal muscles of mice injected with myoblasts expressing high VEGF doses, treated with Fc or EphrinB2-Fc, and sacrificed at 2 weeks after cell injection. Size bars= 50 μ m.

References

1. G. Dragneva, P. Korpisalo, S. Yla-Herttuala, Promoting blood vessel growth in ischemic diseases: challenges in translating preclinical potential into clinical success. *Disease models & mechanisms* **6**, 312 (Mar, 2013).
2. B. H. Annex, Therapeutic angiogenesis for critical limb ischaemia. *Nature reviews. Cardiology*, (May 14, 2013).
3. H. Karvinen, S. Yla-Herttuala, New aspects in vascular gene therapy. *Current opinion in pharmacology* **10**, 208 (Apr, 2010).
4. C. Emanuelli, P. Madeddu, Changing the logic of therapeutic angiogenesis for ischemic disease. *Trends in molecular medicine* **11**, 207 (May, 2005).
5. A. Alfranca, VEGF therapy: a timely retreat. *Cardiovascular research* **83**, 611 (Sep 1, 2009).
6. S. Reginato, R. Gianni-Barrera, A. Banfi, Taming of the wild vessel: promoting vessel stabilization for safe therapeutic angiogenesis. *Biochemical Society transactions* **39**, 1654 (Dec, 2011).
7. C. R. Ozawa et al., Microenvironmental VEGF concentration, not total dose, determines a threshold between normal and aberrant angiogenesis. *The Journal of clinical investigation* **113**, 516 (Feb, 2004).
8. A. Banfi et al., Therapeutic angiogenesis due to balanced single-vector delivery of VEGF and PDGF-BB. *FASEB journal : official publication of the Federation of American Societies for Experimental Biology* **26**, 2486 (Jun, 2012).

9. A. Armulik, G. Genove, C. Betsholtz, Pericytes: developmental, physiological, and pathological perspectives, problems, and promises. *Developmental cell* **21**, 193 (Aug 16, 2011).
10. M. Potente, H. Gerhardt, P. Carmeliet, Basic and therapeutic aspects of angiogenesis. *Cell* **146**, 873 (Sep 16, 2011).
11. R. K. Jain, Molecular regulation of vessel maturation. *Nature medicine* **9**, 685 (Jun, 2003).
12. E. Pardali, M. J. Goumans, P. ten Dijke, Signaling by members of the TGF-beta family in vascular morphogenesis and disease. *Trends in cell biology* **20**, 556 (Sep, 2010).
13. P. Carmeliet, R. K. Jain, Principles and mechanisms of vessel normalization for cancer and other angiogenic diseases. *Nature reviews. Drug discovery* **10**, 417 (Jun, 2011).
14. O. Salvucci, G. Tosato, Essential roles of EphB receptors and EphrinB ligands in endothelial cell function and angiogenesis. *Advances in cancer research* **114**, 21 (2012).
15. S. S. Foo et al., Ephrin-B2 controls cell motility and adhesion during blood-vessel-wall assembly. *Cell* **124**, 161 (Jan 13, 2006).
16. O. Salvucci et al., EphrinB reverse signaling contributes to endothelial and mural cell assembly into vascular structures. *Blood* **114**, 1707 (Aug 20, 2009).
17. H. Misteli et al., High-throughput flow cytometry purification of transduced progenitors expressing defined levels of vascular endothelial growth factor induces controlled angiogenesis in vivo. *Stem cells* **28**, 611 (Mar 31, 2010).

18. G. von Degenfeld, A. Banfi, M. L. Springer, H. M. Blau, Myoblast-mediated gene transfer for therapeutic angiogenesis and arteriogenesis. *British journal of pharmacology* **140**, 620 (Oct, 2003).
19. E. P. Bottinger et al., The recombinant proregion of transforming growth factor beta1 (latency-associated peptide) inhibits active transforming growth factor beta1 in transgenic mice. *Proceedings of the National Academy of Sciences of the United States of America* **93**, 5877 (Jun 11, 1996).
20. P. Lin et al., Inhibition of tumor angiogenesis using a soluble receptor establishes a role for Tie2 in pathologic vascular growth. *The Journal of clinical investigation* **100**, 2072 (Oct 15, 1997).
21. S. He et al., Soluble EphB4 inhibition of PDGF-induced RPE migration in vitro. *Investigative ophthalmology & visual science* **51**, 543 (Jan, 2010).
22. A. Banfi, M. L. Springer, H. M. Blau, Myoblast-mediated gene transfer for therapeutic angiogenesis. *Methods in enzymology* **346**, 145 (2002).
23. M. Kimura et al., Soluble form of ephrinB2 inhibits xenograft growth of squamous cell carcinoma of the head and neck. *International journal of oncology* **34**, 321 (Feb, 2009).
24. R. Gianni-Barrera et al., VEGF over-expression in skeletal muscle induces angiogenesis by intussusception rather than sprouting. *Angiogenesis* **16**, 123 (Jan, 2013).
25. G. von Degenfeld et al., Microenvironmental VEGF distribution is critical for stable and functional vessel growth in ischemia. *FASEB journal : official publication of the Federation of American Societies for Experimental Biology* **20**, 2657 (Dec, 2006).

26. K. Kullander, R. Klein, Mechanisms and functions of Eph and ephrin signalling. *Nature reviews. Molecular cell biology* **3**, 475 (Jul, 2002).
27. F. Baffert et al., Cellular changes in normal blood capillaries undergoing regression after inhibition of VEGF signaling. *American journal of physiology. Heart and circulatory physiology* **290**, H547 (Feb, 2006).
28. C. Ito, T. Akimoto, T. Ioka, T. Kobayashi, E. Kusano, TGF-beta inhibits vascular sprouting through TGF-beta type I receptor in the mouse embryonic aorta. *The Tohoku journal of experimental medicine* **218**, 63 (May, 2009).
29. M. Ramsauer, P. A. D'Amore, Contextual role for angiopoietins and TGFbeta1 in blood vessel stabilization. *Journal of cell science* **120**, 1810 (May 15, 2007).
30. P. ten Dijke, H. M. Arthur, Extracellular control of TGFbeta signalling in vascular development and disease. *Nature reviews. Molecular cell biology* **8**, 857 (Nov, 2007).
31. B. Styp-Rekowska, R. Hlushchuk, A. R. Pries, V. Djonov, Intussusceptive angiogenesis: pillars against the blood flow. *Acta physiologica* **202**, 213 (Jul, 2011).
32. J. L. Williams et al., Differential gene and protein expression in abluminal sprouting and intraluminal splitting forms of angiogenesis. *Clinical science* **110**, 587 (May, 2006).
33. G. Thurston et al., Angiopoietin 1 causes vessel enlargement, without angiogenic sprouting, during a critical developmental period. *Development* **132**, 3317 (Jul, 2005).

34. A. Anisimov *et al.*, Vascular endothelial growth factor-angiopoietin chimera with improved properties for therapeutic angiogenesis. *Circulation* **127**, 424 (Jan 29, 2013).
35. N. Arsic *et al.*, Induction of functional neovascularization by combined VEGF and angiopoietin-1 gene transfer using AAV vectors. *Molecular therapy : the journal of the American Society of Gene Therapy* **7**, 450 (Apr, 2003).
36. I. Kim *et al.*, EphB ligand, ephrinB2, suppresses the VEGF- and angiopoietin 1-induced Ras/mitogen-activated protein kinase pathway in venous endothelial cells. *FASEB journal : official publication of the Federation of American Societies for Experimental Biology* **16**, 1126 (Jul, 2002).
37. X. H. Lin, K. Dahlin-Huppe, W. B. Stallcup, Interaction of the NG2 proteoglycan with the actin cytoskeleton. *Journal of cellular biochemistry* **63**, 463 (Dec 15, 1996).

Increasing VEGF doses impair vascular stabilization by directly inhibiting the Sema3A/CD11b⁺ NP-1⁺ monocyte/TGF- β 1 axis

Elena Groppa MSc¹, Silvia Reginato PhD¹, Roberto Gianni-Barrera PhD¹, Manuele G. Muraro PhD², Michael Heberer MD^{1,2} and Andrea Banfi MD¹

¹Cell and Gene Therapy and ²Oncology, Department of Biomedicine, University of Basel, and Department of Surgery, Basel University Hospital, Basel, Switzerland

Introduction

Therapeutic Angiogenesis (TA) is an attractive strategy that aims to induce normal, stable, and functional blood vessels by delivering angiogenic factors to ischemic tissues. Vascular Endothelial Growth Factor (VEGF) is the master regulator of vascular growth in both development and postnatal life, and it has long been recognized as the major molecular target to achieve TA (1). However, several studies have showed that uncontrolled and sustained VEGF expression by delivery of plasmid DNA (2, 3), adenoviral (4, 5) and adeno-associated (6, 7) vectors, or genetically engineered myoblasts (8, 9) has the potential to cause the growth of aberrant vascular structures and angioma-like tumors in both normal and ischemic tissues. On the other hand, *in vivo* inducible systems (10, 11) and systemic treatment with blocking reagents (12) showed that short-term VEGF

expression of less than about four weeks is insufficient to stabilize newly induced vessels, which regress after stimulus cessation. Therefore, it is desirable to accelerate vascular stabilization to enable short-term therapy.

The best understood mechanisms leading to newly induced vessel stabilization is the recruitment of pericytes that suppress endothelial cell proliferation and release endothelial cell-survival signals such as Angiopoietin-1 (Ang-1) and low levels of VEGF (13-15). Bone marrow (BM)-derived mononuclear cells have also been described to home to the sites of VEGF-induced adult angiogenesis, where they do not incorporate into the newly formed vessels (16, 17) and have been suggested to secrete paracrine factors beneficial for vessel development and cell survival (18). Recently, Zacchigna and coworkers have showed that a specific population of BM-derived myeloid cells, expressing both the monocyte marker CD11b and the VEGF co-receptor Neuropilin-1 (NP-1) and named therefore Neuropilin-Expressing Monocytes (NEM), favor vascular stabilization by secreting several paracrine factors, among which Transforming Growth Factor- β (TGF- β) and Platelet-Derived Growth Factor-BB (PDGF-BB) (19). Further, it was found that NEM recruitment can be increased by Semaphorin 3A (Sema3A), a glycoprotein that is expressed by endothelial cells and can act as an anti-angiogenic factor (19, 20).

During developmental angiogenesis, VEGF activity is exquisitely dose-dependent, since changes in its expression levels as small as a 50% reduction or a two- to three-fold increases result in severe vascular defects and embryonic lethality (21-23). Also in the setting of therapeutic VEGF overexpression in adult tissues, the growth of either normal capillary networks or aberrant angioma-like

structures is strictly controlled by the dose of VEGF localized in the microenvironment around each expressing cell (12, 24). On the other hand, very low VEGF levels efficiently generate normal angiogenesis, but fail to restore perfusion in ischemic tissue (24). Therefore, safe and effective angiogenesis requires VEGF expression in a specific therapeutic window of doses. However, it is unknown whether VEGF dose may also regulate vascular stabilization.

Here we took advantage of a highly controlled gene delivery platform we previously developed, based on monoclonal populations of VEGF-expressing transduced myoblasts (25, 26), to rigorously investigate whether different microenvironmental doses of VEGF regulate vessel stabilization independently from the transition from normal to aberrant angiogenesis, as well as the underlying mechanism. We found that VEGF negatively regulates vascular stabilization in a dose-dependent fashion, not by affecting pericyte recruitment, but rather by directly inhibiting the endothelial Sema3A/NEM/TGF- β 1 paracrine axis.

Materials and Methods

Cell culture

Primary myoblasts isolated from C57BL/6 mice were transduced to express the β -galactosidase marker gene (lacZ) from a retroviral promoter (27) and over-infected at high efficiency with retroviruses carrying the cDNA of murine VEGF₁₆₄, and a truncated murine CD8a as marker linked through an IRES sequence (Internal-Ribosome-Entry-Site) (28). The isolation and characterization of early

passage myoblast clones homogeneously expressing specific VEGF levels have been previously described (26). Briefly, myoblast clones were isolated using a FACS Vantage SE cell sorter (Becton Dickinson) and single cell isolation was confirmed visually. By ELISA assay we assessed the stability of the VEGF secretion periodically. All myoblast populations were cultured in 5% CO₂ on collagen-coated dishes with a growth medium consisting of 40% F10, 40% DMEM low glucose (1000 mg glucose/liter) and 20% fetal bovine serum, supplemented with 2.5 ng/ml basic fibroblast growth factor (FGF-2), as previously described (29).

Implantation of myoblasts into mice

Six-eight week-old, male SCID CB17 mice (Charles River Laboratories, Sulzfeld, Germany) were treated in accordance with the Swiss Federal guidelines for animal welfare, after approval from the Veterinary Office of the Canton of Basel-Stadt (Basel, Switzerland). SCID mice were used to avoid any immunologic response to myoblasts expressing xenogenic proteins. Myoblasts were dissociated in trypsin and resuspended in PBS with 0.5% BSA. We injected 1x10⁶ myoblasts in 10 µl into the posterior auricular muscle, midway up the dorsal aspect of the external ear, and into the tibialis anterior and gastrocnemius muscles in the calf, using a syringe with a 29½-gauge needle.

VEGF-Trap_{R1R2}

VEGF-Trap_{R1R2}, which consists of portions of extracellular domain of VEGFR-1 and VEGFR-2 coupled to human Fc, is a soluble form of VEGF receptors that can be used to deplete active VEGF *in vivo* (30). Mice were treated with VEGF-Trap_{R1R2} (25 mg/kg; 100 µl intraperitoneally) in PBS (40 mM phosphate and 20 mM NaCl, pH

7.4) or with vehicle (PBS; 100 µl intraperitoneally) 2 and 4 days before tissue harvest. On days 14 and 21, the vasculature was stained by injection of biotinylated *Lycopersicon esculentum* lectin intravascularly to examine the morphological changes (n= 5 mice per group).

Tissue staining

The entire vascular network of the ear could be visualized following intravascular staining with a biotinylated *Lycopersicon esculentum* lectin (50 µg in 100 µl; Vector Laboratories). Mice were anesthetized, lectin was injected intravenously and 4 minutes later the tissues were fixed by vascular perfusion of 1% paraformaldehyde and 0.5% glutaraldehyde in PBS pH 7.4. Ears were then removed, bisected in the plane of the cartilage, and stained with X-gal staining buffer (1 mg/ml 5-bromo-4-chloro-3-indoyl-β-D-galactoside, 5 mM potassium ferricyanide, 5 mM potassium ferrocyanide, 0.02% Nonidet P-40, 0.01% sodium deoxycholate, 1 mM MgCl₂ in PBS pH 7.4). Tissues were stained using avidin-biotin complex-diaminobenzidine histochemistry (Vector Laboratories), dehydrated through an alcohol series, cleared with toluene and whole-mounted on glass slides with Permount embedding medium (Fisher Scientific). Vascular morphology was analyzed at 2 and 3 weeks post-injection. To study vessel perfusion *in vivo* fluorescein isothiocyanate (FITC)-labeled *Lycopersicon esculentum* lectin (50 µg in 50 µl; Vector Laboratories) was injected into the femoral vein and allowed to circulate for 4 hours before perfusion of fixative (24).

For tissue sections, mice were anesthetized and fixed by vascular perfusion of 1% paraformaldehyde in PBS pH 7.4. *Tibialis anterior* and *Gastrocnemius*

muscles were harvested, embedded in OCT compound (Sakura Finetek), frozen in freezing isopentane, and cryosectioned. Immunofluorescence staining was performed on cryosection of 10 µm in thickness; sections were permeabilized by incubation with 0.3% Triton (Sigma-Aldrich) and 2% goat serum (Invitrogen) in PBS for 1 hour at room temperature. The following primary antibodies and dilutions were used: rat monoclonal anti-mouse PECAM-1 (BD Pharmingen) at 1:100; mouse monoclonal anti-mouse α -SMA (MP Biomedicals) at 1:400; rabbit polyclonal anti-NG2 (Millipore) at 1:200; rat monoclonal anti-CD11b (Abcam) at 1:100; rabbit polyclonal anti-NP-1 (Abcam) at 1:50; rabbit polyclonal anti-p-SMAD2/3 (Santa Cruz) at 1:100. Fluorescently labeled secondary antibodies (Molecular Probes, Invitrogen) were used at 1:200. Antibodies incubation was performed at room temperature for 1 hour.

Immunohistochemistry

Frozen sections prepared as previously described, were incubated with blocking solution, i.e. 1:20 goat serum in Tris buffer solution (TBS) for 10 minutes at room temperature. After three wash steps with TBS, primary polyclonal antibody rabbit anti Sema3A (Abcam) was used in a dilution 1:50 in TBS/1% BSA and incubated for 1 hour at room temperature. After rinsing, the immunobinding was detected with biotinylated secondary antibodies anti rabbit and using the appropriate Vectastain ABC kits. The red signal was developed with the Fast Red kit (Dako Cytomation) and sections counterstained by Haematoxylin. All images were acquired using Olympus BX61 microscope (Olympus, Volketswil, Switzerland).

Vessel analysis

Vessel length density was quantified in whole mounts ears stained with *Lycopersicon esculentum* lectin. We analyzed 3-6 fields per ear (n=5) by tracing the total length of vessels in the acquired field (20x objective), and dividing it by the area of the fields. Vessel resistant fraction was calculated as ratio between VLD after TRAP treatment and VLD before TRAP treatment, where each VLD was previously normalized with the control one (calculated on muscles injected with saline solution). All images were acquired using Olympus BX61 microscope (Olympus, Volketswil, Switzerland), and analyzed with AnalySIS D software (Soft Imaging System).

Vessel perfusion quantification was performed on sections of leg muscles derived from animals perfused with fluorescent lectin, prepared as previously described. After immunofluorescence co-staining the sections with antibodies against endothelium CD31, we traced vascular structures positive for lectin and CD31. The index of vessel perfusion was obtained by the ratio between lectin positive/CD31 positive vascular segments.

Vessel coverage quantification was performed on sections of leg muscles, prepared as explained above and co-stained with fluorescently labeled antibodies against endothelium (CD31) and pericyte (NG2). Area positive for CD31 and NG2 were calculated by ImageJ software, and the ratio between the two provided the degree of pericyte-coverage of the vessels (31).

For both vessel perfusion and coverage, we analyzed from 3 to 5 fields from each of 3 analyzed legs per group (n = 3). All images were taken with a 40X objective on a Carl Zeiss LSM710 3-laser scanning confocal microscope (Carl Zeiss,

Feldbach, Switzerland), and analyses were conducted with Cell Sense software (Olympus, Volketswil, Switzerland).

FACS sorting based ex-vivo cell isolation

Twenty skeletal muscles of CB17 SCID mice, including *Tibialis anterior* and *Gastrocnemius*, were injected with a specific VEGF-expressing myoblast clone and harvested at 7 days post injection. Muscles injected with the same myoblast clone were pooled together and treated as individual sample. Tissues were minced with scalpels into small pieces and digested with a final concentration of 0.2 mg/mL DNase (Sigma-Aldrich), 484 U/mL Collagenase type IV (Worthington), 0.5 mg/mL Collagenase I (Sigma-Aldrich), and 0.5 mg/mL Collagenase II (Sigma-Aldrich) in a 30 mL volume of DMEM low glucose (Sigma-Aldrich) into 50 mL standard polypropylene conicals, for 45 minutes at 37°C under constant shaking. Every 15 minutes cell suspensions were pipetted in order to fracture clumps. To eliminate connective tissue and fibers, samples were filtered through 100 and 70 µm nylon cell strainers (BD Falcon). Digested tissues were centrifuged for 5 minutes at 300 g and the pellet washed twice with a 20 mL volume of cold PBS. Finally collected cells were resuspended in 5 mL volume of FACS buffer (PBS supplemented with 1% EDTA and 0.5% fetal calf serum), counted, and stained with fluorescently labeled antibodies: PE anti-mouse CD31 (BioLegend) at 1:20; PE Cy7 anti-mouse CD11b (BD Pharmingen) at 1:20; antibody incubation was performed at 4°C for 30 minutes. Samples were washed twice with FACS buffer and resuspended in FACS buffer. The isolation of CD31⁺ and CD11b⁺ cell subsets was performed using a BD Influx cell sorter (Becton, Dickinson and Company). Single colour controls were prepared for

setting the software compensation and propidium iodide was used to stain samples immediately before sorting in order to gate and purify alive cells.

In vitro assay with MAECs

Mouse aortic endothelial cells (MAEC) were provided by collaborators and cultured in DMEM high glucose (Sigma-Aldrich) supplemented with 10% FBS (HyClone), 1 mM sodium pyruvate (Gibco, Invitrogen), 0.1 mM MEM Non Essential Amino Acids (Gibco, Invitrogen), 2mM glutamine (Gibco, Invitrogen), 100 U/ml penicillin and 100 µg/ml streptomycin (Gibco, Invitrogen). We seeded 1×10^5 cells/well into 24-well cell culture plates and cultured them to confluency. Cells were stimulated with mouse VEGF-A₁₆₄ or human TGF-β₁ (R&D System) at different concentrations (0 ng/mL, 1 ng/mL, 2.5 ng/mL, 10 ng/mL, and 20 ng/mL) in DMEM with 0.5% FBS, at 37°C. MAEC were collected after 24 hours post stimulation. RNA extraction, reverse-transcription into cDNA, and qRT-PCR was performed as explained above.

Quantitative Real-Time PCR

For RNA extraction from the total tissue, muscle previously injected with transgenic myoblasts were freshly harvested and disrupted using a Qiagen Tissue Lyser (Qiagen) in 1 ml of PBS 1% Trizol (Invitrogen). RNA was extracted according to manufacturer's instruction. RNA from mouse aortic endothelial cells (MAEC) and FACS sorted bone-marrow derived cells and endothelial cells was extracted with RNeasy Mini Kit (Qiagen). Total RNA from total muscles and MAECs was reverse transcribed into cDNA with the Omniscript Reverse Transcription kit (Qiagen) at 37 °C for 60 minutes; RNA from ex-vivo purified cell substes was

transcribed into cDNA with the Sensiscript RT Kit (Qiagen). Quantitative Real-Time PCR (qRT-PCR) was performed on an ABI 7300 Real-Time PCR system (Applied Biosystems). Expression of genes of interest was determined using commercial TaqMan gene expression assays (Applied Biosystems). The cycling parameters were: 50°C for 2 minutes, followed by 95°C for 10 minutes and 40 cycles of denaturation at 95°C for 15 seconds and annealing/extension at 60°C for 1 minute. Reactions were performed in triplicate for each template, averaged, and normalized to expression of the GAPDH housekeeping gene.

Statistics

Data are presented as mean \pm standard error. The significance of differences was evaluated using analysis of variance (ANOVA) followed by the Bonferroni test (for multiple comparisons); $p < 0.05$ was considered statistically significant.

Results

Vascular stabilization is impaired by increasing VEGF doses

To rigorously determine the role of VEGF dose on the vascular stabilization kinetics, we took advantage of a well-characterized pool of monoclonal populations of retrovirally transduced mouse myoblasts that express specific VEGF₁₆₄ doses, thereby ensuring homogeneous microenvironmental levels (12, 26). We selected 3 clones expressing increasing VEGF levels *in vitro*, previously shown to induce either normal (low and medium) or aberrant angiogenesis (high): V Low=11.0 \pm 0.4 ng/10⁶ cells/day, V Med=61.0 \pm 2.9 ng/10⁶ cells/day, and V

High=133.2±9.7 ng/10⁶ cells/day. Myoblast populations were implanted into the *auricularis posterior* (ear) muscle of adult SCID mice, which is amenable to whole-mount analysis of 3D vascular networks (12). Vessel stabilization was determined by quantifying the vessel length density (VLD) after systemic treatment with VEGF-Trap_{R1R2} (Trap), a potent receptor-body blocker of VEGF signaling (30), or saline control. As expected, after 2 and 3 weeks both low and medium VEGF levels yielded a network of homogeneous capillaries (Fig. 1B, D, I, and K), whereas high VEGF levels led to aberrant bulbous structures (Fig. 1F and M). In areas remote from the site of myoblast implantation in saline-treated mice, the mean VLD of pre-existing muscle capillaries was 80±4.5 mm/mm² and the VLD increase above this value represents the amount of newly induced vessels. Trap treatment showed that, after 2 weeks, 37±1.3% of the vessels induced by low VEGF were already VEGF-independent, whereas similarly normal vessels induced by medium VEGF regressed completely, as well the aberrant structures induced by high VEGF, reducing VLD to the same value as the pre-existing capillary networks in control areas (Fig. 1C, E, G, and O). By 3 weeks, the fraction of stabilized new vessels induced by low VEGF increased to 49±1.5%, while 33±14.5% became VEGF-independent with medium VEGF levels (Fig. 1J, L, and P). Aberrant vascular structures induced by high VEGF were still completely sensitive to VEGF deprivation (Fig. 1N and P). Immunofluorescence staining on sections of leg skeletal muscles collected from animals implanted with the same clones and treated with saline or TRAP, confirmed the stabilization pattern observed by the lectin staining on the whole mount ears. In fact, by 2 weeks after cell

implantation, some vessels induced by low VEGF levels were already resistant to Trap treatment, while almost none of those induced by either V Med or V High

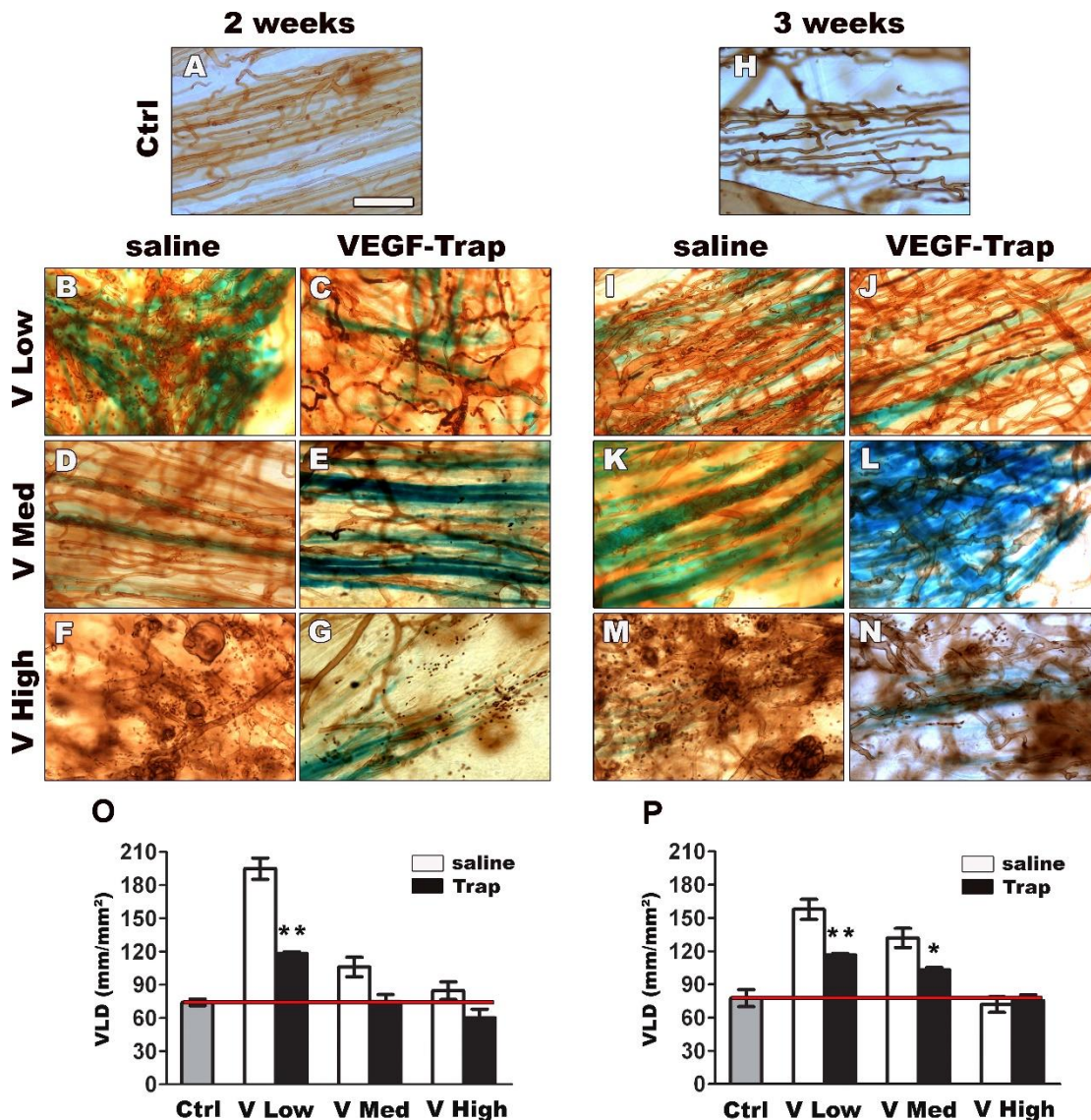


Figure 1 Increasing VEGF doses impair vessel stabilization. Myoblasts expressing different VEGF levels were implanted in ear skeletal muscles. Blood vessels were visualized in whole-mount preparations after intravascular lectin perfusion (in brown) at 2 weeks (A-G) and 3 weeks (H-N). TRAP treatment was applied to abrogate VEGF signaling, whereas saline solution was provided to the control group. Implanted myoblasts were identified by X-gal staining (blue). Scale bar= 100µm. Quantification of vascular length density (O, P) revealed that a fraction of capillaries induced by low VEGF levels become stable by 2 weeks post cell implantation, whereas normal and aberrant vessels induced by medium and high doses respectively, regressed completely (O). At 3 weeks post myoblast implantation, low and medium VEGF levels induced a similar amount of VEGF-independent normal vessels, instead, structures formed by high VEGF doses regressed (P). * $P < 0.05$, ** $P < 0.01$, vs Ctrl (*).

persisted (Fig. 2B-G). By 3 weeks after myoblast injection, some VEGF-independent vascular structures were detectable in both V Low- and V Med-

injected muscles, whereas all vessels induced by high VEGF levels still regressed (Fig. 2I-N).

Therefore, these results show that increasing VEGF amounts, within the range that induces only normal angiogenesis, impair the stabilization of newly induced capillaries in a dose-dependent fashion.

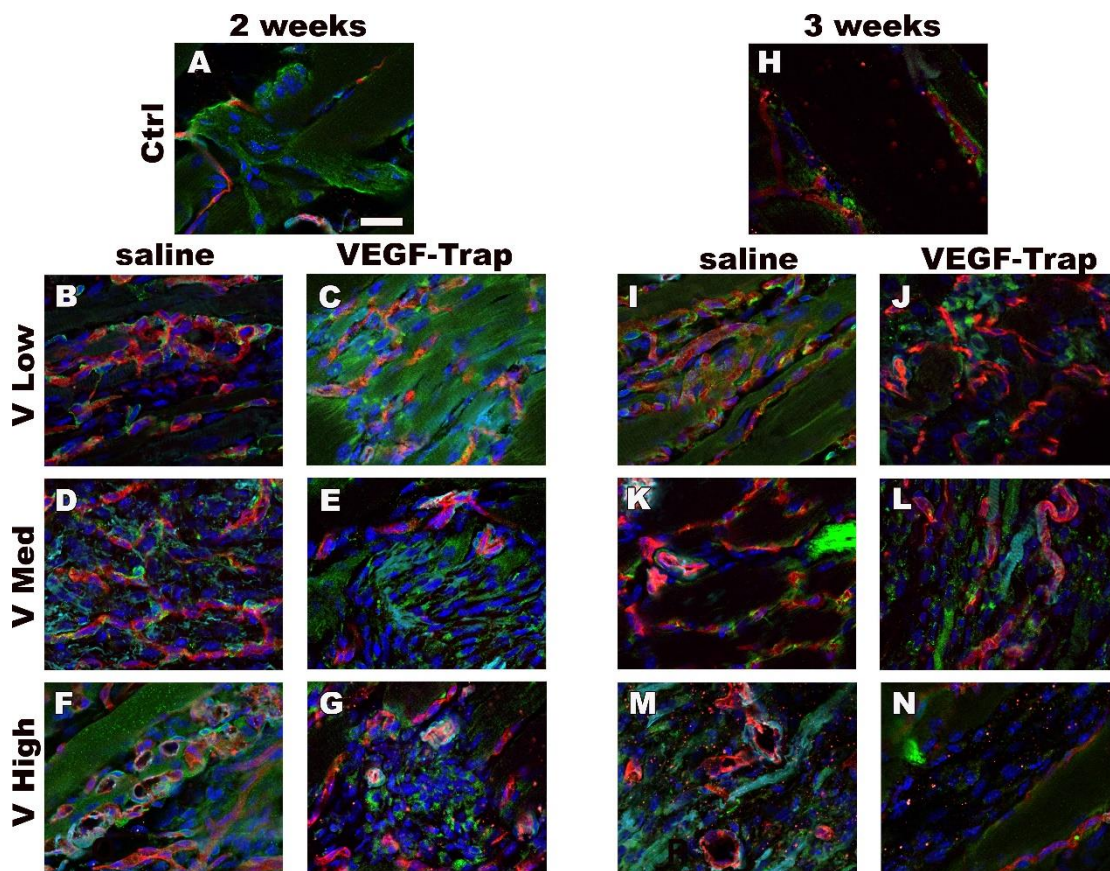


Figure 2 Impaired vascular stabilization rate by increasing VEGF doses does not correlate with pericyte coverage. Immunofluorescence staining of endothelium (CD31, in red), pericytes (NG2, in green), and smooth muscle cell (α -SMA, in cyan) on frozen sections of leg skeletal muscles of mice injected with VEGF-expressing myoblast clones, treated with or without TRAP, and sacrificed at 2 and 3 weeks after cell injection. All normal vessels induced by low and medium VEGF doses displayed a similar coverage by normal pericytes (B, D, I, and K). Instead, high VEGF-induced abnormal structures were covered with α -SMA-positive smooth muscle cells (F and M). A fraction of capillaries induced by low VEGF were already Trap-resistant by 2 weeks after myoblast implantation, but none of those induced by medium VEGF, despite similar pericyte coverage (C and E). By 3 weeks, low and medium VEGF levels induced a similar amount of VEGF-independent normal vessels, while, structures produced by high VEGF doses regressed at both time-points (G, J, L, and N). Size bar= 25 μ m.

The stabilization rate does not correlate with differential pericyte coverage or vascular perfusion

Both pericyte recruitment and establishment of functional flow have been shown to provide crucial signals for the stabilization of nascent vascular structures (13). Pericyte coverage of newly induced vessels was quantified 2 weeks after implantation of the different clones in hind limb muscles by measuring their maturation index, i.e. the ratio of the NG2-positive/CD31-positive areas after immunofluorescence staining. As shown in Fig. 2 (B, D, I, and K), the normal capillaries induced by both low and medium VEGF levels were tightly associated with NG2⁺/α-SMA⁻ pericytes, with a similar maturation index (Ctrl: 0.6 ± 0.08 , V Low 0.4 ± 0.02 , and V Med 0.4 ± 0.06). As previously described (12), aberrant structures induced by high VEGF levels were covered by a smooth muscle coat rather than pericytes (Fig. 2F and M), and therefore their maturation index was not quantified. These observations indicated that the different stabilization kinetics of normal vessels induced by low and medium VEGF doses did not correlate with differential pericyte recruitment.

The establishment of functional blood flow in newly induced vascular structures was assessed by intravenous injection of FITC-labeled tomato lectin, which binds to the luminal endothelial surface of vessels only if they are perfused by the systemic circulation (24). As shown in Fig. 3 (A-L), both normal vessels and aberrant structures induced by all VEGF doses were stained by lectin and therefore functionally perfused. Further, the quantification of the ratio between lectin-positive and CD31-positive areas did not show any significant difference

among the groups (Fig. 3M). Very few non-perfused endothelial structures were visible in every condition with similar frequency. These results suggest that establishment of functional flow was not responsible for the different stabilization rates of vessels induced by increasing VEGF doses.

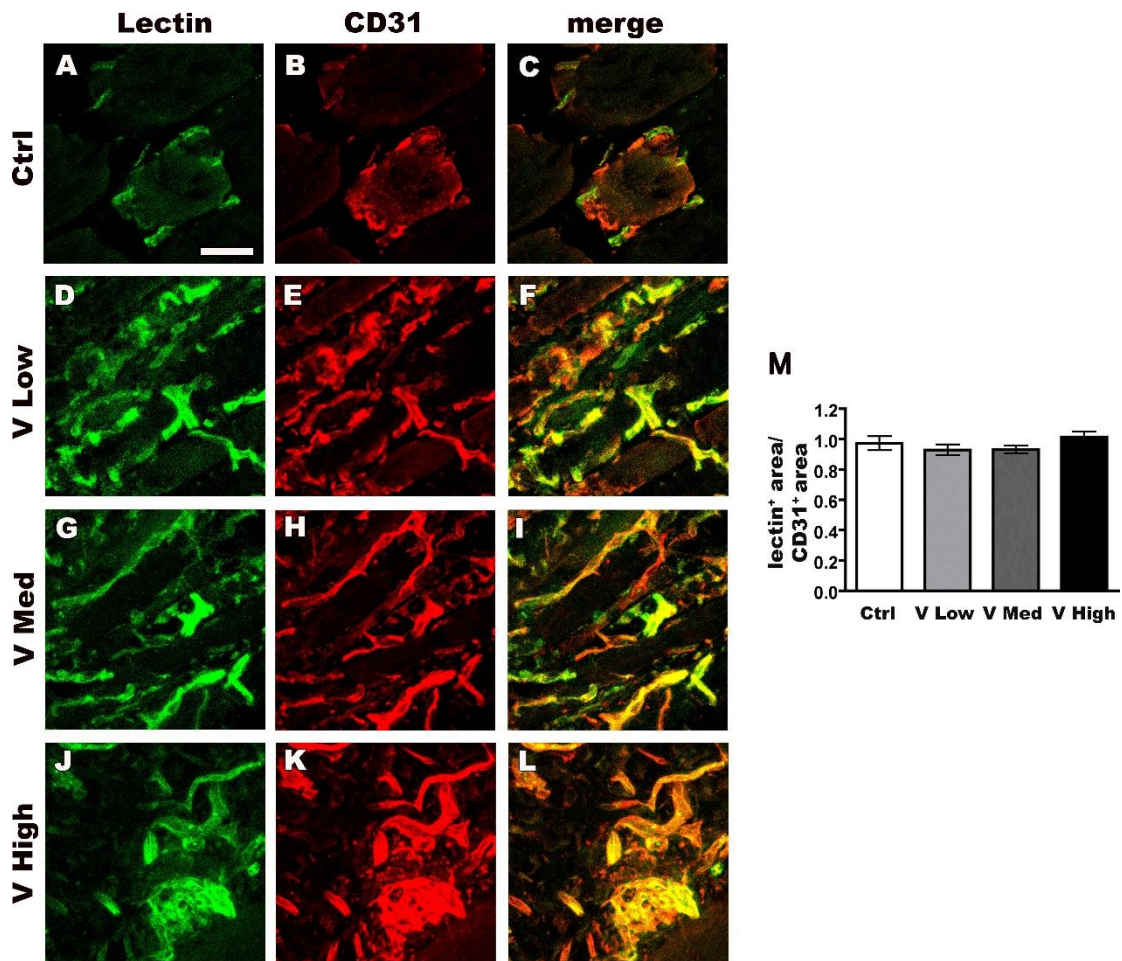


Figure 3 Vessels induced by different VEGF doses are similarly perfused. Mice received intravenous injections of FITC-lectin 2 weeks after implantation of VEGF myoblast clones. Frozen sections were immunostained for the endothelial marker CD31 (red) and perfused structures were visualized by FITC-lectin (green) (A-L). Scale bar= 25 μ m. No significant differences in perfusion were detectable either in the normal capillaries or aberrant structures induced by the different VEGF doses, as indicated by quantification of the perfusion index (lectin-positive area/CD31-positive area) (M).

TGF- β 1 and Sema3A are down-regulated in tissues exposed to increasing VEGF doses

To investigate the mechanism by which increasing VEGF doses induced similarly normal and pericyte-covered capillaries, but with distinct stabilization rates, we quantified the expression of the principal vascular maturation factors (PDGF-BB, Ang-1, TGF- β 1, and Sema3A) in muscles injected with the 3 VEGF-expressing clones or control myoblasts. As the differences in vascular stabilization were detected with VEGF-Trap treatment starting 10 days after cell implantation, gene expression was measured at day 7. As shown in Fig. 4A, PDGF-BB and Ang-1 were moderately up-regulated in tissues exposed to low VEGF, but their expression patterns were substantially stable with increasing VEGF doses and did not correlate with the observed downward trend in stabilization rates. On the other hand, both Sema3A and TGF- β 1 expression was robustly increased 4- to 5-fold compared to control levels by low VEGF and significantly down-regulated by higher VEGF doses. Gene expression data were confirmed by immunostaining for Sema3A protein on tissue sections, which showed a clear and progressive reduction of Sema3A abundance down to control levels in the areas of active angiogenesis by increasing VEGF doses (Fig. 4B-I). Further, the different myoblast populations expressed low levels of Sema3A that were unrelated to the amount of VEGF, thereby excluding that the VEGF-expressing cells may be the source of the different Sema3A amounts observed *in vivo* (Fig. S1).

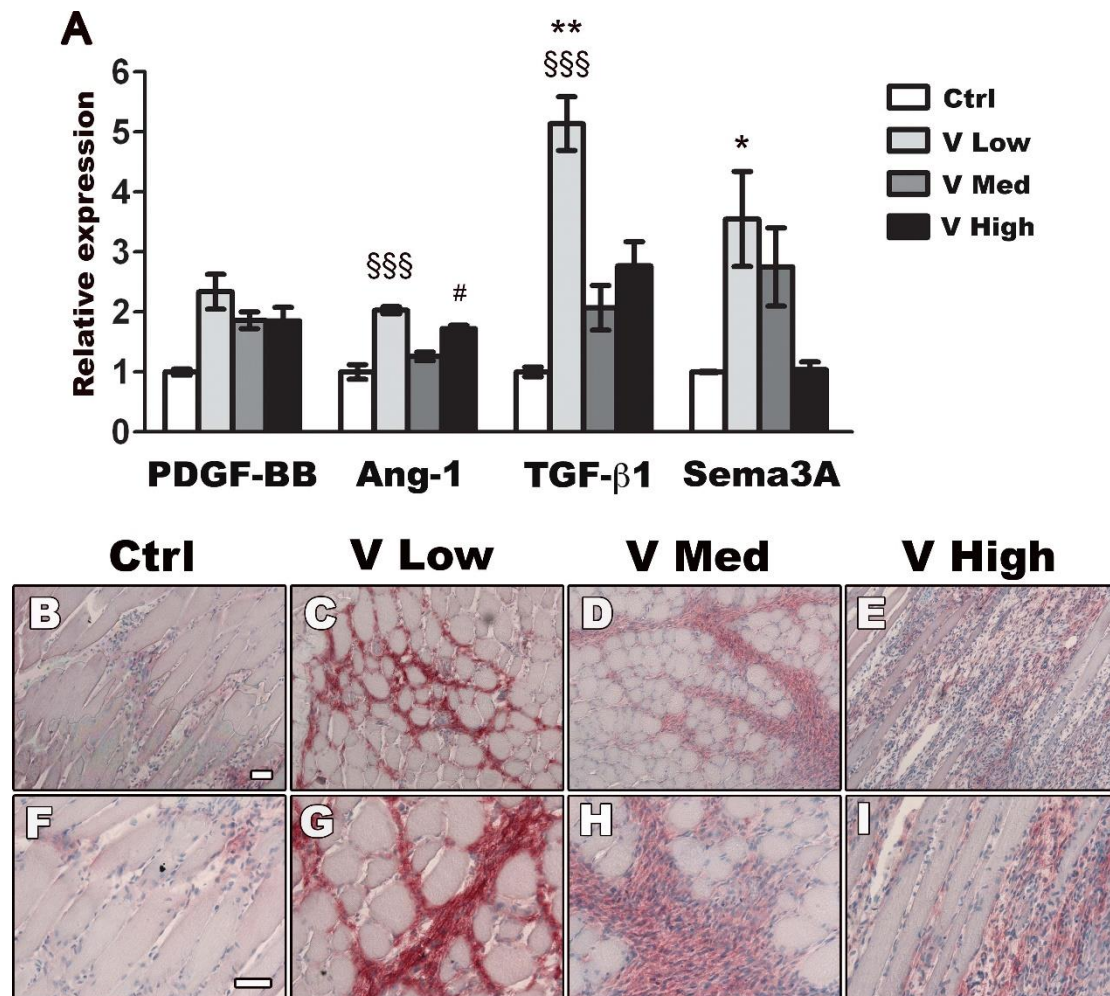


Figure 4 **TGF- β 1 and Sema3A, but not PDGF-BB and Ang-1, are down-regulated by increasing VEGF doses.** Muscles were harvested 7 days after implantation of V Low, V Med, V High clones, and control cells (Ctrl). Relative mRNA expression of PDGF-BB, Ang-1, TGF- β 1, and Sema3A was quantified by RT-PCR and normalized to control muscles (A). * $P < 0.05$, ** $P < 0.01$, V Low vs V High (*); \$\$\$ $P < 0.001$, V Low vs V Med (\$); # $P < 0.05$ V High vs V Med (#). Immunohistochemistry on frozen muscle section confirmed a decrease of Sema3A expression in the area of neovascularization by increasing VEGF doses (B-I). Scale bar = 50 μ m.

Increasing VEGF doses impair endothelial Sema3A expression and NEM recruitment

Both VEGF and Sema3A are able to recruit a specific population of bone marrow-derived neuropilin1-expressing monocytes (NEM), which have been shown to have a vascular stabilization function by secreting maturation factors such as PDGF-BB and TGF- β 1 (19). NEMs were previously shown to co-express both

NP-1 and the monocyte marker CD11b (19), and immunostaining confirmed that all CD11b⁺ cells recruited to muscle implanted with VEGF-expressing clones were also positive for NP-1 (Fig. S2). Since NP-1 is also expressed on endothelium, for clarity in subsequent experiments NEMs were identified only by CD11b staining, as previously described (19). One week after implantation of VEGF-expressing myoblasts, increased numbers of CD11b⁺ cells were recruited to the areas of active angiogenesis compared to controls. However, their frequency was clearly and progressively reduced in the presence of increasing VEGF doses (Fig. 5A-L). NEM frequency was quantified on histological sections and normalized to the amount of angiogenesis in the different conditions (CD11b⁺ cells/cm of vessel length), showing that increasing VEGF levels impaired NEM recruitment in a dose-dependent fashion (Fig. 5M). In order to analyze cell-specific changes in gene expression, CD31⁺ endothelial cells and CD11b⁺ NEM were isolated *ex-vivo* by FACS sorting from muscles implanted with the different clones (Fig. 5N). Flow cytometry quantification confirmed the VEGF dose-dependent impairment in NEM recruitment (Fig. 5N). As shown in Fig. 5O, endothelial cells isolated from tissues exposed to increasing VEGF levels significantly down-regulated *Sema3A* expression by 5-fold in a gradual and VEGF dose-dependent fashion, similarly to the results obtained from whole-tissue analyses in Fig. 4A. On the other hand, neither PDGF-BB nor TGF- β 1 expression in isolated endothelial cells was regulated by VEGF dose. CD11b⁺ isolated from tissues implanted with the different VEGF-expressing clones expressed similar levels of both NP-1 and TGF- β 1 (Fig. 5P). Furthermore, NEM expressed 2- to 3-fold more TGF- β 1 than endothelial cells without differences between VEGF doses (Fig. S3). Taken together, these results

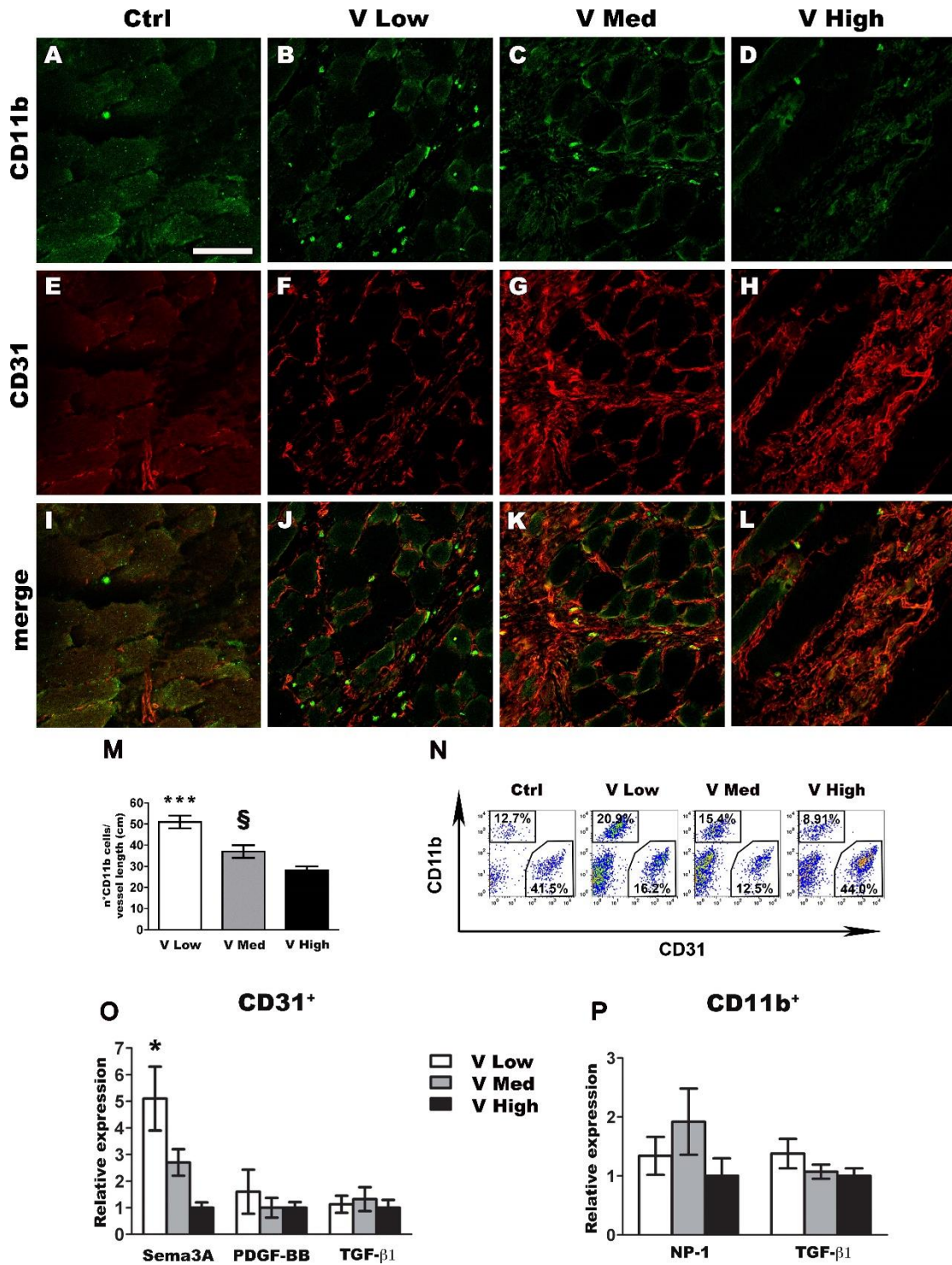


Figure 5 Increasing VEGF doses inhibit NEM recruitment and Sema3A expression in endothelial cells. Immunofluorescence staining of endothelial cells (CD31, in red) and NEMs (CD11b, in green) on cryosections from skeletal muscles 1 week after injection with VEGF-expressing myoblast clones (A-L). Quantification of NEMs/cm of vessel length indicated a reduction of CD11b⁺ cells recruited to the sites of new angiogenesis by increasing VEGF doses (M). Scale bar= 100μm. ****P*<0.001, V Low vs V High (*); §*P*<0.05, V Med vs V High (§). Muscles injected with the same myoblast clones were digested to purify endothelial cells (CD31⁺) and NEMs (CD11b⁺) by FACS sorting (N). RT-PCR analysis revealed that Sema3A is expressed by endothelial cells and down-regulated by increasing VEGF levels, whereas PDGF-BB and TGF-β1 were similarly expressed. On the other hand, expression of TGF-β1 and NP-1 by CD11b⁺ cells did not show any differences among the three groups. Relative expression was normalized to V High group (O-P). **P*<0.05, V Low vs V High (*).

show that increasing VEGF doses specifically impaired endothelial expression of Sema3A and NEM recruitment, but did not regulate TGF- β 1 expression by either endothelium or NEM, causing a reduction in total TGF- β 1 indirectly through inhibition of NEM recruitment.

Increasing VEGF doses inhibit the TGF- β 1 pathway activity in the endothelium of newly induced vessels

TGF- β 1 can promote both endothelial activation and maturation/stabilization by activating distinct intracellular signaling pathways through the phosphorylation of the SMAD1/5 and SMAD2/3 complexes, respectively (32). Therefore, we sought to determine whether TGF- β signaling was differentially activated in tissues exposed to increasing VEGF doses and which downstream pathway was preferentially stimulated. As shown in Fig. 6A, the expression of Id-1, which is induced by the SMAD1/5 pathway and not by SMAD2/3, was moderately increased 1 week after implantation of the different VEGF-expressing clones, but did not change in relation to the different VEGF doses. Conversely, the expression of PAI-1, which is induced by the SMAD2/3 pathway and not by SMAD1/5, was robustly increased about 10-fold in tissues exposed to low VEGF levels compared to controls, but this up-regulation was completely abolished by higher VEGF doses. Immunofluorescence staining confirmed that SMAD2/3 was phosphorylated and translocated in the endothelial nuclei of newly induced vessels 1 week after stimulation with low VEGF, but not with high VEGF (Fig. 6B-I). Therefore, the VEGF dose-dependent down-regulation of TGF- β 1 expression resulted in the specific

inhibition of the SMAD2/3 pathway, which mediates endothelial maturation and stabilization, in newly induced vascular structures.

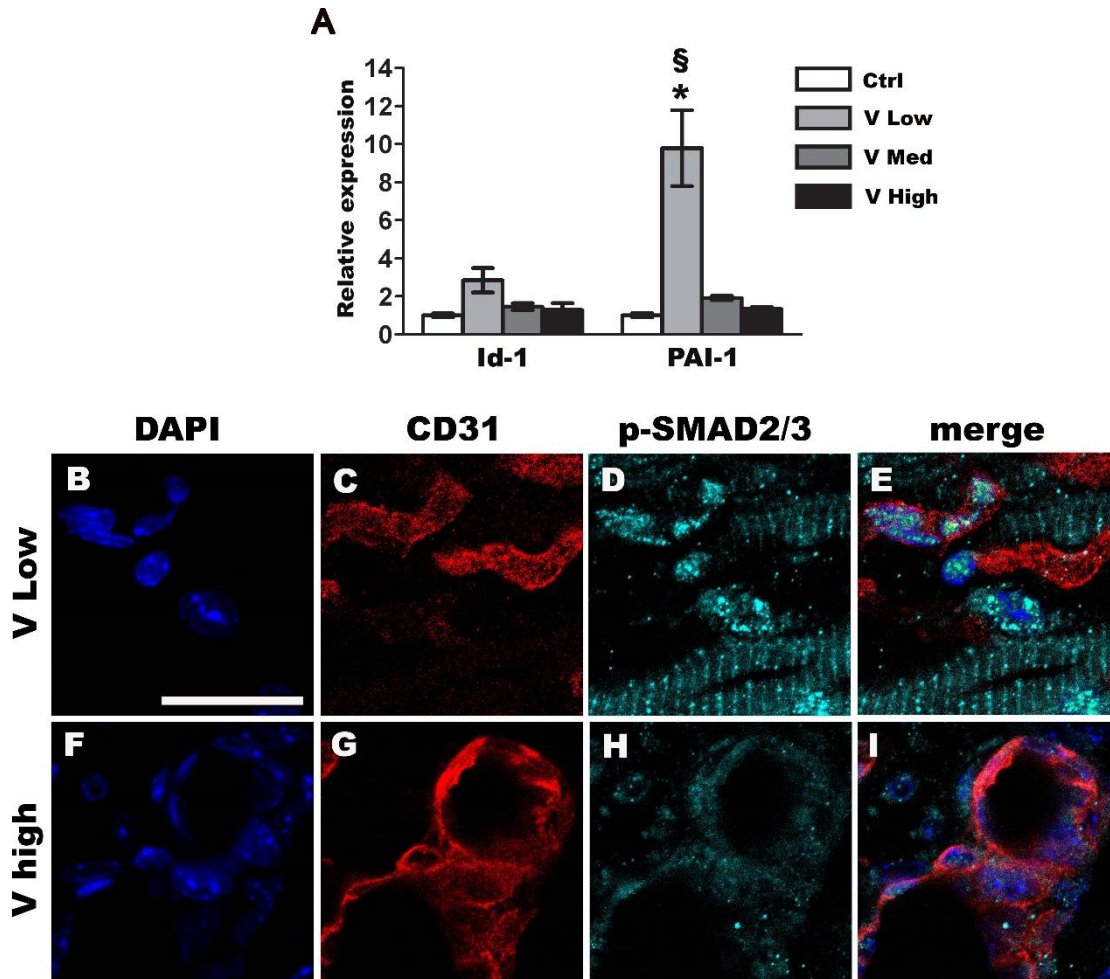
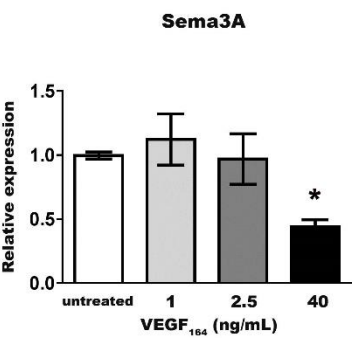


Figure 6 Increasing VEGF doses inhibit TGF- β 1 pathway activity in the endothelium of newly induced vessels. RT-PCR analysis on total muscles indicated that PAI-1 expression, which is specifically induced by activated SMAD2/3, was inhibited by increasing VEGF levels. Conversely, Id-1 expression, which is specifically induced by activated SMAD1/5, was not differentially regulated in the presence of different VEGF levels (A). * $P < 0.05$, V Low vs V High (*), § $P < 0.05$, V Low vs V Med (§). Immunofluorescence staining of endothelium (CD31, in red) and p-SMAD2/3 (cyan) on cryosections from skeletal muscles 1 week after injection with VEGF-expressing myoblast clones revealed that the TGF- β 1 pathway activity in endothelial cells was inhibited by increasing VEGF doses (B-I). Scale bar= 25 μ m.

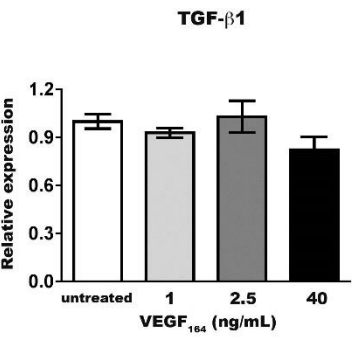
VEGF directly inhibits endothelial *Sema3A* expression and *TGF-β1* stimulates it

In order to determine whether VEGF regulated *Sema3A* expression by endothelial cells directly or indirectly, we performed *in vitro* assays using mouse aortic endothelial cells (MAEC). MAECs were stimulated with increasing VEGF

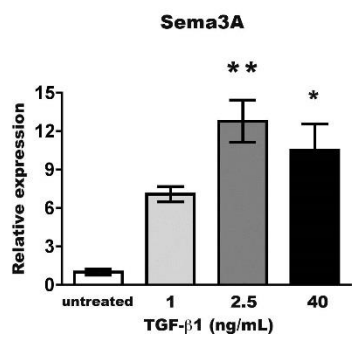
A



B



C



doses for 24 hours before RNA extraction and gene expression analysis. *Sema3A* expression was directly down-regulated by increasing VEGF doses, consistently with the results obtained both in total muscles and *ex-vivo* purified endothelial cells (Fig. 7A). On the other hand, different VEGF doses did not induce any change in *TGF-β1* expression, again consistently with the results obtained in *ex-vivo* isolated endothelial cells (Fig. 7B). Interestingly, the stimulation of MAECs with increasing *TGF-β1* doses resulted in an up-regulation of *Sema3A* expression (Fig. 7C), consistently with the results obtained *in vivo*, showing that *Sema3A* expression was increased in conditions of high *TGF-β1* activity.

Figura 7 **In vitro *Sema3A* expression in endothelial cells is inhibited by VEGF and stimulated by *TGF-β1*.** Mouse aortic endothelial cells were stimulated with increasing doses of VEGF or *TGF-β1* for 24 hours. *Sema3A* expression was quantified by RT-PCR and normalized to non-stimulated cells. VEGF inhibited *Sema3A* expression, but did not alter *TGF-β1* expression (A-B), whereas *TGF-β1* up-regulated *Sema3A* expression (C). **P*<0.05, ***P*<0.001, vs untreated (*).

Discussion

Taking advantage of the same highly controlled myoblast-mediated gene delivery platform employed here, we previously found that, while uncontrolled VEGF expression causes the growth of angioma-like vascular tumors, a wide range of doses below a threshold level induce only normal and functional angiogenesis (12, 24). Here we found that increasing VEGF doses, within the range that induces only normal angiogenesis, actually impair the stabilization of newly induced vessels, without affecting pericyte recruitment, but rather by directly inhibiting endothelial expression of *Sema3A* and the NEM/TGF- β 1 axis. Taken together, our *in vivo* and *in vitro* results suggest a model for the regulation of vascular stabilization by low to moderate VEGF doses, which lie in the therapeutic range, cause the growth only of normal microvascular networks and do not interfere with pericyte recruitment (Fig. 8): 1) in the presence of low VEGF levels, activated endothelial cells express *Sema3A*, which recruits large numbers of NEM that in turn lead to high levels of TGF- β 1 in the tissue. TGF- β 1 not only activates SMAD2/3 signaling in endothelial cells, known to induce quiescence and vessel stabilization, but also stimulates them to express further *Sema3A*, thereby providing a positive feedback loop to maintain the stabilizing signals. On the other hand, higher levels of VEGF directly inhibit endothelial expression of *Sema3A* and lead to the reversal of the above-described events, resulting in delayed stabilization of the newly induced vessels.

It has been shown that VEGF can negatively regulate pericyte function by inhibiting PDGFR- β phosphorylation through the formation of a non-functional

VEGFR2/PDGFR- β heterodimer (33). Therefore, increasing VEGF doses might interfere with endogenous PDGF-BB signaling and prevent pericyte recruitment. This provides a likely mechanism for the switch between normal and aberrant angiogenesis induced by very high VEGF levels, which is in fact characterized by a loss of physiological pericyte cover in the initial stages of vascular induction (34). Further, we recently found that this transition is not a fixed property of VEGF dose, but depends on the balance between VEGF and PDGF-BB signaling *in vivo* (35). However, it is unlikely that the competition between VEGF and PDGF-BB for PDGFR- β may explain the negative effect of increasing VEGF doses on vascular stabilization. In fact, such a mechanism would regulate stabilization through differential pericyte recruitment, whereas all normal capillaries induced by both low and medium VEGF doses showed no differences in either quantity or quality of pericyte recruitment.

The role of pericytes in protecting from vascular regression is complex. Studies on vascular regression in the retina, under hyperoxia conditions, and in tumors, after VEGF withdrawal, demonstrated a protecting role by pericytes against regression (36, 37). However, in retina and tumors, vessel regression has been described also for pericyte-covered vessels (38, 39). Our data showed that all normal capillaries induced by low and medium VEGF levels were similarly covered by pericytes by 2 weeks, but stabilization was still incomplete and further increased by 3 weeks. Therefore, pericyte recruitment is necessary, but complete stabilization requires further steps that are independent of pericytes and can be modulated by VEGF dose.

Sema3A has been recently described to antagonize VEGF₁₆₅ activity in the endothelium through the shared receptor NP-1, thereby limiting vessel growth (20, 40, 41). Furthermore, Sema3A has also been shown to be a powerful attractant of circulating myeloid cells named NEM, which prompt vessel stabilization by secreting maturation factors like TGF- β 1 (19). In agreement with this, we found that Sema3A down-regulation in skeletal muscles and *ex-vivo* purified endothelial cells by increasing VEGF doses correlated with reduced NEM recruitment to the area of newly induced angiogenesis. Despite the fact that also VEGF has been described to attract NEM by binding NP-1 (18, 19), we found that tissue-recruited NEM were severely reduced in the presence of very high VEGF levels. A likely explanation is provided by previous observations suggesting that Sema3A is more effective than VEGF in recruiting NEM (19), whereby the loss of Sema3A signaling caused by high VEGF doses cannot be compensated by the increase in VEGF expression itself. This is supported by the fact that monocytes also express VEGFR1, which can prevent NP-1 binding to VEGF₁₆₅ and therefore negatively regulate VEGF signaling activity via NP-1 (42, 43).

TGF- β 1 expression by *ex-vivo* purified NEM was independent of VEGF dose, suggesting that the amount of factor in tissue is a function exclusively of the number of recruited NEM.

TGF- β 1 is a pleiotropic factor and can either stimulate endothelial activation or promote maturation/stabilization, contributing to the establishment of basement membrane around new vessels and favoring endothelial cell quiescence (44), by activating distinct intracellular signaling pathways through the phosphorylation of the SMAD1/5 and SMAD2/3 complexes, respectively (32). Our

data show that in the setting of VEGF over-expression in skeletal muscle TGF- β 1 had a stabilizing function. In fact, the observed changes in its expression correlated with corresponding changes in SMAD2/3 phosphorylation in endothelial cells and in expression of the SMAD2/3-specific downstream gene PAI-1, but not of Id-1, which is instead specifically regulated by the SMAD1/5 pathway. Even though pericyte coverage was not affected by increasing VEGF doses, it is possible that changes in pericyte expression of TGF- β 1 or other factors, directly or indirectly caused by VEGF, may contribute to the observed differences in vascular stabilization kinetics. Further investigations on *ex-vivo* purified pericytes isolated from the different conditions will provide valuable data.

In conclusion, our results show that VEGF dose impairs vessel stabilization by directly inhibiting Sema3A/NEM/TGF- β 1 signaling. This finding has implications for the design of safe and effective approaches for therapeutic angiogenesis. In fact, we have previously found that VEGF doses within the range inducing only normal angiogenesis are not therapeutically equivalent (24). In particular, the lower doses, which we found here to allow the fastest stabilization, are not effective to restore blood flow in ischemia, due to the excessively small size of the induced vessels, and functional improvement requires higher doses, which induce larger vessels, but also inhibit Sema3A expression and delay stabilization. Therefore, these results suggest that delivery of controlled doses of VEGF will not be able to achieve both therapeutic angiogenesis and an accelerated stabilization. However, based on our findings, co-delivery of Sema3A would be expected to significantly accelerate stabilization of micro-vascular networks induced by therapeutic doses of VEGF, thereby enabling short-term and safer therapeutic

approaches, such as the sustained release of recombinant factors from biomaterial depots.

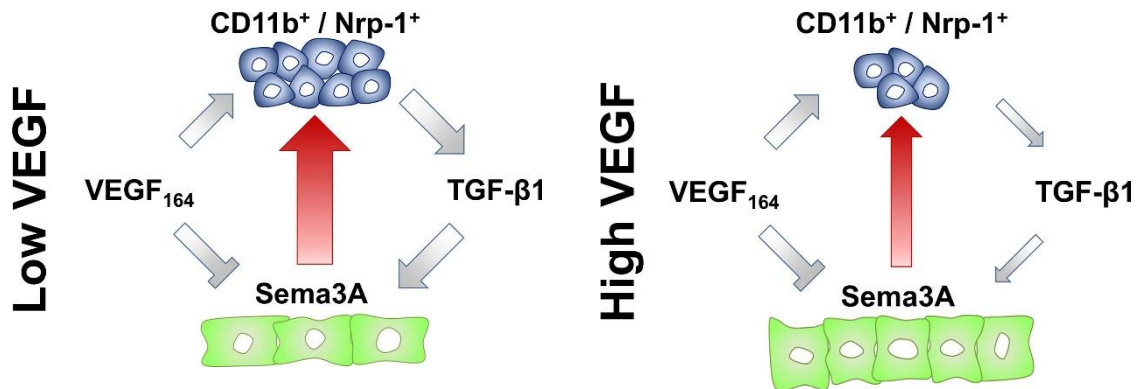
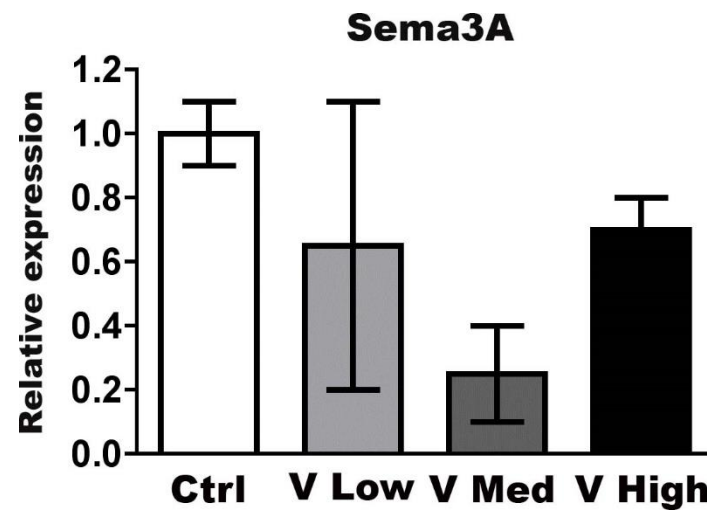
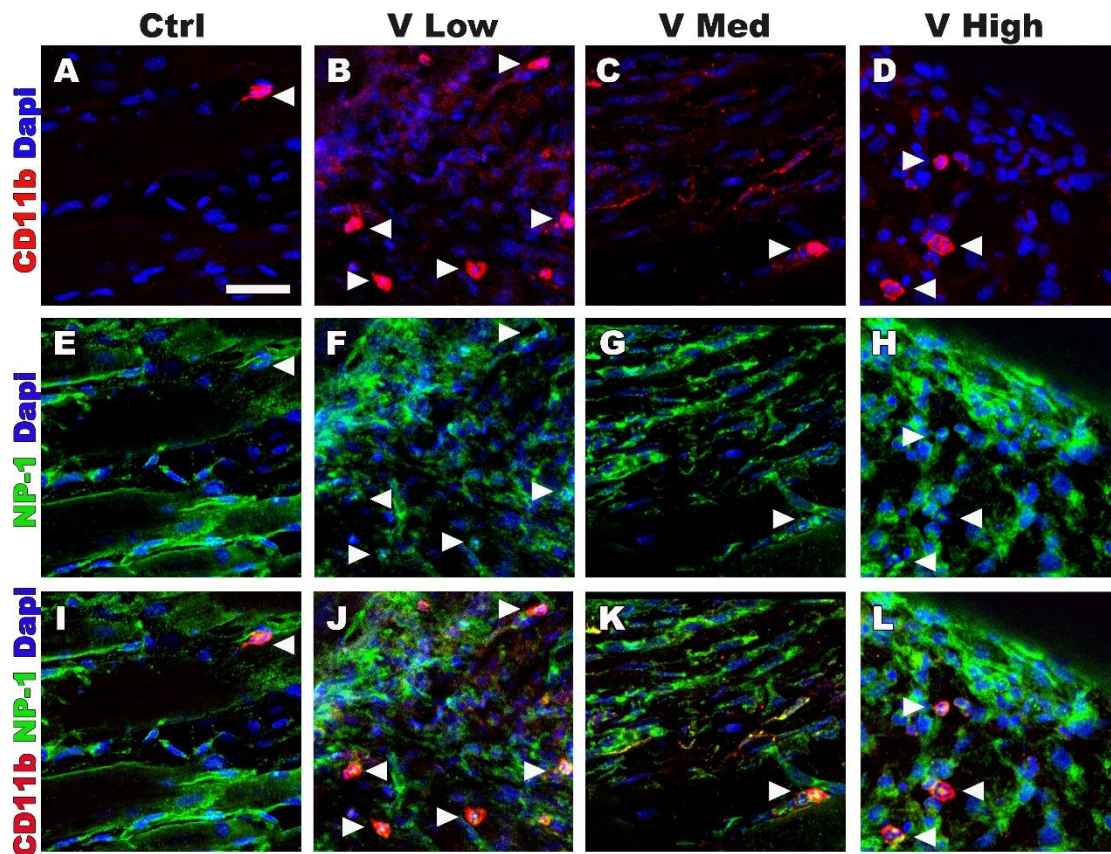


Figura 8 **Working model of the mechanisms by which VEGF dose regulates vascular stabilization.** In the presence of low VEGF levels, Sema3A produced by endothelial cells recruits NEM that home to the area of new angiogenesis and express TGF- β 1. TGF- β 1 on one hand activates the SMAD2/3 pathway to promote vascular stabilization and on the other stimulates Sema3A expression by endothelial cells, thereby maintaining a pro-stabilization positive feedback loop. However, high levels of VEGF directly inhibit Sema3A expression by endothelial cells, the Sema3A/NEM/TGF- β 1/Sema3A loop is impaired and stabilization is delayed.

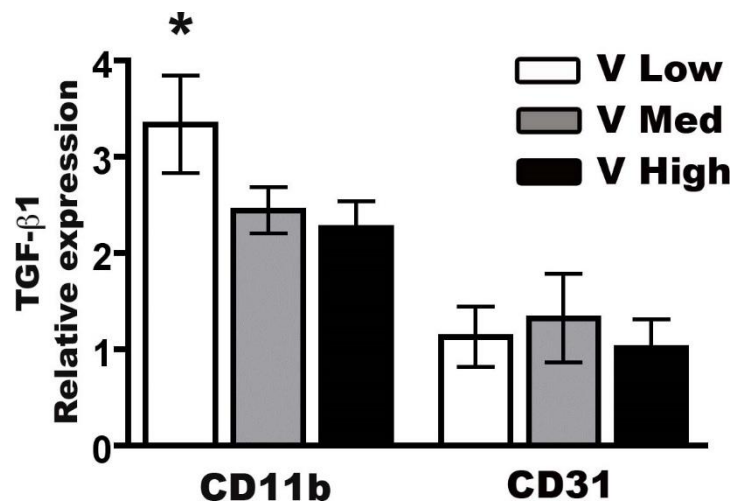
Supplementary Informations



Suppl. Figure 1 **Figure 1. VEGF expressing myoblasts do not express significantly different levels of Sema3A.** Sema3A gene expression analysis was performed on V Low, V Med, V High, and Ctrl myoblasts cultured *in vitro*. No statistically significant difference was detected.



Suppl. Figure 2 **Mononuclear cells expressing both CD11b and NP-1 are recruited to the sites of VEGF-induced neovascularization.** Immunofluorescence staining for CD11b (red) and NP-1 (green) on cryosections from skeletal muscles 1 week after injection of VEGF-expressing myoblast clones. All CD11b-positive cells also expressed NP-1. Nuclei positive for NP-1 but not for CD11b marker belong to endothelial cells. Scale bar= 20 μ m.



Suppl. Figure 3 **Ex-vivo purified NEMs express higher levels of TGF- β 1 than endothelial cells.** TGF- β 1 gene expression analysis performed on FACS-purified NEMs and endothelial cells. * P <0.05, CD11b V Low vs CD31 V Low (*).

References

1. M. Giacca, S. Zacchigna, VEGF gene therapy: therapeutic angiogenesis in the clinic and beyond. *Gene therapy* **19**, 622 (Jun, 2012).
2. J. M. Isner et al., Clinical evidence of angiogenesis after arterial gene transfer of phVEGF165 in patient with ischaemic limb. *Lancet* **348**, 370 (Aug 10, 1996).
3. E. R. Schwarz et al., Evaluation of the effects of intramyocardial injection of DNA expressing vascular endothelial growth factor (VEGF) in a myocardial infarction model in the rat--angiogenesis and angioma formation. *Journal of the American College of Cardiology* **35**, 1323 (Apr, 2000).
4. A. Pettersson et al., Heterogeneity of the angiogenic response induced in different normal adult tissues by vascular permeability factor/vascular endothelial growth factor. *Laboratory investigation; a journal of technical methods and pathology* **80**, 99 (Jan, 2000).
5. C. Sundberg et al., Glomeruloid microvascular proliferation follows adenoviral vascular permeability factor/vascular endothelial growth factor-164 gene delivery. *The American journal of pathology* **158**, 1145 (Mar, 2001).
6. S. Zacchigna et al., In vivo imaging shows abnormal function of vascular endothelial growth factor-induced vasculature. *Human gene therapy* **18**, 515 (Jun, 2007).

7. H. Karvinen *et al.*, Long-term VEGF-A expression promotes aberrant angiogenesis and fibrosis in skeletal muscle. *Gene therapy* **18**, 1166 (Dec, 2011).
8. M. L. Springer, A. S. Chen, P. E. Kraft, M. Bednarski, H. M. Blau, VEGF gene delivery to muscle: potential role for vasculogenesis in adults. *Molecular cell* **2**, 549 (Nov, 1998).
9. R. J. Lee *et al.*, VEGF gene delivery to myocardium: deleterious effects of unregulated expression. *Circulation* **102**, 898 (Aug 22, 2000).
10. Y. Dor *et al.*, Conditional switching of VEGF provides new insights into adult neovascularization and pro-angiogenic therapy. *The EMBO journal* **21**, 1939 (Apr 15, 2002).
11. S. Tafuro *et al.*, Inducible adeno-associated virus vectors promote functional angiogenesis in adult organisms via regulated vascular endothelial growth factor expression. *Cardiovascular research* **83**, 663 (Sep 1, 2009).
12. C. R. Ozawa *et al.*, Microenvironmental VEGF concentration, not total dose, determines a threshold between normal and aberrant angiogenesis. *The Journal of clinical investigation* **113**, 516 (Feb, 2004).
13. M. Potente, H. Gerhardt, P. Carmeliet, Basic and therapeutic aspects of angiogenesis. *Cell* **146**, 873 (Sep 16, 2011).
14. P. Carmeliet, R. K. Jain, Principles and mechanisms of vessel normalization for cancer and other angiogenic diseases. *Nature reviews. Drug discovery* **10**, 417 (Jun, 2011).

15. G. Ferrari *et al.*, TGF-beta1 induces endothelial cell apoptosis by shifting VEGF activation of p38(MAPK) from the prosurvival p38beta to proapoptotic p38alpha. *Molecular cancer research : MCR* **10**, 605 (May, 2012).
16. T. Ziegelhoeffer *et al.*, Bone marrow-derived cells do not incorporate into the adult growing vasculature. *Circulation research* **94**, 230 (Feb 6, 2004).
17. L. Zentilin *et al.*, Bone marrow mononuclear cells are recruited to the sites of VEGF-induced neovascularization but are not incorporated into the newly formed vessels. *Blood* **107**, 3546 (May 1, 2006).
18. P. Korpisalo *et al.*, Vascular endothelial growth factor-A and platelet-derived growth factor-B combination gene therapy prolongs angiogenic effects via recruitment of interstitial mononuclear cells and paracrine effects rather than improved pericyte coverage of angiogenic vessels. *Circulation research* **103**, 1092 (Nov 7, 2008).
19. S. Zacchigna *et al.*, Bone marrow cells recruited through the neuropilin-1 receptor promote arterial formation at the sites of adult neoangiogenesis in mice. *The Journal of clinical investigation* **118**, 2062 (Jun, 2008).
20. F. Maione *et al.*, Semaphorin 3A is an endogenous angiogenesis inhibitor that blocks tumor growth and normalizes tumor vasculature in transgenic mouse models. *The Journal of clinical investigation* **119**, 3356 (Nov, 2009).
21. N. Ferrara *et al.*, Heterozygous embryonic lethality induced by targeted inactivation of the VEGF gene. *Nature* **380**, 439 (Apr 4, 1996).
22. P. Carmeliet *et al.*, Abnormal blood vessel development and lethality in embryos lacking a single VEGF allele. *Nature* **380**, 435 (Apr 4, 1996).

23. L. Miquerol, B. L. Langille, A. Nagy, Embryonic development is disrupted by modest increases in vascular endothelial growth factor gene expression. *Development* **127**, 3941 (Sep, 2000).
24. G. von Degenfeld et al., Microenvironmental VEGF distribution is critical for stable and functional vessel growth in ischemia. *FASEB journal : official publication of the Federation of American Societies for Experimental Biology* **20**, 2657 (Dec, 2006).
25. G. von Degenfeld, A. Banfi, M. L. Springer, H. M. Blau, Myoblast-mediated gene transfer for therapeutic angiogenesis and arteriogenesis. *British journal of pharmacology* **140**, 620 (Oct, 2003).
26. H. Misteli et al., High-throughput flow cytometry purification of transduced progenitors expressing defined levels of vascular endothelial growth factor induces controlled angiogenesis in vivo. *Stem cells* **28**, 611 (Mar 31, 2010).
27. T. A. Rando, H. M. Blau, Primary mouse myoblast purification, characterization, and transplantation for cell-mediated gene therapy. *The Journal of cell biology* **125**, 1275 (Jun, 1994).
28. M. L. Springer, H. M. Blau, High-efficiency retroviral infection of primary myoblasts. *Somatic cell and molecular genetics* **23**, 203 (May, 1997).
29. A. Banfi, M. L. Springer, H. M. Blau, Myoblast-mediated gene transfer for therapeutic angiogenesis. *Methods in enzymology* **346**, 145 (2002).
30. J. Holash et al., VEGF-Trap: a VEGF blocker with potent antitumor effects. *Proceedings of the National Academy of Sciences of the United States of America* **99**, 11393 (Aug 20, 2002).

31. F. Li et al., Endothelial Smad4 maintains cerebrovascular integrity by activating N-cadherin through cooperation with Notch. *Developmental cell* **20**, 291 (Mar 15, 2011).
32. P. ten Dijke, H. M. Arthur, Extracellular control of TGFbeta signalling in vascular development and disease. *Nature reviews. Molecular cell biology* **8**, 857 (Nov, 2007).
33. J. I. Greenberg et al., A role for VEGF as a negative regulator of pericyte function and vessel maturation. *Nature* **456**, 809 (Dec 11, 2008).
34. R. Gianni-Barrera et al., VEGF over-expression in skeletal muscle induces angiogenesis by intussusception rather than sprouting. *Angiogenesis* **16**, 123 (Jan, 2013).
35. A. Banfi et al., Therapeutic angiogenesis due to balanced single-vector delivery of VEGF and PDGF-BB. *FASEB journal : official publication of the Federation of American Societies for Experimental Biology* **26**, 2486 (Jun, 2012).
36. I. Helfrich et al., Resistance to antiangiogenic therapy is directed by vascular phenotype, vessel stabilization, and maturation in malignant melanoma. *The Journal of experimental medicine* **207**, 491 (Mar 15, 2010).
37. L. E. Benjamin, I. Hemo, E. Keshet, A plasticity window for blood vessel remodelling is defined by pericyte coverage of the preformed endothelial network and is regulated by PDGF-B and VEGF. *Development* **125**, 1591 (May, 1998).
38. T. Inai et al., Inhibition of vascular endothelial growth factor (VEGF) signaling in cancer causes loss of endothelial fenestrations, regression of

- tumor vessels, and appearance of basement membrane ghosts. *The American journal of pathology* **165**, 35 (Jul, 2004).
39. D. von Tell, A. Armulik, C. Betsholtz, Pericytes and vascular stability. *Experimental cell research* **312**, 623 (Mar 10, 2006).
 40. M. Narazaki, G. Tosato, Ligand-induced internalization selects use of common receptor neuropilin-1 by VEGF₁₆₅ and semaphorin_{3A}. *Blood* **107**, 3892 (May 15, 2006).
 41. A. Vacca *et al.*, Loss of inhibitory semaphorin 3A (SEMA_{3A}) autocrine loops in bone marrow endothelial cells of patients with multiple myeloma. *Blood* **108**, 1661 (Sep 1, 2006).
 42. G. Fuh, K. C. Garcia, A. M. de Vos, The interaction of neuropilin-1 with vascular endothelial growth factor and its receptor flt-1. *The Journal of biological chemistry* **275**, 26690 (Sep 1, 2000).
 43. C. A. Staton, I. Kumar, M. W. Reed, N. J. Brown, Neuropilins in physiological and pathological angiogenesis. *The Journal of pathology* **212**, 237 (Jul, 2007).
 44. M. T. Holderfield, C. C. Hughes, Crosstalk between vascular endothelial growth factor, notch, and transforming growth factor-beta in vascular morphogenesis. *Circulation research* **102**, 637 (Mar 28, 2008).

Summary and Future Prospective

VEGF is the master regulator of angiogenesis and is the most investigated factor in therapeutic angiogenesis approaches to induce the growth of new vessels that could restore oxygen and nutrients supply in tissues affected by ischemia, for example in peripheral or coronary artery diseases (1). Several VEGF-based therapies have been tested in clinical trials, but, despite a good safety profile, they could not prove therapeutic efficacy (2). Retrospective analyses in light of current knowledge of VEGF biology have identified several issues with the VEGF gene delivery approaches used in those trials (3), among which the dose and duration of expression are key parameters that define the narrow therapeutic window of VEGF (4).

Therefore, here we sought to investigate the cellular and molecular mechanisms regulating the switch between normal and aberrant angiogenesis and the achievement of vascular stabilization in the presence of increasing VEGF doses, in order to identify novel and potentially more specific molecular targets to improve both the safety and the efficacy of VEGF-based strategies for therapeutic angiogenesis (4). For this purpose we took advantage of a highly controlled gene delivery platform previously developed by our group, based on monoclonal populations of transduced myoblasts that express specific VEGF₁₆₄ doses, thereby ensuring homogeneous microenvironmental levels in skeletal muscle (5-7).

The first part of this thesis aimed at identifying the pericyte-derived signaling pathways that determine the transition from normal to aberrant angiogenesis by

increasing VEGF doses. In particular, we investigated the TGF- β 1/TGF β R, Ang-1/Tie2, and EphrinB2/EphB4 signaling pathways, which were previously found to have key functions in the mural cell-endothelial cell crosstalk during both embryonic and adult angiogenesis (8). Each of these pathways was inhibited in vivo by co-expressing a soluble blocker together with a low VEGF dose that induces only normal angiogenesis when delivered alone. While neither TGF- β 1/TGF β R nor Ang-1/Tie2 blockade affected normal vascular growth induced by low VEGF levels, loss and gain of function experiments revealed EphrinB2/EphB4 to be a crucial pathway in determining whether VEGF induces normal or aberrant angiogenesis in skeletal muscle. In fact, inhibition of this pathway led to a switch from normal pericyte-coated vessels to aberrant smooth muscle-covered angioma-like structures, despite expression of a low VEGF dose. EphrinB2/EphB4 inhibition affected VEGF-induced angiogenesis during the remodeling phase, i.e. between 4 and 7 days after cell implantation, when it caused an increase in the degree of vascular enlargement and the loss of NG2-positive pericytes, replaced by NG2- and α -SMA-double positive mural cells. Conversely, the stimulation of EphB4 signaling with a recombinant EphrinB2-Fc fusion protein caused the reverse switch from aberrant to normal angiogenesis despite expression of high VEGF levels, re-establishing a well-organized network of normal capillaries with physiological pericyte coverage. Current experiments aim to define which cellular processes are affected by modulating EphrinB2/EphB4 signaling in VEGF-induced angiogenesis, such as cell proliferation, adhesion, and motility.

These findings suggest that EphrinB2 may be exploited to normalize aberrant angiogenesis to overcome the issues of uncontrolled VEGF expression in a

therapeutically relevant gene therapy approach. For example, adeno-associated viral (AAV) vectors provide several attractive features for a clinical application, such as low immunogenicity, high efficiency of transduction and long duration of expression (9). Nevertheless, several studies have shown that also VEGF delivery by AAV has the potential to induce aberrant vascular structures due to the long-term uncontrolled expression (10). Therefore, an EphrinB2-based combined therapy to prompt normalization of VEGF-induced aberrant angiogenesis would benefit the development of safer therapeutic strategies with AAV gene delivery, i.e. with a bicistronic AAV that co-express VEGF and EphrinB2. However, monomeric soluble EphrinB2 is actually an inhibitor of the EphB4 receptor, since in order to activate the signaling an oligomerization of the ligand/receptor complex is required, which physiologically takes place thanks to the fact that both ligand and receptor are cell membrane bound (11). In order to generate a soluble version of the EphrinB2 ligand that could be secreted after in vivo delivery of a viral vector, but that at the same time would retain the physiological ability to oligomerize, we are currently developing an engineered version of the soluble truncated extracellular portion of EphrinB2 fused to a chimeric immunoglobulin Fc portion comprising the 18 aa tail-piece of human IgM Fc attached to the human IgG1 Fc. This engineered IgM-IgG Fc molecule exploits the property of IgM immunoglobulins to physiologically assemble into pentamers and has been shown to spontaneously create hexameric complexes (12). We will therefore test the hypothesis that a spontaneously multimerizing version of soluble EphrinB2 can ensure homogeneously normal angiogenesis despite uncontrolled levels of VEGF

over-expression when co-delivered with a clinically relevant AAV vector in skeletal muscle.

The experiments described in this part of the thesis were based on educated guesses investigating pathways previously found to have a role in vascular maturation. In order to have a complete understanding of the molecular pathways underlying the transition from normal to aberrant angiogenesis by increasing VEGF levels, we have planned to perform an unbiased transcriptomic analysis on FACS-purified endothelial cells (CD31⁺) and pericytes (NG2⁺) derived from skeletal muscles injected with VEGF-expressing myoblasts. Cells will be isolated 4 and 7 days after implantation of clones expressing either low or high VEGF doses, since we have previously found that the initial vascular response in both conditions is a circumferential enlargement by 4 days, followed by differential remodeling to either normal or aberrant vascular structures by 7 days (7). Next generation RNA sequencing of the mRNA and miRNA transcriptome and state-of-the-art bioinformatics analysis in collaboration with Hoffman-La Roche, using pathway, miRNA and transcription factor enrichment analyses, are expected to identify regulatory networks that are differentially regulated during the switch from normal to aberrant angiogenesis by increasing VEGF doses.

In the second part of this thesis, we investigated whether VEGF dose also controls vessel stabilization, independently from vascular morphogenesis, i.e. the switch between normal capillary networks and aberrant angioma-like structures. Taking advantage of clonal myoblast populations expressing specific VEGF doses that induce either normal (low and medium VEGF) or aberrant angiogenesis high VEGF) (5), we found that increasing VEGF levels impair vascular stabilization in a

dose-dependent fashion. In particular, normal vessels generated by low and medium VEGF levels displayed similar morphology, pericyte coverage and functional blood flow, but stabilized faster the lower the VEGF dose. Further, we found that VEGF impairs vascular stabilization by directly inhibits the endothelial *Sema3A*/NEM/TGF- β 1 paracrine axis, according to the following model: 1) in the presence of low VEGF levels, activated endothelial cells express *Sema3A*, which recruits large numbers of circulating Neuropilin-expressing Monocytes (NEM) by binding the receptor neuropilin-1 (NP-1). NEM in turn express TGF- β 1, which not only induces endothelial quiescence and vessel stabilization by activating SMAD2/3 signaling in endothelial cells, but also stimulates them to express further *Sema3A*, thereby providing a positive feedback loop to maintain the stabilizing signals. On the other hand, higher levels of VEGF directly inhibit endothelial expression of *Sema3A* and lead to the reversal of the above-described events, resulting in delayed stabilization of the newly induced vessels.

As an immediate extension of these data, it would be interesting to test the potential of *Sema3A* overexpression to also normalize VEGF-induced aberrant angiogenesis. In fact, recent data show that *Sema3A* may normalize tumor vasculature, leading to improved perfusion and greater efficacy of anti-tumor treatments (13, 14). Furthermore, NEM recruited by *Sema3A* are also a rich source PDGF-BB (13). While the data described above show that pericyte recruitment is not involved in the impairment of stabilization by increasing VEGF doses in the low to moderate range, we have previously found that the transition between normal and aberrant angiogenesis at high VEGF levels is critically regulated by the balance between VEGF and PDGF-BB signaling, as shown by the induction of

homogeneously normal angiogenesis by co-delivery of VEGF and PDGF-BB at balanced levels from a single bicistronic construct, despite uncontrolled and high VEGF expression (15, 16). Therefore, it will be interesting to test the hypothesis that Sema3A co-expression can normalize aberrant angiogenesis by high VEGF doses taking advantage of the highly controlled myoblast-based gene delivery platform described here. If the proof of principle was confirmed, the results should be extended to a clinically relevant gene therapy vector, such as the co-expression of VEGF and Sema3A from a single AAV construct.

Regardless of whether Sema3A may have a normalization function, its role in regulating vascular stabilization in VEGF-induced angiogenesis could be exploited to accelerate vascular stabilization in short-term delivery systems. For example, biodegradable biomaterials easily allow the delivery of homogeneous and controlled VEGF doses, but it is challenging to sustain release for at least 4 weeks. Sema3A incorporation in such biomaterials together with a safe VEGF dose is an attractive approach to accelerate the stabilization of the newly induced normal angiogenesis despite short duration of factor release.

Lastly, a fascinating opportunity could be provided by the combination of the normalization features of Ephrin pathway stimulation with the stabilization effect of Sema3A, for example using a tri-cistronic vector. However, recent work by the group of K. Alitalo (Helsinki, Finland), suggests that it could be possible to develop a single bifunctional chimeric protein by fusing together the receptor-binding region of each molecule, to be co-expressed with VEGF (17).

In conclusion, we have identified some mechanisms of vascular morphogenesis and stabilization underlying normal and aberrant vascular growth induced by

VEGF over-expression at specific doses. These results suggest novel targets that have the potential to modulate the dose-dependent effects of VEGF gene delivery in combinatorial therapeutic approaches.

References

1. M. Giacca, S. Zacchigna, VEGF gene therapy: therapeutic angiogenesis in the clinic and beyond. *Gene therapy* **19**, 622 (Jun, 2012).
2. B. H. Annex, Therapeutic angiogenesis for critical limb ischaemia. *Nature reviews. Cardiology*, (May 14, 2013).
3. S. Yla-Herttuala, T. T. Rissanen, I. Vajanto, J. Hartikainen, Vascular endothelial growth factors: biology and current status of clinical applications in cardiovascular medicine. *Journal of the American College of Cardiology* **49**, 1015 (Mar 13, 2007).
4. S. Reginato, R. Gianni-Barrera, A. Banfi, Taming of the wild vessel: promoting vessel stabilization for safe therapeutic angiogenesis. *Biochemical Society transactions* **39**, 1654 (Dec, 2011).
5. C. R. Ozawa *et al.*, Microenvironmental VEGF concentration, not total dose, determines a threshold between normal and aberrant angiogenesis. *The Journal of clinical investigation* **113**, 516 (Feb, 2004).
6. H. Misteli *et al.*, High-throughput flow cytometry purification of transduced progenitors expressing defined levels of vascular endothelial growth factor induces controlled angiogenesis in vivo. *Stem cells* **28**, 611 (Mar 31, 2010).
7. R. Gianni-Barrera *et al.*, VEGF over-expression in skeletal muscle induces angiogenesis by intussusception rather than sprouting. *Angiogenesis* **16**, 123 (Jan, 2013).

8. M. Potente, H. Gerhardt, P. Carmeliet, Basic and therapeutic aspects of angiogenesis. *Cell* **146**, 873 (Sep 16, 2011).
9. M. Giacca, S. Zacchigna, Virus-mediated gene delivery for human gene therapy. *Journal of controlled release : official journal of the Controlled Release Society* **161**, 377 (Jul 20, 2012).
10. H. Karvinen et al., Long-term VEGF-A expression promotes aberrant angiogenesis and fibrosis in skeletal muscle. *Gene therapy* **18**, 1166 (Dec, 2011).
11. O. Salvucci, G. Tosato, Essential roles of EphB receptors and EphrinB ligands in endothelial cell function and angiogenesis. *Advances in cancer research* **114**, 21 (2012).
12. D. N. Mekhaie et al., Polymeric human Fc-fusion proteins with modified effector functions. *Scientific reports* **1**, 124 (2011).
13. F. Maione et al., Semaphorin 3A overcomes cancer hypoxia and metastatic dissemination induced by antiangiogenic treatment in mice. *The Journal of clinical investigation* **122**, 1832 (May 1, 2012).
14. G. Chakraborty, S. Kumar, R. Mishra, T. V. Patil, G. C. Kundu, Semaphorin 3A suppresses tumor growth and metastasis in mice melanoma model. *PloS one* **7**, e33633 (2012).
15. S. Zacchigna et al., Bone marrow cells recruited through the neuropilin-1 receptor promote arterial formation at the sites of adult neoangiogenesis in mice. *The Journal of clinical investigation* **118**, 2062 (Jun, 2008).
16. A. Banfi et al., Therapeutic angiogenesis due to balanced single-vector delivery of VEGF and PDGF-BB. *FASEB journal : official publication of the Federation of American Societies for Experimental Biology* **26**, 2486 (Jun, 2012).

17. A. Anisimov *et al.*, Vascular endothelial growth factor-angiopoietin chimera with improved properties for therapeutic angiogenesis. *Circulation* **127**, 424 (Jan 29, 2013).

CURRICULUM VITAE ET STUDIORUM

ELENA GROPPA

PERSONAL INFORMATION

Full Name	Elena, GROPPA
Place and Date of Birth	Vicenza (Italy), February 15 th , 1984
Address	Spalenring 64, Basel, CH-4055 Basel
Mobile	+41 77 472 0061
e-mail - personal	elena.groppa@hotmail.it
- work	elena.groppa@usb.ch
Nationality	Italian

EDUCATION & TRAINING

June 2013	PhD Degree Institute for Surgical Research and Hospital Management, Cell and Gene Therapy Laboratory - 20, Hebelstrasse CH-4031 Basel, Switzerland Thesis title: Mechanisms of vascular morphogenesis and stabilization by VEGF dose
December 2008	Master's degree in Industrial Biotechnology (110/110 <i>cum laude</i>) University of Padua, Faculty of Mathematics Physics and Natural Sciences, Department of Biology - Via Ugo Bassi, 35121 Padova, Italy Thesis title: A Novel 3-D co-culture model of adipocytes and endothelial cells
July 2006	Bachelor's degree in Biotechnology (107/110) University of Padua, Faculty of Mathematics Physics and Natural Sciences, Department of Biology - Via Ugo Bassi, 35121 Padova, Italy Thesis title: Phylogenetic analysis of superoxide dismutase Cu-Zn
June 2003	Scientific Diploma (98/100) Liceo Scientifico N.Tron - 4, Via Alessandro Luzio, 36015 Schio (VI), Italy

WORK EXPERIENCE

June 2013 -	Research Fellow Institute for Surgical Research and Hospital Management, Cell and Gene Therapy Laboratory, Supervisor Dr Andrea Banfi - 20, Hebelstrasse CH-4031 Basel, Switzerland <u>Research Project:</u> perform an unbiased transcriptomic analysis on FACS-purified endothelial cells (CD31 ⁺) and pericytes (NG2 ⁺) derived from skeletal muscles injected with VEGF-expressing myoblasts in order to have a complete understanding of the molecular pathways underlying the transition from normal to aberrant angiogenesis by increasing VEGF levels.
November 2009 - June 2013	PhD Student position Institute for Surgical Research and Hospital Management, Cell and Gene Therapy Laboratory, Supervisor Dr Andrea Banfi - 20, Hebelstrasse CH-4031 Basel, Switzerland

	<p><u>Research Project:</u> my PhD project aimed to 1) investigate the paracrine signals between pericyte and endothelium that determine the switch from normal to aberrant angiogenesis by increasing VEGF dose 2) study the effect of VEGF dose on vessel stabilization and identify the molecular and cellular mechanisms that prompt vessels newly induced to become VEGF-independent.</p>
March 2013	<p>Visitor researcher</p> <p>Erasmus Stem Cell Institute, Department of Cell Biology, Supervisor Dr Mihaela Crisan - 3000 CA Rotterdam, The Netherlands</p> <p><u>Research Topic:</u> angiogenesis. During this scientific exchange, I learnt and optimized protocols for histological analysis and Fluorescence-Activated Cell Sorting (FACS) experiments in order to characterize and isolate vascular cell subsets.</p>
January 2008 - November 2008	<p>Foreign training as undergraduate student</p> <p>University of Regensburg, Faculty of Pharmacy, Department of Pharmaceutical Technology, Supervisor Prof Stefano Mammi and Prof Torsten Blunk - 31, Universitätsstraße, 93053 Regensburg, Germany</p> <p><u>Research Project:</u> establish and characterize a novel 3-D co-culture model culturing preadipocytes (3T3-L1) and microvascular endothelial cells (HMVEC) in spheroids, in order to develop engineered adipose tissue for clinical and basic research purposes.</p>
May 2006 - July 2006	<p>Internal training as undergraduate student</p> <p>University of Padua, Faculty of Mathematics Physics and Natural Sciences, Department of Biology, Supervisor Prof Santovito Gianfranco - Via Ugo Bassi, 35121 Padova, Italy</p> <p><u>Research Project:</u> phylogenetic analysis of superoxide dismutase in Antarctic and not Antarctic species in order to understand the conservation degree of superoxide dismutase Cu-Zn.</p>

PERSONAL SKILLS AND COMPETENCES

<i>Mother tongue</i>	Italian
<i>Other language(s)</i>	<p>English (Speaking: Good; Writing: Good; Reading: Good)</p> <p>German (Speaking: Intermediate; Writing: Intermediate; Reading: Intermediate)</p>
<i>Technical skills and competences</i>	<p>Cell culture handling in conventional mono-layer and in spheroid system with primary cells and cell lines</p> <p>Cell transfection and transduction</p> <p>Isolation of specific cell subsets from skeletal muscles by Fluorescence-Activated Cell Sorting (FACS)</p> <p>Cytofluorimetric analysis with BD FACS Calibur and Beckman Coulter Cyan</p> <p>Bacteria culture and cloning</p> <p>RNA and DNA Extraction, Quantitative Real Time PCR</p> <p>Immunohistochemistry, immunofluorescence techniques and imaging by confocal microscopy (Carl Zeiss LSM 710 controlled via the ZEN software utility)</p> <p>Elisa, Western Blot, Gene Reporter Assay</p> <p>In-vivo experiments (with mice)</p>
<i>Computer skills and competences</i>	<p>OS: Windows and Macintosh</p> <p>Good command of internet and Microsoft Office tools, in particular Word, Power Point, Excel, and Access</p> <p>FlowJo, GraphPad Prism, Adobe Photoshop, and ImageJ</p>
<i>Driving licence</i>	Italian driving licence, category B

PUBLICATION LIST

- Groppa E., Reginato S., Gianni-Barrera R., Muraro M.G., Heberer M., Banfi A. **Increasing VEGF doses impair vascular stabilization by directly inhibiting the Sema3A/CD11b⁺ NP-1⁺ monocyte/TGF- β 1 axis** (submitted).
- Groppa E., Sacchi V., Trani M., Muraro M.G., Heberer M., Banfi A. **EphrinB2/EphB4 signaling controls the switch from normal to aberrant angiogenesis caused by VEGF dose** (in preparation).
- Sacchi V., Mittermayr R., Hartinger J., Martino M.M., Lorentz K.M., Wolbank S., Hofmann A., Largo R.A., Marschall J.S., Groppa E., Gianni-Barrera R., Ehrbar M., Hubbell J.A., Redl H., Banfi, A. **Long-lasting fibrin matrices ensure stable and functional angiogenesis by highly tunable, sustained delivery of recombinant VEGF164** (PNAS, 2014).
- Helmrich U., Di Maggio N., Güven S., Groppa E., Melly L., D Largo R, Heberer M., Martin I., Scherberich A., Banfi A. **Increased osteogenic graft vascularization and bone resorption by VEGF-expressing human mesenchymal progenitors** (Biomaterials, 2013).

PARTECIPATION AT CONFERENCES AND SYMPOSIA

- | | |
|----------------------------|--|
| Oral Presentation | VEGF dose negatively regulates the stabilization of newly induced vessels by inhibiting the Sema3A/NP-1⁺CD11b⁺monocytes/TGF-β1 axis. International Vascular Biology Meeting, in Wiesbaden, Germany (2012) |
| Poster Presentation | <p>EphrinB2/EphB4 signaling controls the switch from normal to aberrant angiogenesis caused by VEGF dose. Cardiovascular & Metabolic Research Conference 2014, in Fribourg, Switzerland (2014) - Best Poster prize</p> <p>Molecular mechanisms of endothelium-pericyte crosstalk for therapeutic angiogenesis. Advances in the Cellular and Molecular Biology of Angiogenesis, in Birmingham, UK (2011)</p> <p>Molecular mechanisms of endothelium-pericyte crosstalk for therapeutic angiogenesis. 8th International Symposium on the Biology of Endothelial Cells, in Zurich, Switzerland (2011)</p> <p>Role of pericyte signaling pathways in the normalization of VEGF-induced angiogenesis by PDGF-BB co-expression. Cardiovascular Biology and Clinical Implications Meeting, in Muntelier, Switzerland (2010) - Best Poster prize</p> |

ADDITIONAL INFORMATION

- | | |
|---------------------------|--|
| Personal interests | Travelling, Reading, Listening music, Enjoy with friends |
| Sports | Jogging, Biking, Handball, Hiking, Skiing, Swimming |

REFERENCES:

- PD, Dr Andrea Banfi: andrea.banfi@usb.ch
- Dr Mihaela Crisan: m.crisan@erasmusmc.nl
- Prof Giacca Mauro: giacca@icgeb.org
- Prof Torsten Blunk: Blunk_T@klinik.uni-wuerzburg.de
- Prof Stefano Mammi: stefano.mammi@unipd.it